Table of Contents

1. General Information

Materials and Solvents

All solvents (hexane/petroleum ether, dichloromethane, chloroform, diethyl ether) were used without any purification if not indicated differently. All commercially available compounds were used as received. All amines for Buchwald-Hartwig coupling were recrystallized before use to remove all *N*-oxide species. All presented reactions were carried out in a dry glassware under inert atmosphere of argon. Selected reactions was monitored using thin-layer chromatography (TLC), which was visualized under UV lamp (254 nm). Anhydrous solvents were purchased form Sigma-Aldrich. Chloroform and deuterated chloroform were neutralized with potassium carbonate before use (unless otherwise stated).

NMR spectroscopy

^{1}H NMR spectra were recorded on a high-field spectrometer (^{1}H 600 MHz and 400 MHz, ^{13}C 150 MHz and 100 MHz), equipped with a broadband inverse gradient probehead. Spectra were referenced to the residual solvent signal (chloroform-*d*, 7.26 ppm). Two-dimensional NMR spectra were recorded with 2048 data points in the t2 domain and up to 1024 points in the t1 domain, with a 1 s recovery delay. For concentrated samples (e.g. boron/phosphoryl insertions) baseline was corrected using multipoint baseline correction.

Mass Spectrometry

The ESI-MS analysis was performed on Bruker qTOF (Bremen, Germany) equipped with a standard ESI source. Spectra were recorded using DCM or MeOH. The instruments parameters were as follows: positive-ion mode, calibration with the Tunemix™ mixture (Agilent Technologies, Palo Alto, CA, USA), mass accuracy was better than 5 ppm, scan range: 50 - 1600 m/z; drying gas: nitrogen; flow rate: 3.0 L/min, temperature: 200 °C; potential between the spray needle and the orifice: 4.5 kV, analyte was introduced to the ESI source by pump (New Era Pump Systems, Inc., USA) with a flow rate: 3 µL/min.

UV-Vis Spectrophotometry

Electronic spectra were recorded on a Agilent Cary 60 spectrophotometer with a 1 cm optical path in solutions in HPLC grade chloroform in 298 K using standard quartz cuvettes.

X-Ray Crystallography

X-Ray quality crystals were prepared by slow evaporation from HPLC grade DCM/hexane mixture. Diffraction data were collected using a Bruker D8 Quest Eco Photo50 CMOS diffractometer, equipped with MoKα (0.71073 Å) X-ray radiation source, Triumph monochromator, CPAD Photon II detector, and the Oxford CryoStream 800 Plus cooling system. Crystals were mounted in a cryo-loop using paratone oil and kept at 100 K during measurement. Data were processed using the Apex2 software. The structures were solved by intrinsic phasing with SHELXT (2018 release) and refined by full-matrix least-squares methods based F^2 using SHELXL[1] implemented in Olex2[2] software. For all structures, H atoms bound to C atoms were placed in the geometrically idealized positions and treated in riding mode, with C-H = 0.95 Å and $U_{iso}(H) = 1.2U_{eq}(C)$ for C-H groups, and C-H = 0.98 Å and $U_{iso}(H) = 1.5U_{eq}(C)$ for CH_3 groups. All disorders were modelled using similar distance (SADI) restrains.

EPR Spectroscopy

EPR spectra were measured with a Bruker ELEXSYS E500 X-band spectrometer equipped with a super-high-sensitivity ER 4122 SHQE cavity operating at 9.7 GHz and 100 kHz magnetic field modulation. XEpr software was used for spectra acquisition and manipulation. An ER 4111 variable temperature unit was used for precise temperature control. In typical experiments, the spectra were acquired with the microwave power of 2 mW, the modulation amplitude of 1 G, conversion time 83.89 ms, time constant 40.96 ms, and 1 scan were applied. EPR spectra were simulated with the EasySpin software package.[3]

Cyclic Voltammetry

Cyclic voltammograms were recorded in dry degassed dichloromethane under Ar atmosphere on Autolab PGSTAT101 using a glassy-carbon working electrode, platinum wire as the auxiliary electrode, and Ag/AgCl as a reference electrode. The voltammograms were referenced against the halfwave potential of Fc/Fc^+ (internal standard method).

Theoretical calculations

Geometry optimization for **2a** and **3a** was carried out with the Gaussian 09[4] software package within unconstrained C1 symmetry. Counterpoise corrected for adsorption model Becke's three-parameter exchange functional with the gradient-corrected correlation formula of Lee, Yang and Parr (DFT-CAM-B3LYP)[5] were used with the 6-31G(d,p) basis set. Calculations of radical species were performed for doublet state (UCAM-B3LYP/6-31G(d,p), PCM, charge 0, spin 2). For the computation of hyperfine coupling constants EPR-II basis set was used. The polarizable continuum model of solvation was used (PCM, standard chloroform parametrization) for all optimizations. GD3BJ empirical dispersion correction was applied. Harmonic vibrational frequencies were calculated using analytical second derivatives as a verification of local minimum achievement with no negative frequencies observed. Time-dependent DFT (TD-DFT) calculations were performed at the CAM-B3LYP/6-311G(d,p) level of theory including PCM and GD3BJ. A total 50 singlet excited states were computed. Natural transition orbitals (NTOs) were obtained using the IOp(9/40=2) keyword. Atoms in Molecules (AIM) analyses were performed using the Multiwfn 3.8 program,[6] based on the wavefunction files (.fchk) generated at the CAM-B3LYP/6-31G(d,p) level including PCM and GD3BJ. The topology of the electron density was analyzed according to Bader's QTAIM theory.[7] Bond critical points (BCPs) were located, and electron densities and their Laplacians at BCPs were used to calculate energies of interactions. Visualizations of the electron density topology were generated in Multiwfn and further processed in VMD software.

2. Experimental

2.1. General Procedures

General Procedure 1. (**GP1**) The dry Schlenk tube was charged with bromoamine (1 equiv), tris(dibenzylideneacetone)dipalladium(0) (5 mol%), 1,1'-bis(diphenylphosphino)ferrocene (10 mol%), and sodium *tert*-butoxide (1.5 equiv) and dried under vacuum for 2-5 hours. Then, 2-iodobromobenzene (1.1 equiv) dissolved in dry degassed toluene (5 mL per 1 mmol of amine) was added, and the obtained mixture was refluxed for 20 hours (oil bath). After this time, the dark reaction mixture was diluted with diethyl ether and passed through celite. The product was purified by automatic flash chromatography with a silica column (230-400 mesh) using a 0-5% gradient of ethyl acetate in petroleum ether.

General Procedure 2. (**GP2**) (**A**) The Schlenk tube was charged with *N*-Boc-pyrrole-2-boronic acid (3 equiv), palladium(II) acetate (20 mol%), 2-dicyclohexylphosphino-2',6'-dimethoxybiphenyl (SPhos, 7 mol%), and potassium phosphate tribasic (3 equiv) and dried under vacuum for 1 hour. Then, the solution of dibromoderivative (1 equiv) in the degassed mixture of n-butanol and water (95:5; 60 mL per 1 mmol of dibromoderivative) was added. The obtained solution was refluxed for 2-4 hours (heating block), cooled down, diluted with diethyl ether, and passed through celite. The product was purified by automatic flash chromatography with a silica column (230-400 mesh) using a 0-3% gradient of ethyl acetate in petroleum ether and submitted directly to the deprotection reaction. The use of THF instead of n-butanol decreases the amount of contamination after the reaction. (**B**) The obtained substance was dispersed in ethylene glycol (100 mL per 1 mmol of substrate), heated under reflux for 1 hour (heating block), cooled down to ambient temperature, and diluted with water. Then, the mixture was extracted with ethyl acetate three times (in darkness), and combined organic fractions were washed with distilled water (at least 5 times) and saturated brine. Further drying over anhydrous sodium sulfate, and evaporation led to the light-sensitive product which was used in Vilsmeyer-Haack formylation immediately. (**C**) The dried and argonated two-neck round-bottom flask was charged with dry dimethylformamide (4 equiv) and cooled down to the ice bath temperature. Phosphoryl chloride (4 equiv) was added dropwise and yellowish solid formation was observed. The obtained Vilsmeyer reagent was gently melted down using a heat gun and dissolved in dry 1,2-dichloroethane (25 mL per 1 mmol of substrate). Then, the solution of deprotection product (1 equiv) in 1,2-dichloroethane (25 mL per 1 mmol of substrate) was added dropwise, and obtained brownish solution was refluxed for 2 hours (heating block). After this time, the reaction was quenched with sodium acetate solution (0.5 mol/L) and heated at 70 °C overnight. The product was extracted with ethyl acetate, dried over anhydrous sodium sulfate, passed through a short silica column, and evaporated. Pure dialdehyde was obtained *via* precipitation made by the addition of HPLC grade hexane to the saturated solution of crude in chloroform.

General Procedure 3. (**GP3**) Zinc (75 equiv) and copper(I) iodide (2.4 equiv) were weighed out to the dry three-neck round-bottom flask and dried under vacuum for 30 minutes. Then, dry tetrahydrofuran (0.5 mL per 1 mg of dialdehyde) was added followed by the direct addition of titanium(IV) chloride (38 equiv). The obtained mixture was refluxed for 2 hours (heating mantle). Then, dialdehyde (1 equiv) solution in tetrahydrofuran (0.5 mL per 1 mg of substrate) was added dropwise, and heating under reflux was continued for 1 hour. After cooling the mixture down, 10% potassium carbonate solution was added, and the product was extracted with ethyl acetate, and dried over anhydrous sodium sulfate. After evaporation, the obtained macrocycle was purified by silica column chromatography using a mixture of petroleum ether and hexane (95:5) as an eluent.

General procedure 4. (**GP4**) A macrocycle (1 equiv) was weighed out, dissolved in deuterated chloroform (0.14 mL per 1 µmol of substrate; without any removal of residual acid), and stored in an NMR tube in darkness for a specified time (NMR control).

General Procedure 5. (**GP5**) A macrocycle (1 equiv) was dissolved in chloroform (1 mL per 5.4 µmol of substrate) followed by the addition of ground molecular sieves (3 Å; 10 mg per 5.4 µmol of substrate) and manganese oxide (10 equiv). The obtained mixture was stirred at room temperature for 24 hours, passed through the celite pad, and evaporated.

General procedure 6. (**GP6**) A macrocycle (1 equiv) was weighed out and transferred to the glove box. 1,8-Diazabicyclo[5.4.0]undec-7-ene (10 equiv) was dissolved in deuterated chloroform (75 mL per 1 mmol of macrocycle). Freebase macrocycle was then dissolved in the resulting solution of the base, transferred to the NMR-tube, and closed with a septum stopper. One equivalent of the solution of a heteroatom source (BBr_3, PBr_3, or $POCl_3$) in $CDCl_3$ was added at a time (^{1}H NMR monitoring). Further purification of the product is impossible due to the high sensitivity of these substances.

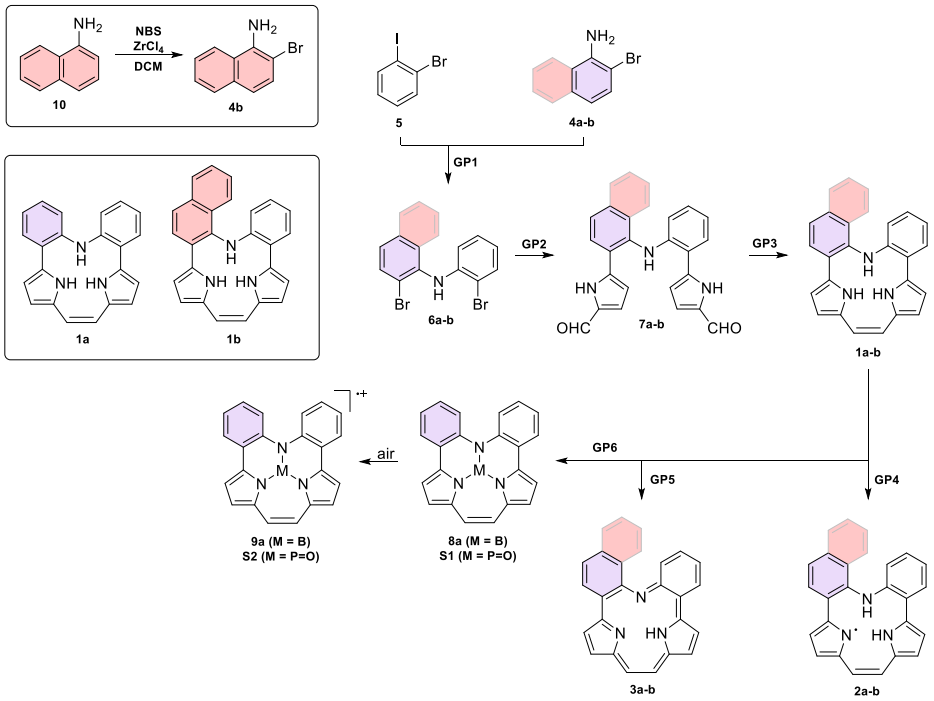

Scheme S1. Synthetic pathways.

2.2. Detailed Procedures

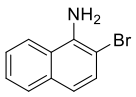

Compound **4b**. A dry round-bottom flask was charged with 1-naphthylamine (12 mmol; 1.718 g; 1 equiv) and zirconium(IV) chloride (0.6 mmol; 140 mg; 5 mol%). Dry dichloromethane (15 mL) was added under an inert atmosphere of argon and the resulting solution was cooled down to -78 °C. Then, the solution of *N*-bromosuccinimide (12 mmol; 2.136 g; 1 equiv) in dichloromethane (90 mL) was added dropwise, and the reaction mixture was stirred at the same temperature for 1.5 hours. The reaction was quenched with the saturated solution of sodium bicarbonate and extracted with dichloromethane. Combined organic layers were dried over anhydrous sodium sulfate and the solvent was then evaporated. The product was purified by automatic flash chromatography with a silica column (230-400 mesh) using a 0-5% gradient of ethyl acetate in petroleum ether. 1.104 g of 2-bromo-1-naphthylamine was obtained as a slightly pink solid with a yield equal to 41%. ^{1}H NMR (400 MHz, $CDCl_3$) δ ppm 7.71-7.84 (m, 2H), 7.41-7.53 (m, 3H), 7.18 (d, *J* = 9.2 Hz, 1H), 4.65 (br. s, 2H).[8]

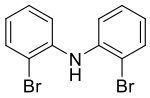

Compound **6a**. **GP1**, 2 mmol scale, colorless oil (crystallizing after some time in the fridge), 0.602 g, isolated yield was equal to 92%. ^{1}H NMR (600 MHz, $CDCl_3$) δ ppm 7.57 (d, *J* = 8.2 Hz, 1H) 7.28 (d, *J* = 8.2 Hz, 2H) 7.21 (t, *J* = 7.6 Hz, 2H) 6.83 (t, *J* = 7.6 Hz, 2H) 6.43 (br. s, 1H).[9]

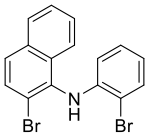

Compound **6b**. **GP1**, 5.9 mmol scale, colorless oil, 1.322 g, isolated yield was equal to 59%. ^{1}H NMR (400 MHz, $CDCl_3$) δ ppm 7.83-7.93 (m, 2 H), 7.71 (d, *J* = 8.7 Hz, 1H), 7.66 (d, *J* = 9.2 Hz, 1H), 7.49-7.58 (m, 2H), 7.46 (td, *J* = 7.8, 1.8 Hz, 1H), 6.94 (td, *J* = 7.8, 1.4 Hz, 1H), 6.68 (td, *J* = 7.6, 1.4 Hz, 1H), 6.28 (br. s, 1H), 6.12 (dd, *J* = 8.2, 1.4 Hz, 1H). ^{13}C NMR (101 MHz, $CDCl_3$) δ ppm 143.0, 135.4, 133.4, 132.5, 131.6, 129.9, 128.3, 128.1, 127.7, 127.2, 126.6, 124.3, 120.1, 119.9, 114.4, 110.5. HRMS (m/z) found 397.9140 $[M+Na]^+$ (expected 397.9150 calcd for $C_{16}H_{11}Br_2N$).

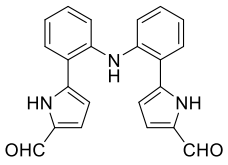

Compound **7a**, **GP2**, 2.6 mmol scale, yellow solid, 0.142 g, isolated yields of Suzuki-Miyaura, deprotection and Vilsmeyer-Haack formylation were equal to 48%, 94%, and 34% respectively. ^{1}H NMR (400 MHz, $CDCl_3$) δ ppm 10.20 (br. s, 2H), 9.48 (s, 2H), 7.49 (dd, *J* = 7.6, 1.6 Hz, 2H), 7.24 (ddd, *J* = 7.8, 7.6, 1.4 Hz, 2H), 7.09 (td, *J* = 7.6, 1.4 Hz, 2H), 7.01 (d, *J* = 8.2 Hz, 2H), 6.99 (dd, *J* = 3.9, 2.5 Hz, 2H), 6.55 (dd, *J* = 3.9, 2.5 Hz, 2H), 5.97 (br. s, 1H). ^{13}C NMR (101 MHz, $CDCl_3$) δ ppm 178.9, 140.6, 136.9, 133.1, 129.9, 129.6, 123.1, 122.9, 121.8, 120.5, 110.8. HRMS (m/z) found 378.1212 $[M+Na]^+$ (expected 378.1213 calcd for $C_{22}H_{17}N_3O_2$).

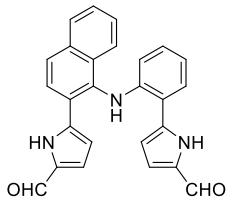

Compound **7b**. **GP2**, 2.9 mmol scale, yellow solid, 0.312 g, isolated yields of Suzuki-Miyaura, deprotection and Vilsmeyer-Haack formylation were equal to 31%, 99%, and 85% respectively. ^{1}H NMR (400 MHz, $CDCl_3$) δ ppm 10.61 (br. s, 1H), 10.45 (br. s, 1H), 9.60 (s, 1H), 9.43 (s, 1H), 7.84-7.93 (m, 3H), 7.80 (d, *J* = 8.7 Hz, 1H), 7.47-7.58 (m, 2H), 7.44 (d, *J* = 7.8 Hz, 1H), 7.11-7.15 (m, 1H), 7.03 (t, *J* = 7.8 Hz, 1H), 6.94-6.98 (m, 1H), 6.91 (t, *J* = 7.4 Hz, 1H), 6.72-6.77 (m, 1H), 6.66-6.72 (m, 1H), 6.29 (d, *J* = 8.2 Hz, 1H), 6.17 (s, 1H). ^{13}C NMR (101 MHz, $CDCl_3$) δ ppm 179.1, 144.0, 137.8, 136.6, 134.3, 133.7, 133.0, 132.9, 131.5, 130.4, 130.3, 128.5, 127.5, 127.0, 125.6, 125.1, 123.1, 122.0, 121.8, 120.2, 118.9, 113.9, 111.6, 111.3. HRMS (m/z) found 406.1532 $[M+H]^+$ (expected 406.1550 calcd for $C_{26}H_{19}N_3O_2$).

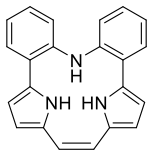

Compound **1a**. **GP3**, 1.1 mmol scale, yellow solid, 0.161 g, isolated yield was equal to 44%. ^{1}H NMR (600 MHz, $CDCl_3$) δ ppm 8.40 (br. s, 2H), 7.58 (br. s, 1H), 7.40 (dd, *J* = 8.3, 0.5 Hz, 2H), 7.36 (dd, *J* = 8.3, 1.7 Hz, 2H), 7.23 (td, *J* = 7.8, 1.7 Hz, 2H), 6.94 (tdd, *J* = 7.8, 1.7, 0.5 Hz, 2H), 6.32 (s, 2H), 6.29 (td, *J* = 2.8, 0.3 Hz, 2H), 6.22 - 6.25 (*J* = 2.8, 0.3 Hz, 2H). ^{13}C NMR (151 MHz, $CDCl_3$) δ ppm 140.6, 130.6, 130.4, 129.6, 128.7, 123.6, 121.1, 117.5, 116.1, 112.4, 110.1. HRMS gave the mass of oxidized form **5a**.

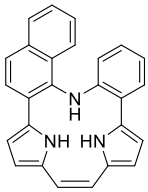

Compound **1b**. **GP3**, 0.14 mmol scale, yellow solid, 30 mg, isolated yield was equal to 57%. ^{1}H NMR (600 MHz, $CDCl_3$) δ ppm 8.92 (br. s, 1H), 7.98 (br. s, 1H), 7.89 (d, *J* = 8.3 Hz, 1H), 7.84 (d, *J* = 8.3 Hz, 1H), 7.80 (d, *J* = 8.6 Hz, 1H), 7.75 (d, *J* = 8.6 Hz, 1H), 7.50 (ddd, *J* = 8.3, 6.9, 1.4 Hz, 1H), 7.45 (ddd, *J* = 8.3, 6.9, 1.4 Hz, 1H), 7.29 (dd, *J* = 7.5, 1.5 Hz, 1H), 6.97 (ddd, *J* = 8.6, 7.5, 1.5 Hz, 1H), 6.80 (td, *J* = 7.5, 1.0 Hz, 1H), 6.51 (dd, *J* = 3.4, 2.7 Hz, 1H), 6.43 (d, *J* = 11.5 Hz, 1H), 6.36-6.41 (m, 2H), 6.34 (t, *J* = 2.9 Hz, 1H), 6.29 (t, *J* = 2.7 Hz, 1H), 6.25 (dd, *J* = 8.6, 1.0 Hz, 1H), 5.96 (s, 1H). ^{13}C NMR (151 MHz, $CDCl_3$) δ ppm 146.5, 133.6, 132.6, 131.9, 131.1, 130.1, 130.0, 129.5, 128.8, 128.3, 127.9, 127.4, 126.8, 126.4, 126.0, 125.3, 121.6, 119.0, 118.1, 116.3, 114.3, 111.5, 111.3, 109.9, 108.2. HRMS gave the mass of oxidized form **5b**.

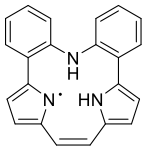

Compound **2a**. **GP4**, 5.0 mmol scale, EPR spectrum was measured without any purification. The value of g_{iso} is equal to 2.0025.

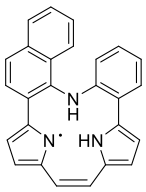

Compound **2b**. **GP4**, 5.0 mmol scale, EPR spectrum was measured without any purification. The value of g_{iso} is equal to 2.0025.

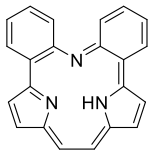

Compound **3a**. **GP5**, 5.4 μmol scale in deuterated chloroform. NMR spectra were measured without any purification due to high sensitivity of the compound (decomposes after evaporation). ^{1}H NMR (600 MHz, $CDCl_3$) δ ppm 9.55 (dd, *J* = 8.6, 1.3 Hz, 2H), 9.38 (d, *J* = 8.9 Hz, 2H), 9.31 (br. s, 1H), 9.05 (d, *J* = 4.3 Hz, 2H), 8.81 (s, 2H), 8.50 (dd, *J* = 4.4, 0.5 Hz, 2H), 8.01 (ddd, *J* = 8.9, 6.5, 1.3 Hz, 2H), 7.87 (ddd, *J*=8.6, 6.6, 0.8 Hz, 2 H). ^{13}C NMR (151 MHz, $CDCl_3$) δ ppm 150.8, 148.1, 147.2, 130.2, 129.3, 127.5, 126.4, 123.2, 122.8, 119.4, 118.0. HRMS (m/z) found 322.1335 $[M+H]^+$ (expected 322.1339 calcd for $C_{22}H_{15}N_3$).

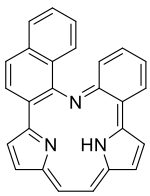

Compound **3b**. **GP5**, 0.11 mmol sale, dark green solid, 39 mg, isolated yield was equal to 98%. ^{1}H NMR (600 MHz, $CDCl_3$) δ ppm 10.80 (br. s, 1H), 9.37 (d, *J* = 8.5 Hz, 1H), 8.94 (d, *J* = 9.1 Hz, 1H), 8.84 (d, *J* = 4.5 Hz, 1H), 8.82 (d, *J* = 4.3 Hz, 1H), 8.73 (d, *J* = 10.3 Hz, 1H), 8.52 (d, *J* = 8.7 Hz, 1H), 8.37-8.42 (m, 2H), 8.35 (d, *J* = 10.3 Hz, 1H), 8.28 (d, *J* = 4.5 Hz, 1H), 8.00 (d, *J* = 7.8 Hz, 1H), 7.88 (d, *J* = 9.1 Hz, 1H), 7.74 (dd, *J* = 8.5, 7.0 Hz, 1H), 7.63 (dd, *J* = 7.8, 7.2 Hz, 1H), 7.53 (ddd, *J* = 8.7, 7.0, 1.0 Hz, 1H), 7.27-7.31 (m, 1H). ^{13}C NMR (151 MHz, $CDCl_3$) δ ppm 154.6, 151.2, 146.8, 146.1, 145.2, 143.6, 131.8, 130.4, 129.4, 128.9, 128.4, 128.3, 127.1, 126.4, 126.2, 126.1, 125.6, 125.4, 123.8, 123.2, 122.9, 122.4, 122.1, 122.0, 120.0, 113.4. HRMS (m/z) found 372.1469 $[M+H]^+$ (expected 372.1495 calcd for $C_{26}H_{17}N_3$).

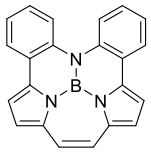

Compound **8a**. **GP6**, 10 µmol scale. NMR spectra were measured without any purification. ^{1}H NMR (400 MHz, $CDCl_3$) δ ppm 7.54 (d, *J* = 8.2 Hz, 2H), 7.43 (dd, *J* = 7.6, 1.6 Hz, 2H), 6.93-7.06 (m, 4H), 6.50 (d, *J* = 3.2 Hz, 2H), 6.15 (d, *J* = 3.2 Hz, 2H), 5.70 (s, 2H).

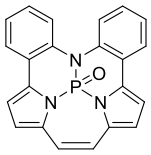

Compound **S1**. **GP6**, 10.0 µmol scale. NMR spectra were measured without any purification. ^{1}H NMR (400 MHz, $CDCl_3$) δ ppm 7.49 (dd, *J* = 7.8, 1.8 Hz, 2H), 7.43 (d, *J* = 8.2 Hz, 2H), 7.05-7.16 (m, 4H), 6.62 (t, *J* = 3.9 Hz, 2H), 6.27 (t, *J* = 3.9 Hz, 2H), 6.11 (s, 2H).

3. NMR Spectra

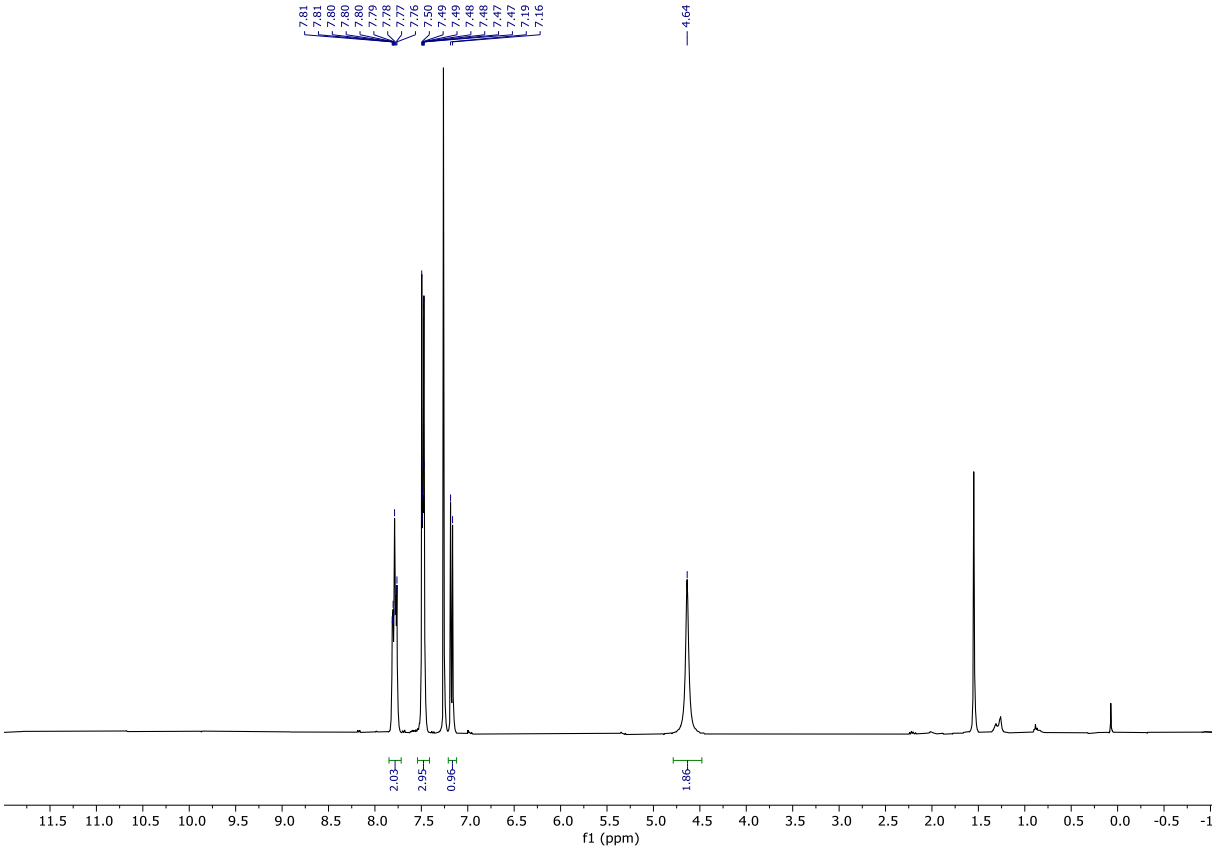

Figure S1. ^{1}H NMR spectrum of **4b** (400 MHz, $CDCl_3$, 293 K).

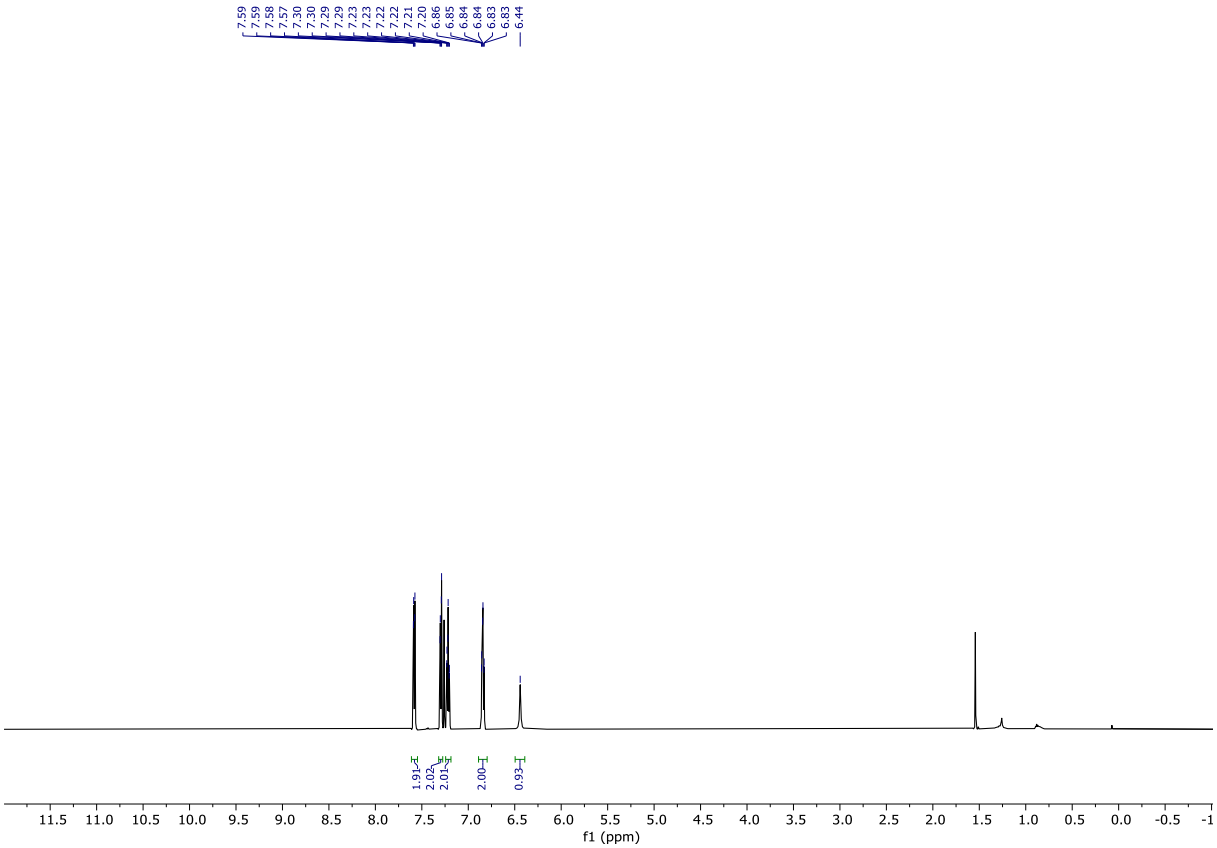

Figure S2. ^{1}H NMR spectrum of **6a** (600 MHz, $CDCl_3$, 293 K).

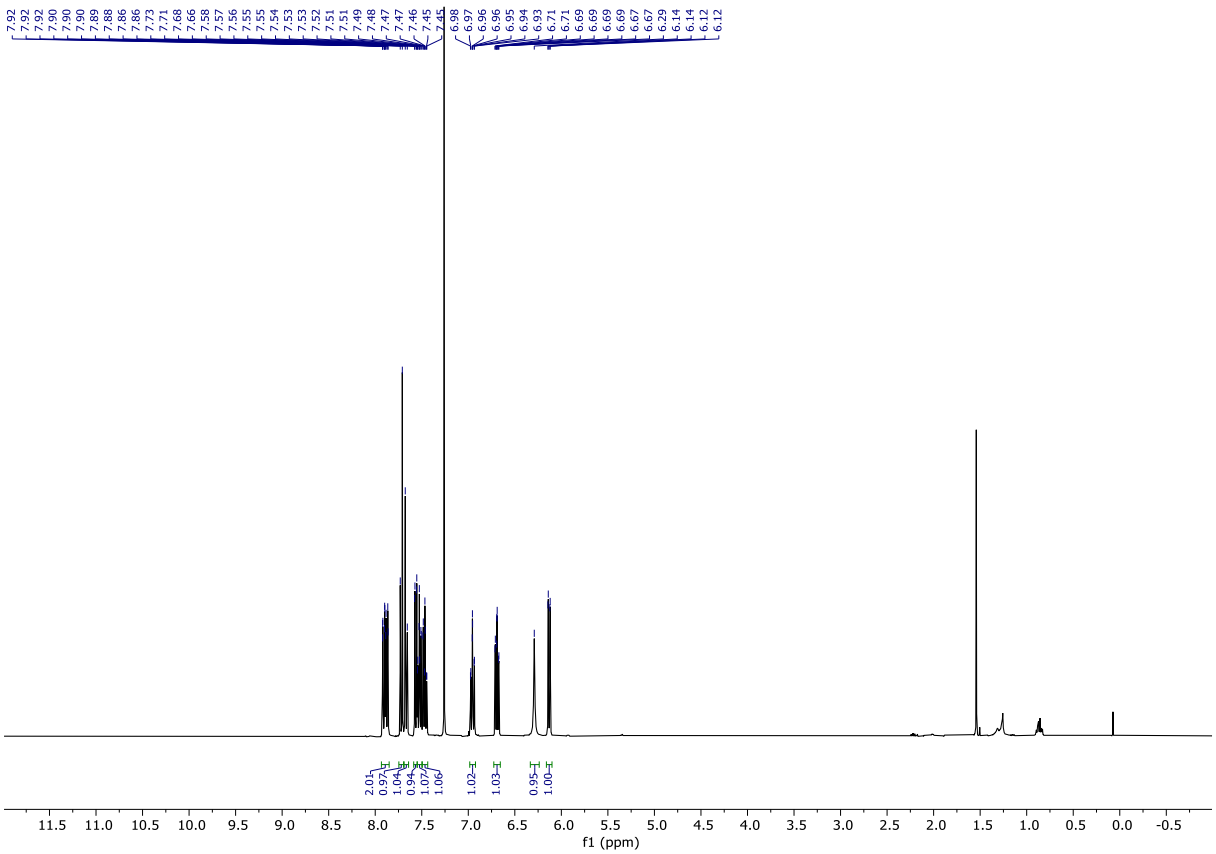

Figure S3. ^{1}H NMR spectrum of **6b** (400 MHz, $CDCl_3$, 293 K).

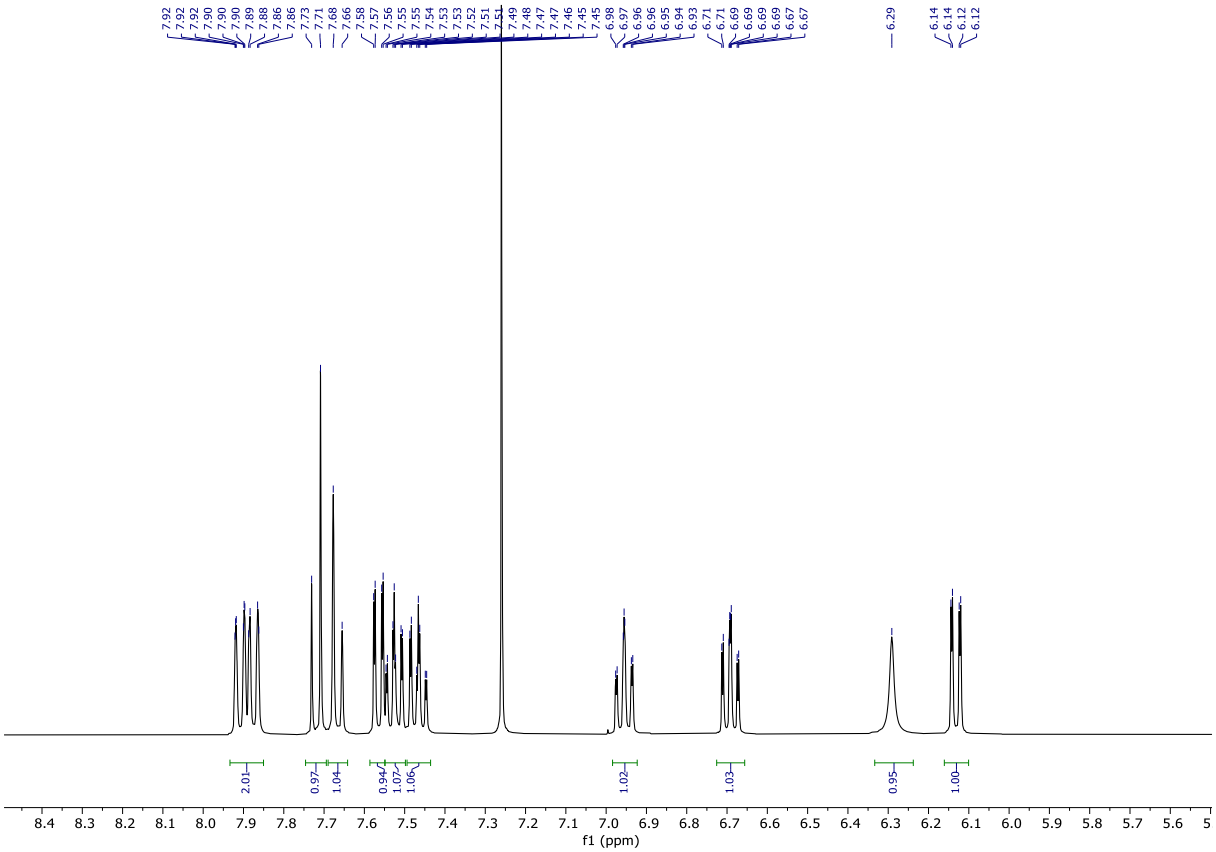

Figure S4. ^{1}H NMR spectrum of **6b** (400 MHz, $CDCl_3$, 293 K, 5.5 – 8.5 ppm region).

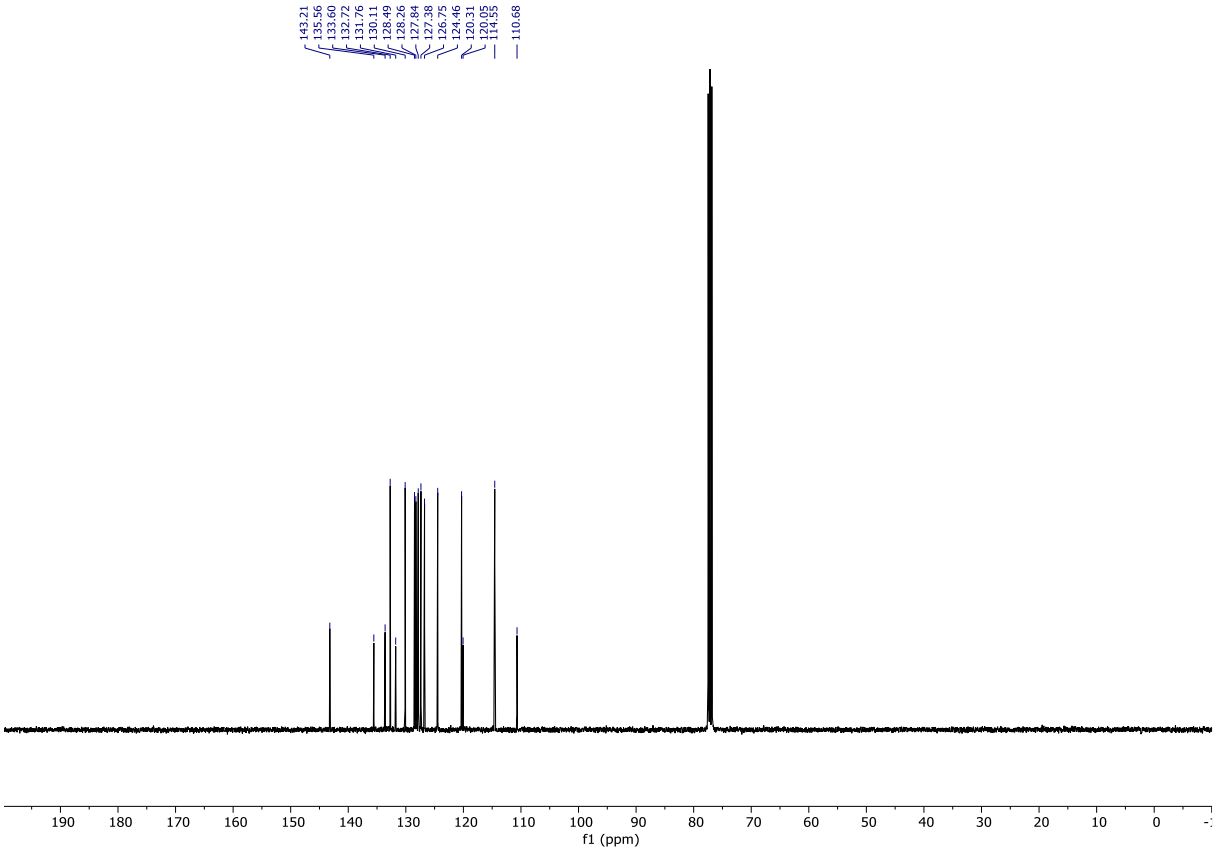

Figure S5. ^{13}C NMR spectrum of **6b** (101 MHz, $CDCl_3$, 293 K).

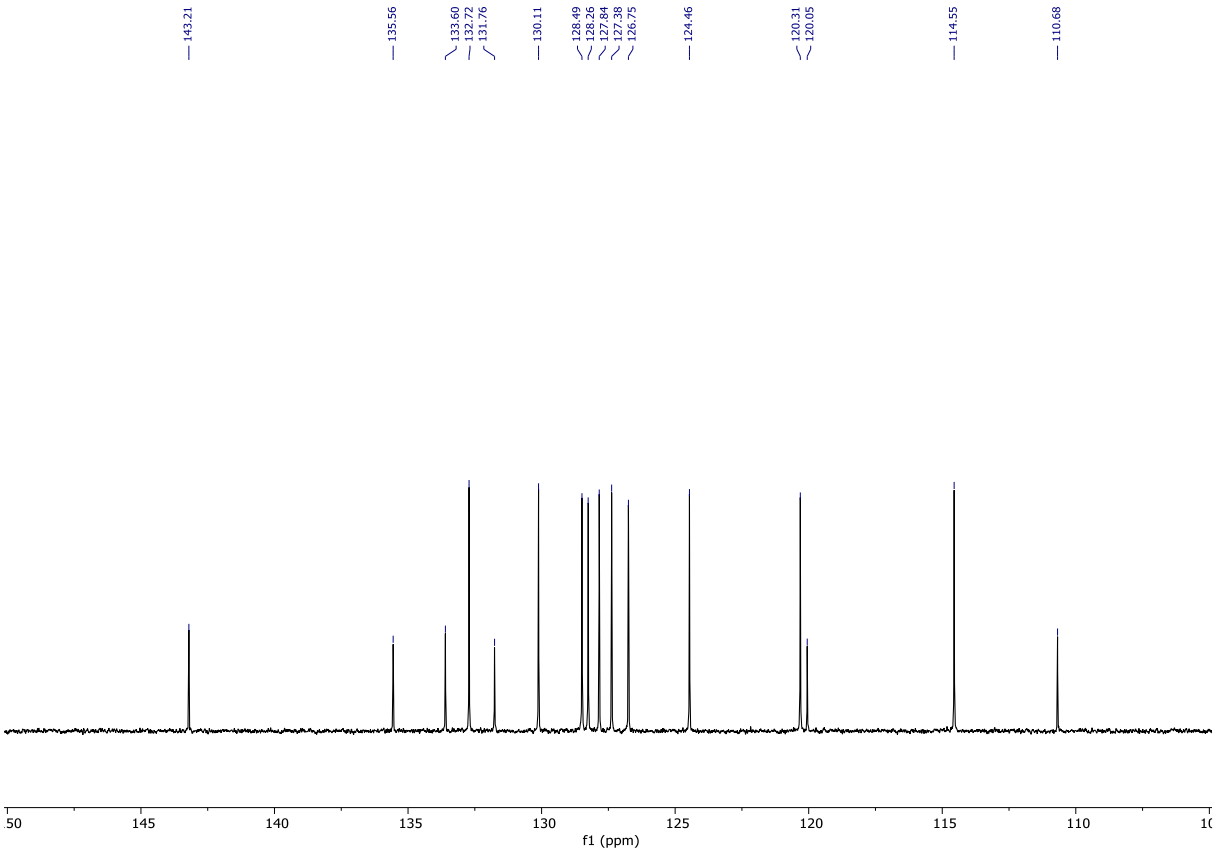

Figure S6. ^{13}C NMR spectrum of **6b** (101 MHz, $CDCl_3$, 293 K, 100 – 150 ppm region).

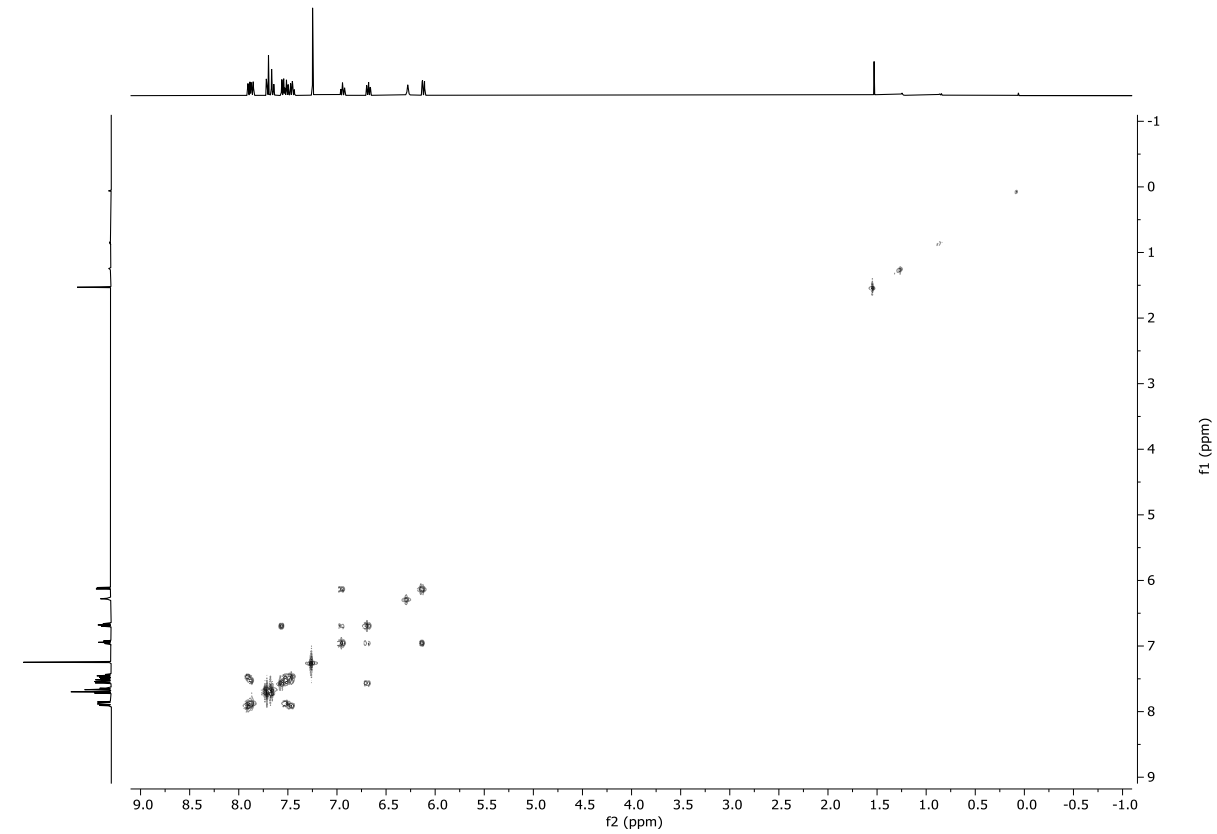

Figure S7. ^{1}H-^{1}H COSY spectrum of **6b** (400 MHz, $CDCl_3$, 293 K).

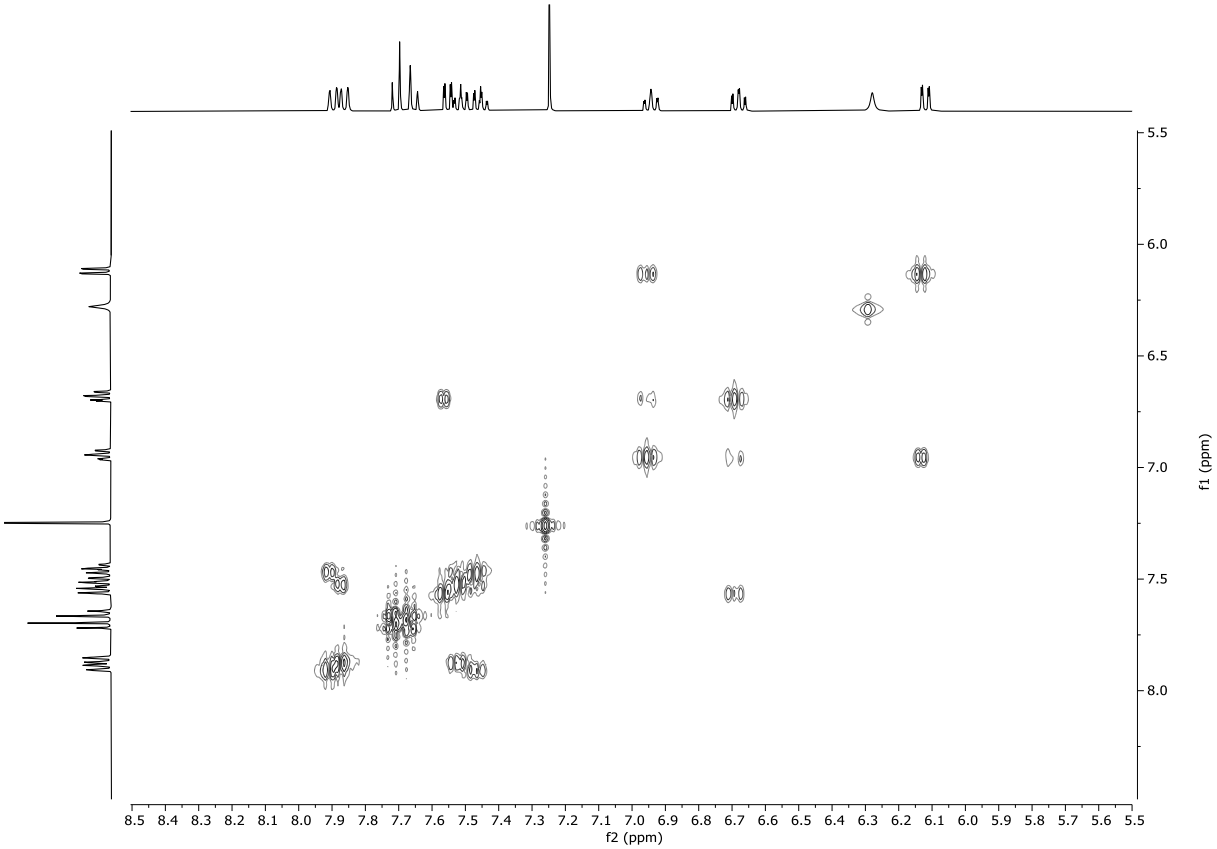

Figure S8. ^{1}H-^{1}H COSY spectrum of **6b** (400 MHz, $CDCl_3$, 293 K, 5.5 – 8.5 ppm region).

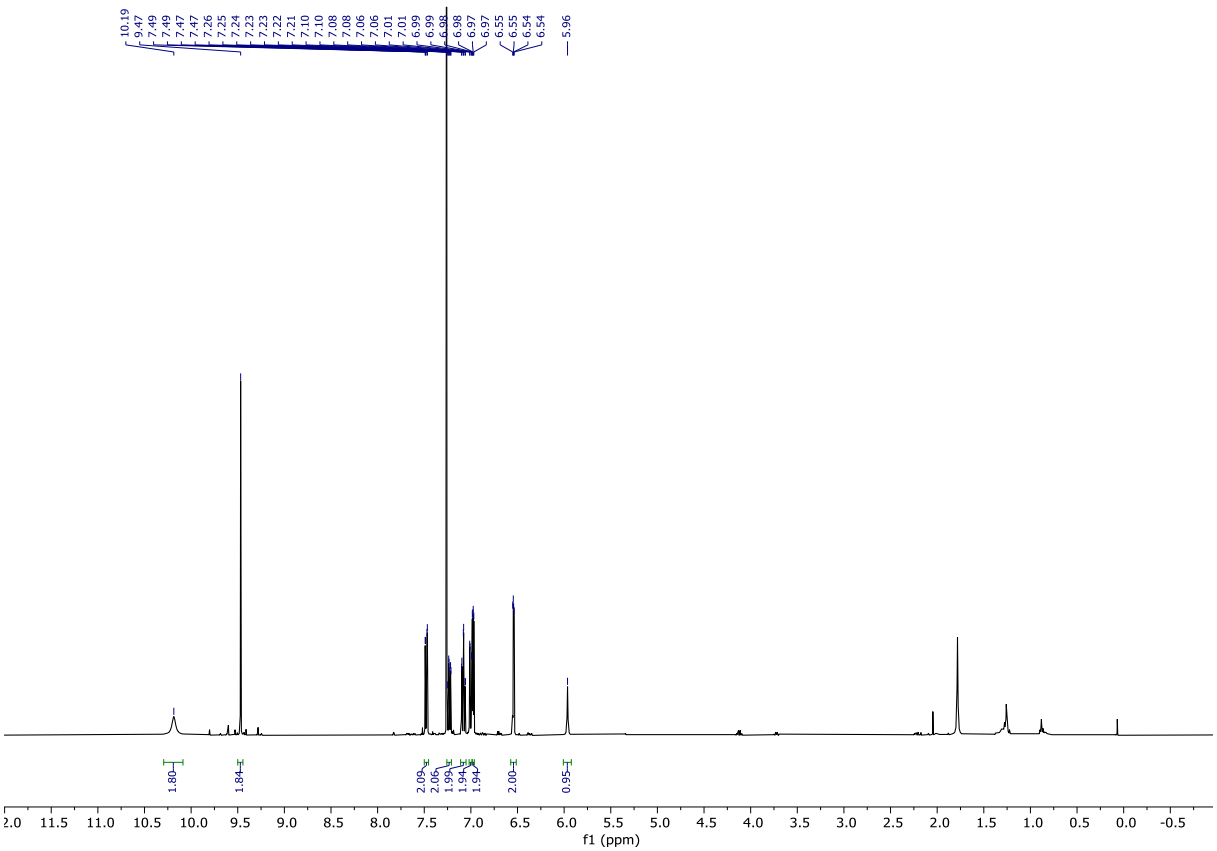

Figure S9. ^{1}H NMR spectrum of **7a** (400 MHz, $CDCl_3$, 293 K).

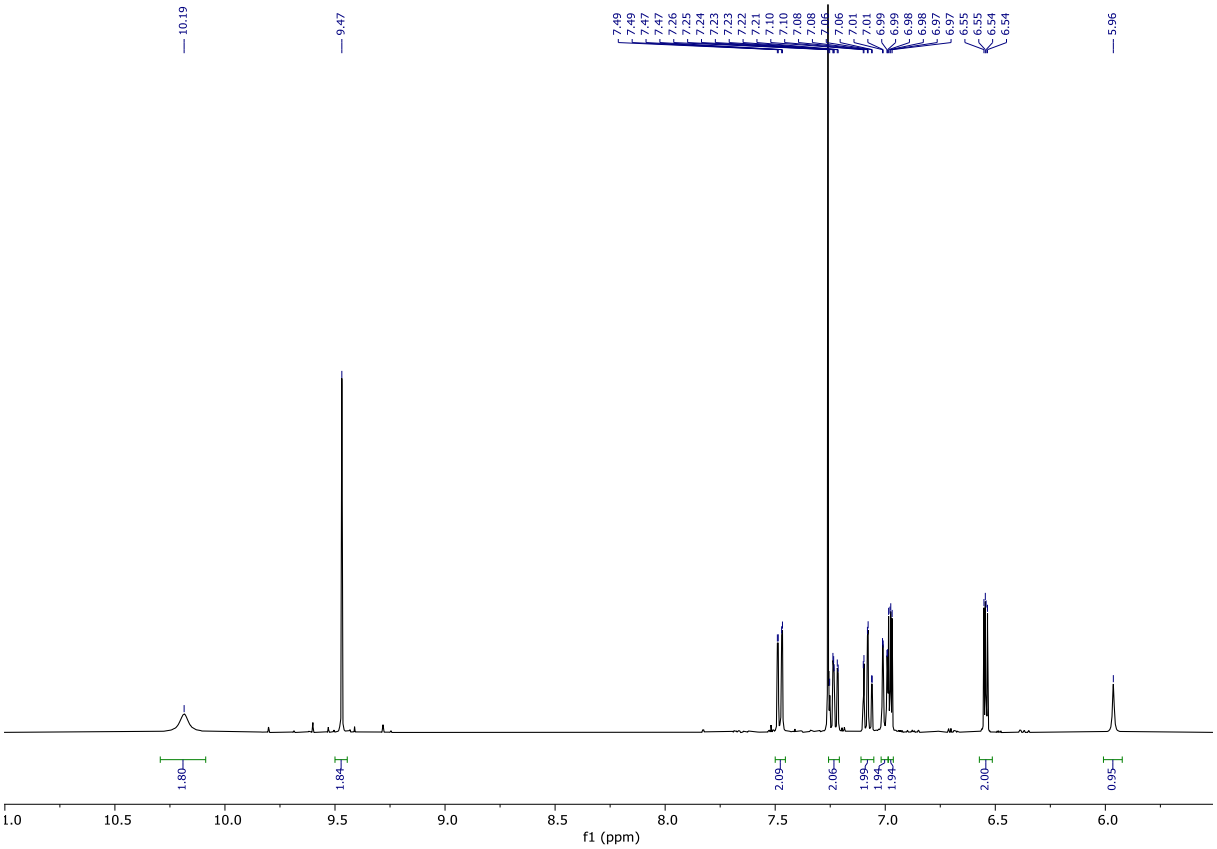

Figure S10. ^{1}H NMR spectrum of **7a** (400 MHz, $CDCl_3$, 293 K, 5.5 – 11.0 ppm region).

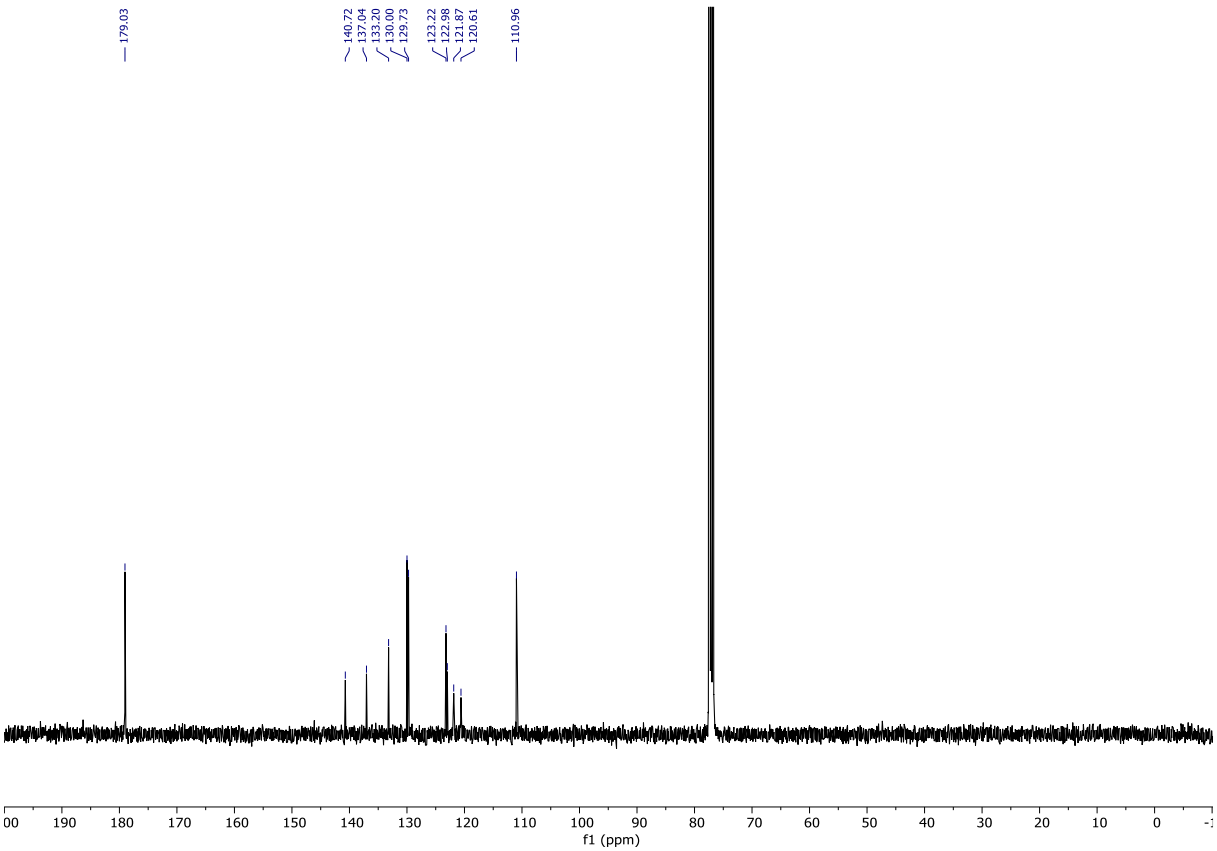

Figure S11. ^{13}C NMR spectrum of **7a** (101 MHz, $CDCl_3$, 293 K).

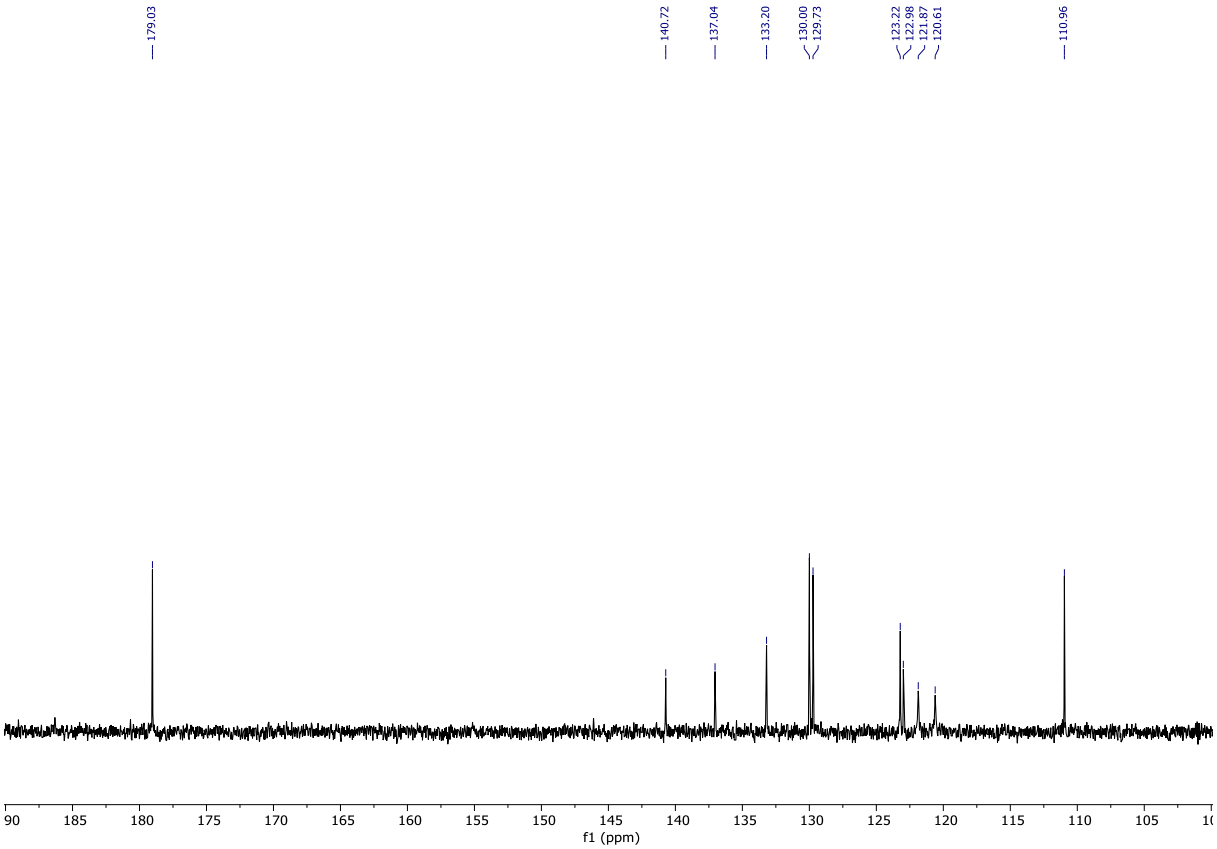

Figure S12. ^{13}C NMR spectrum of **7a** (101 MHz, $CDCl_3$, 293 K, 100 – 190 ppm region).

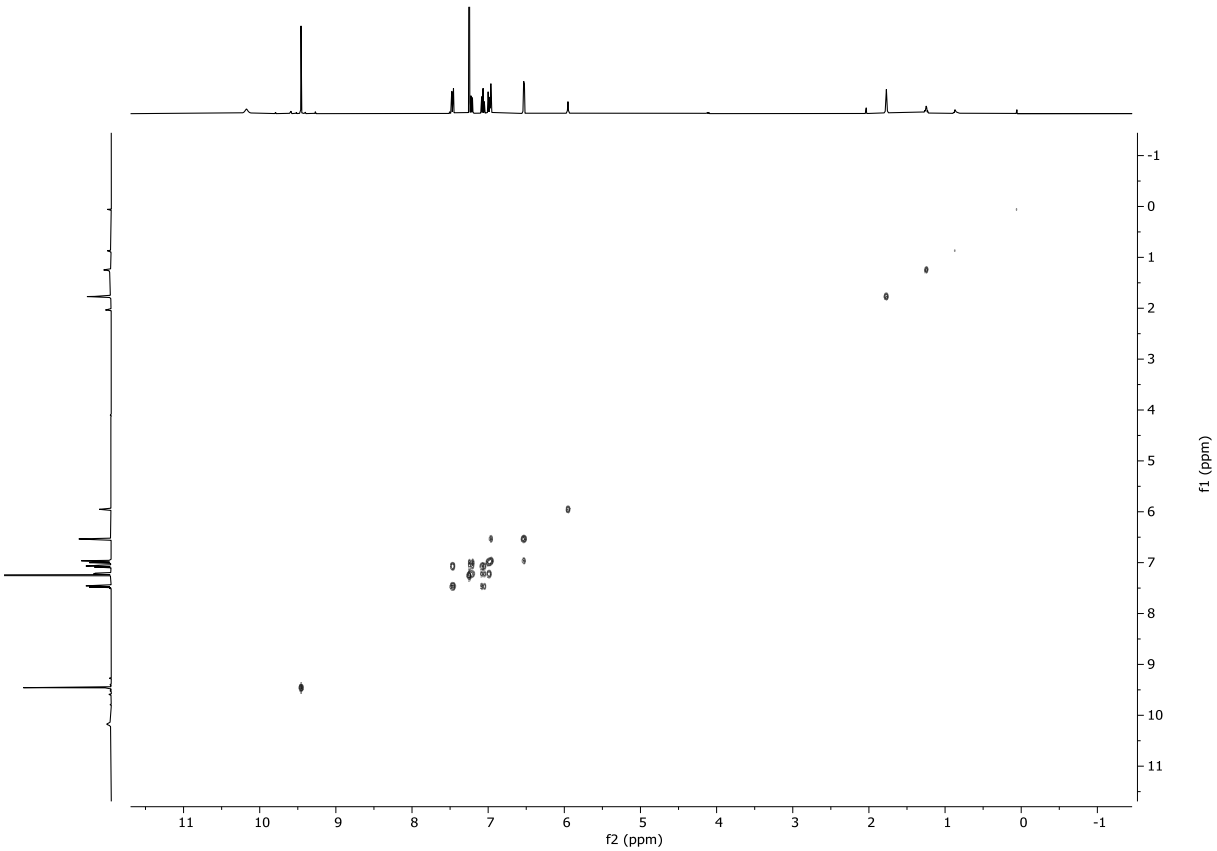

Figure S13. ^{1}H-^{1}H COSY spectrum of **7a** (400 MHz, $CDCl_3$, 293 K).

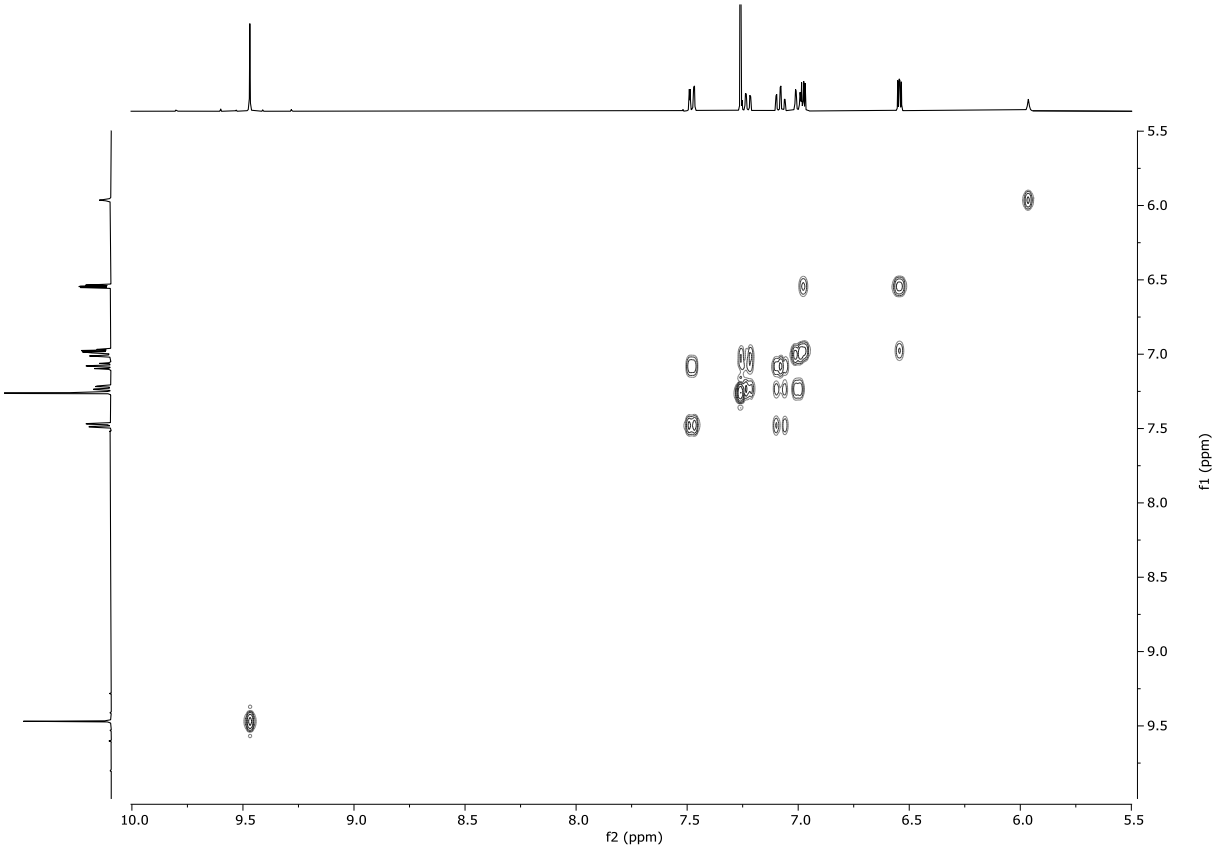

Figure S14. ^{1}H-^{1}H COSY spectrum of **7a** (400 MHz, $CDCl_3$, 293 K, 5.5 – 10.0 ppm region).

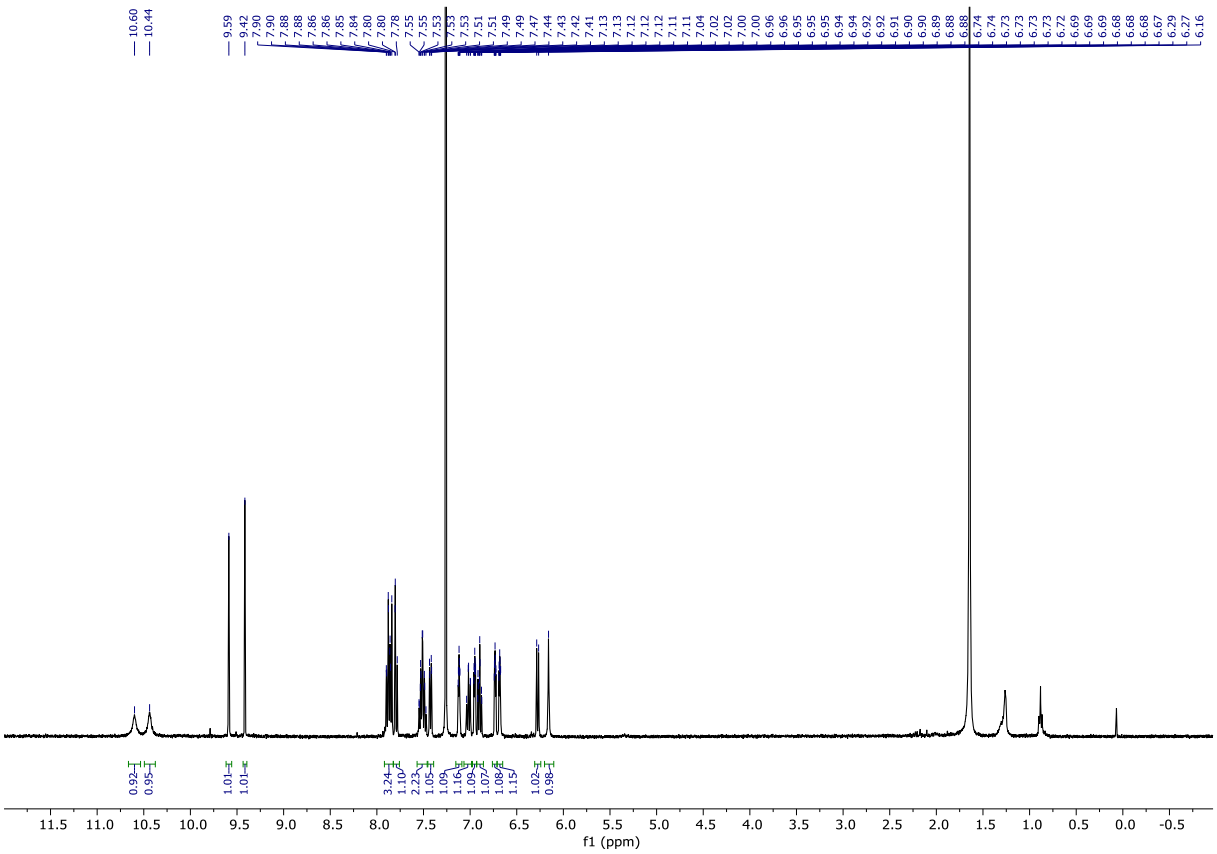

Figure S15. ^{1}H NMR spectrum of **7b** (400 MHz, $CDCl_3$, 293 K).

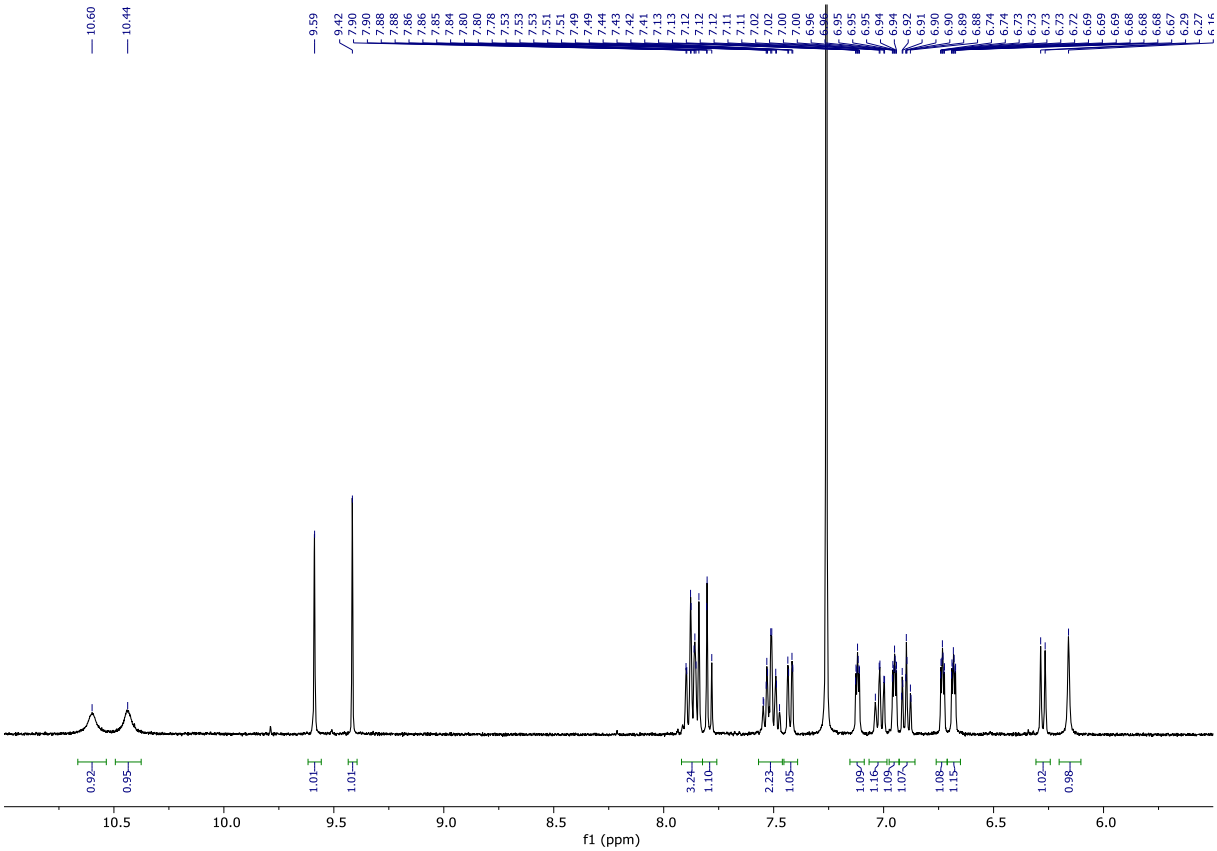

Figure S16. ^{1}H NMR spectrum of **7b** (400 MHz, $CDCl_3$, 293 K, 5.5 – 11.0 ppm region).

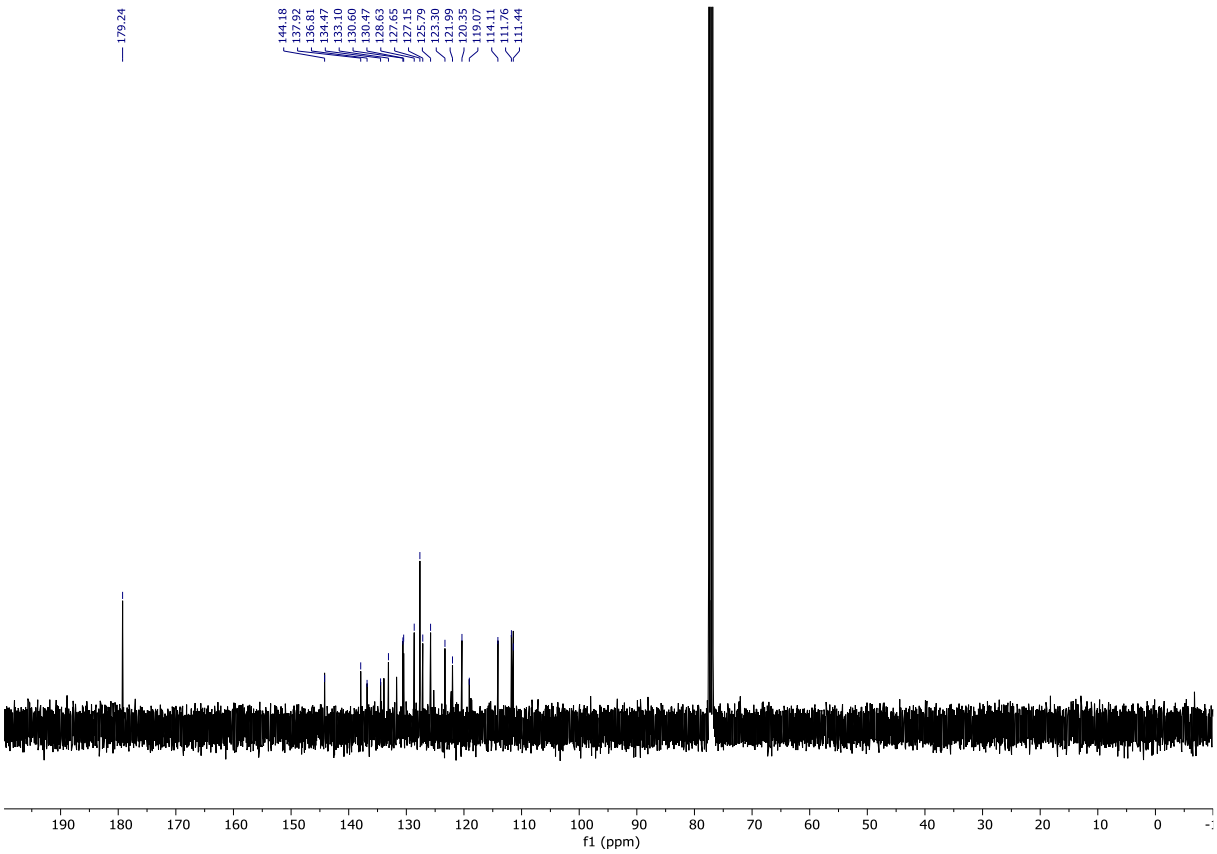

Figure S17. ^{13}C NMR spectrum of **7b** (101 MHz, $CDCl_3$, 293 K).

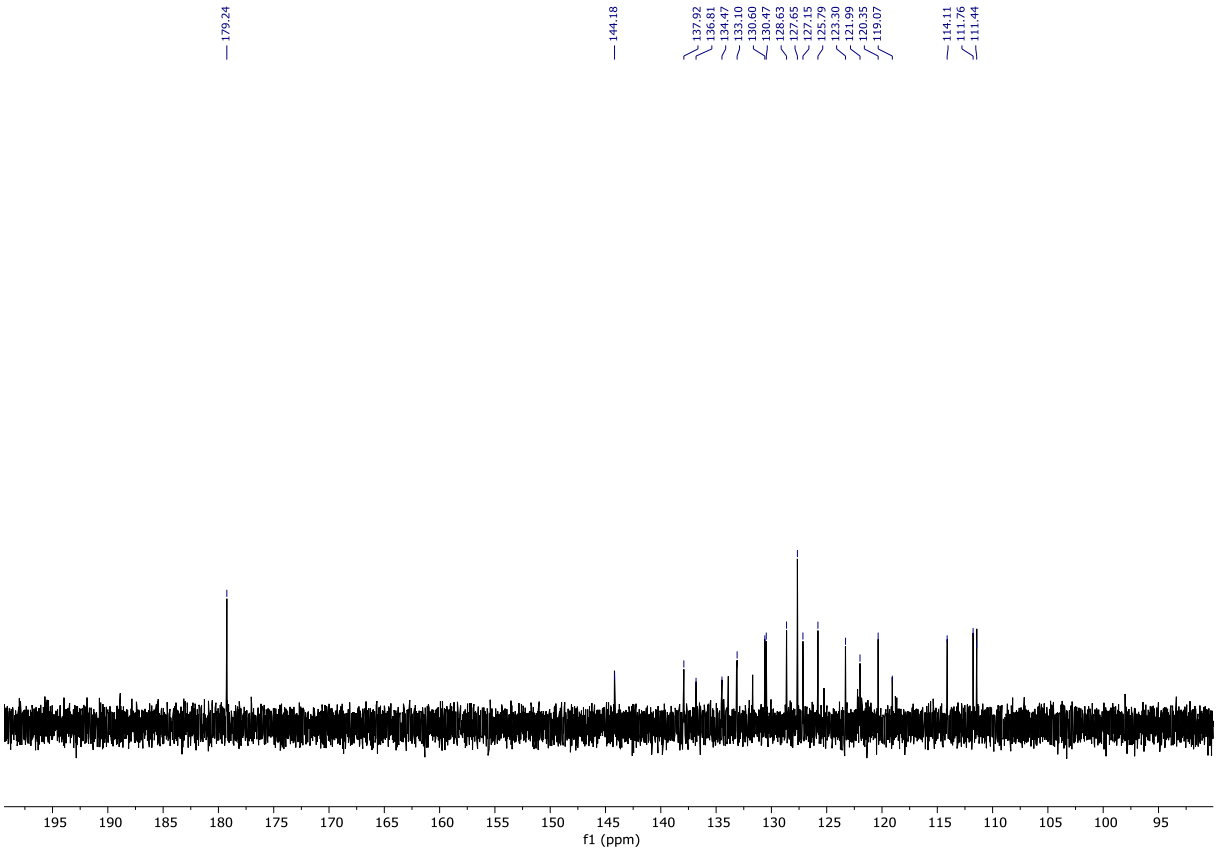

Figure S18. ^{13}C NMR spectrum of **7b** (101 MHz, $CDCl_3$, 293 K, 90 – 200 ppm region).

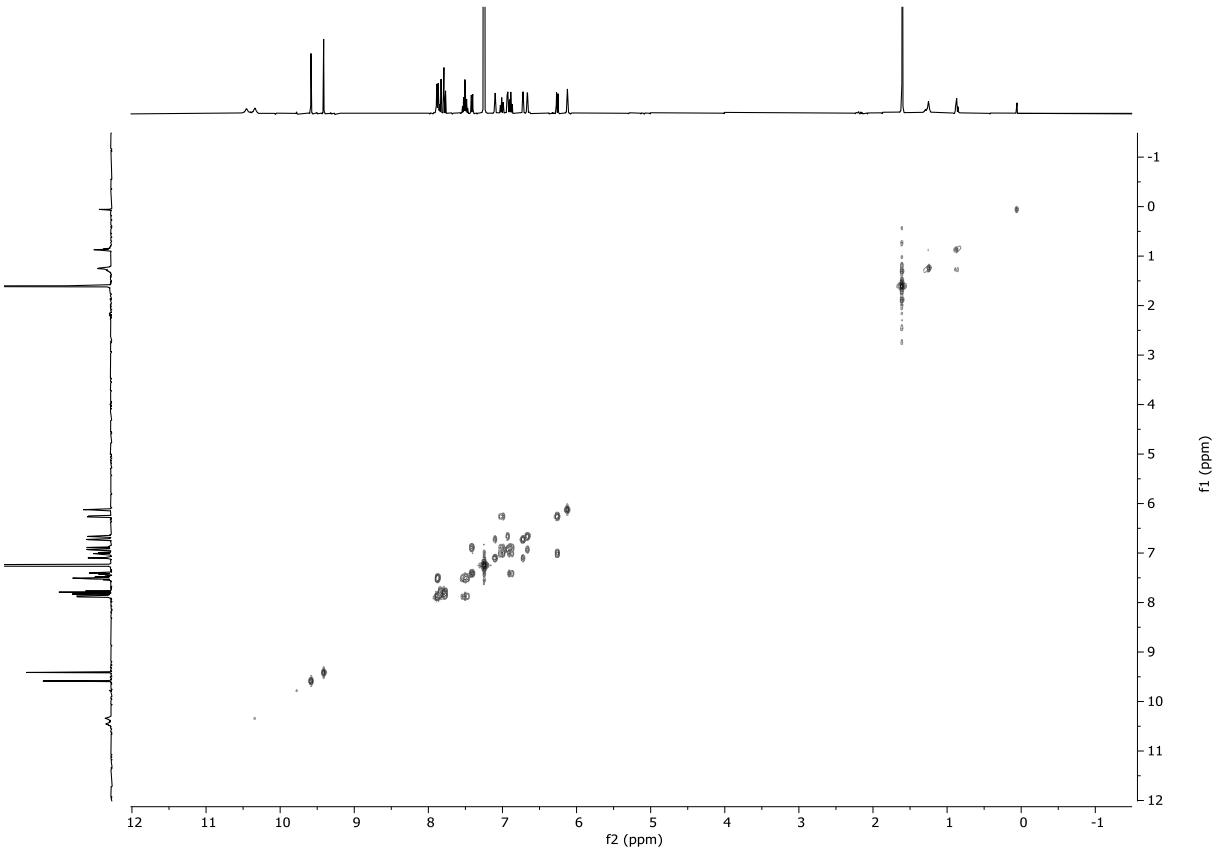

Figure S19. ^{1}H-^{1}H COSY spectrum of **7b** (400 MHz, $CDCl_3$, 293 K).

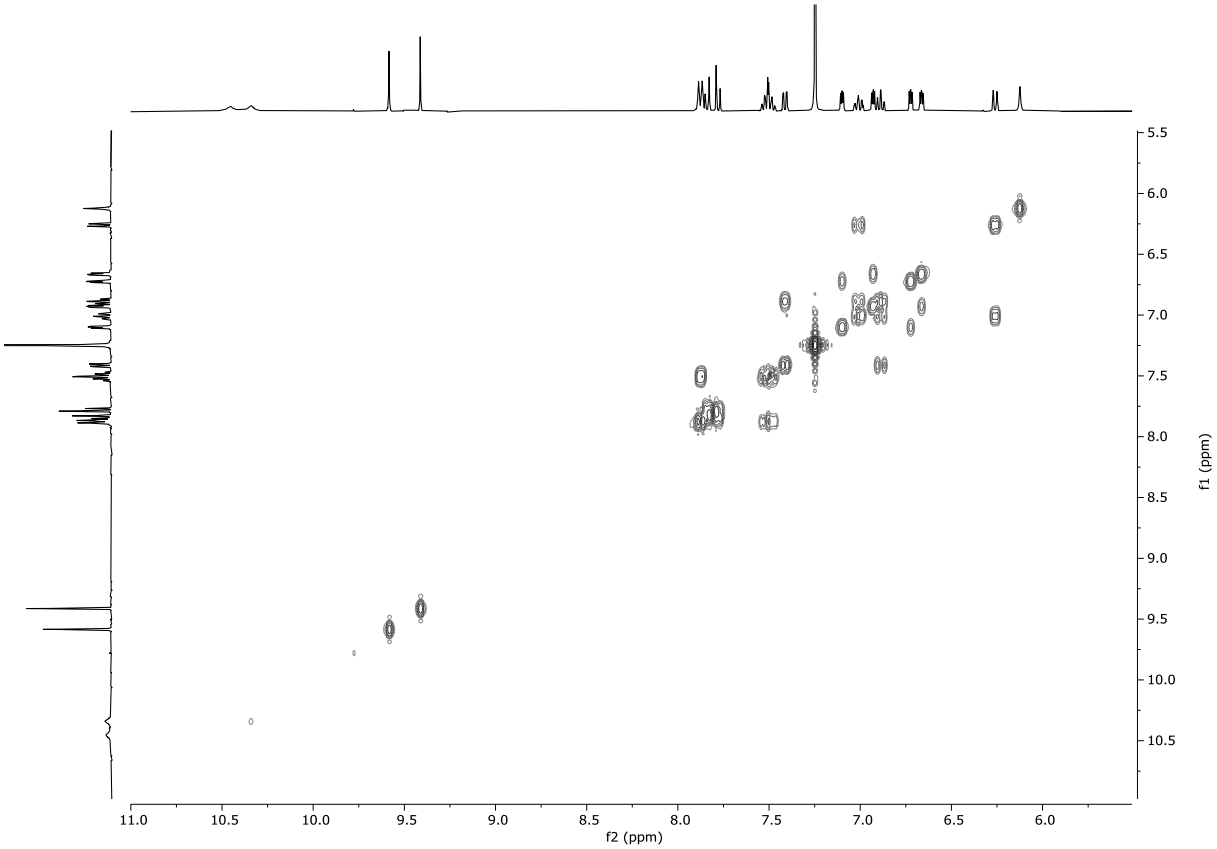

Figure S20. ^{1}H-^{1}H COSY spectrum of **7b** (400 MHz, $CDCl_3$, 293 K, 5.5 – 11.0 ppm region).

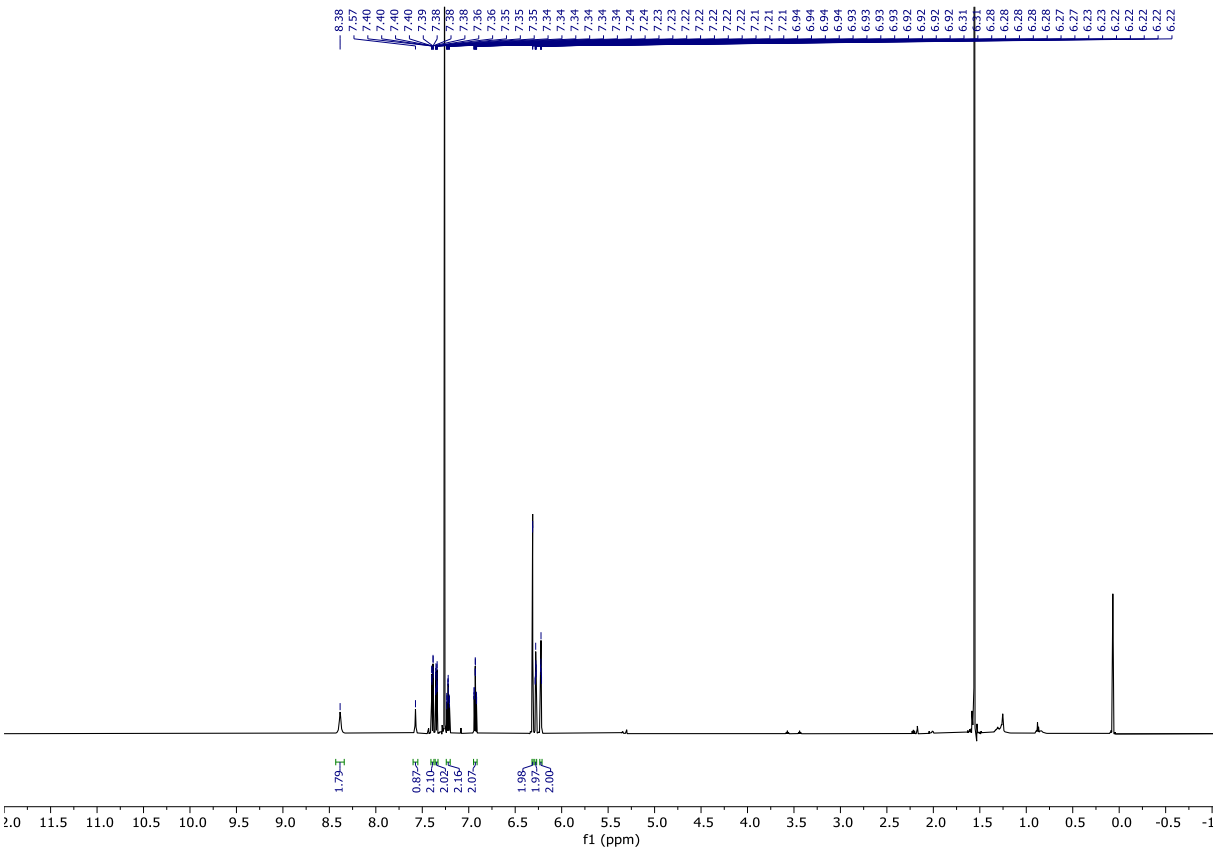

Figure S21. ^{1}H NMR spectrum of **1a** (600 MHz, $CDCl_3$, 293 K).

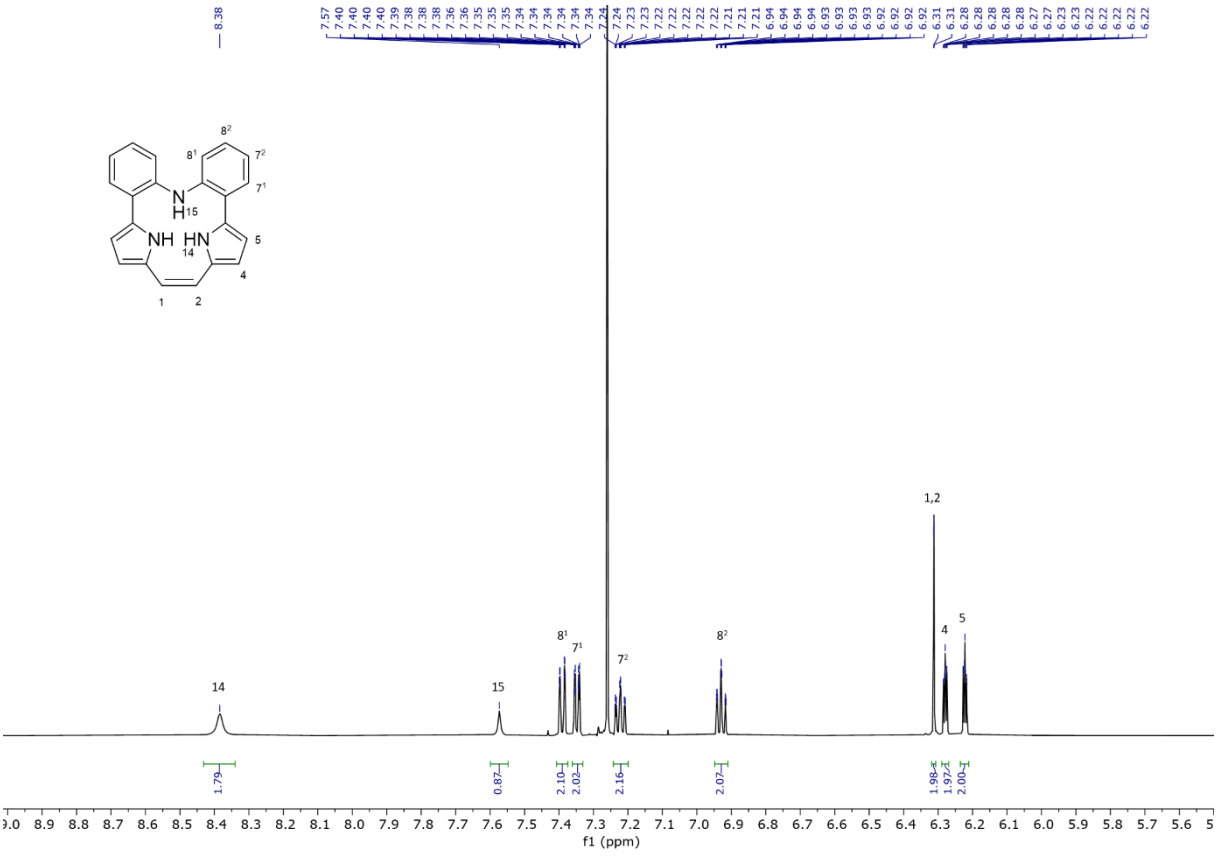

Figure S22. ^{1}H NMR spectrum of **1a** (600 MHz, $CDCl_3$, 293 K, 5.5 – 9.0 ppm region).

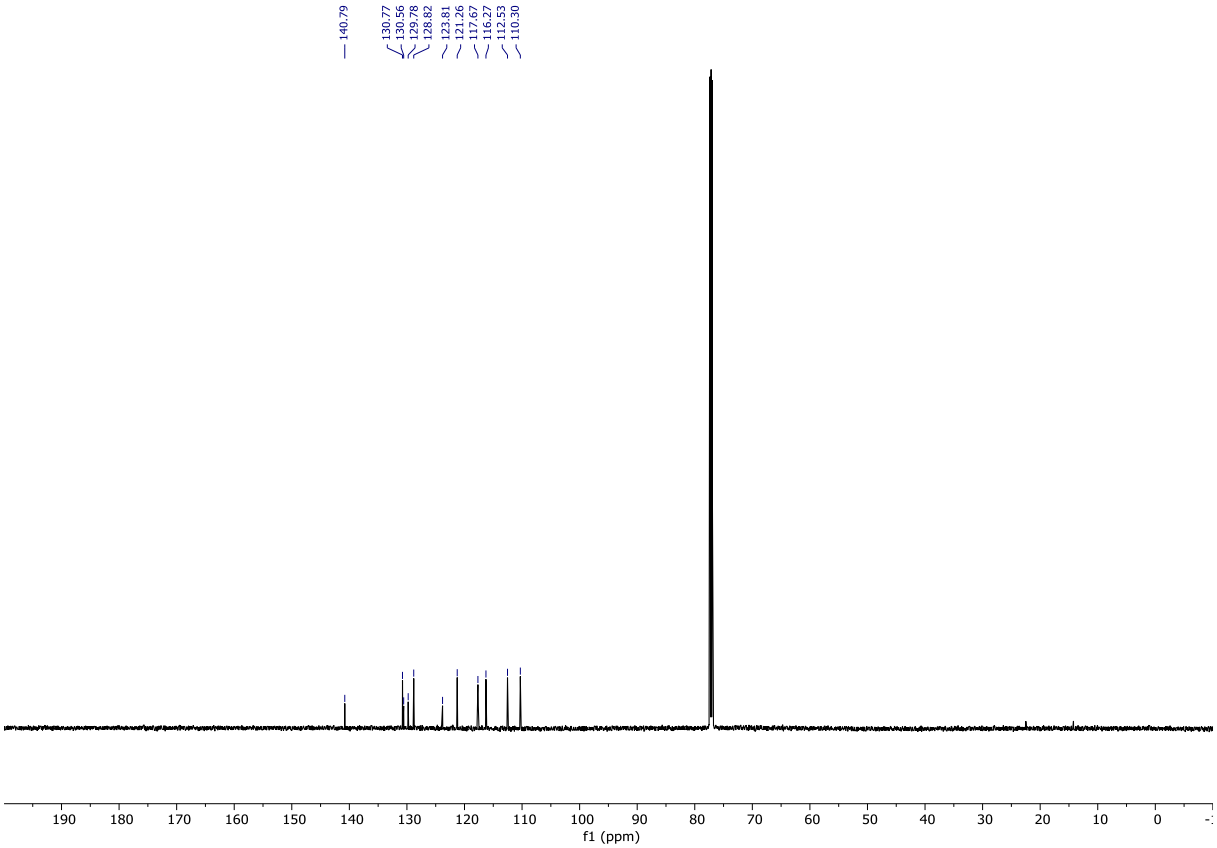

Figure S23. ^{13}C NMR spectrum of **1a** (151 MHz, $CDCl_3$, 293 K).

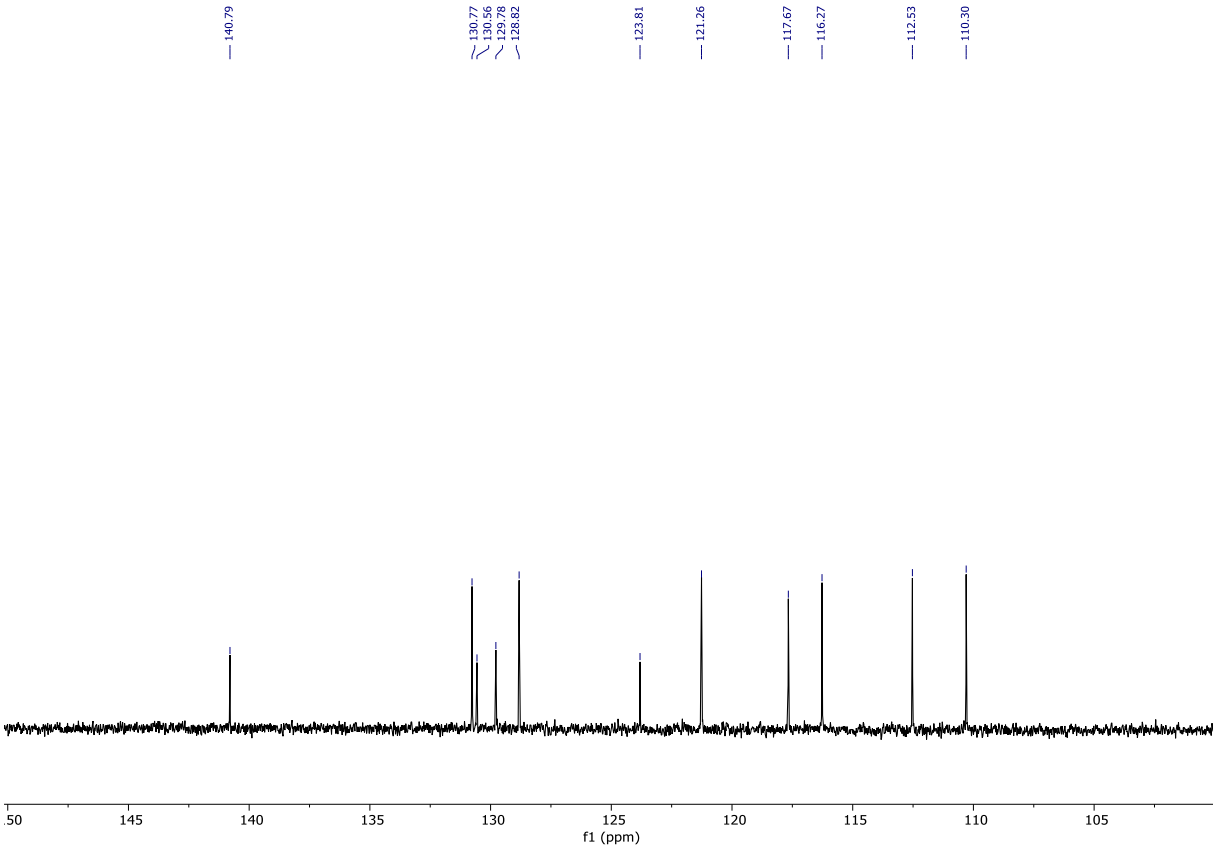

Figure S24. ^{13}C NMR spectrum of **1a** (151 MHz, $CDCl_3$, 293 K, 100 – 150 ppm region).

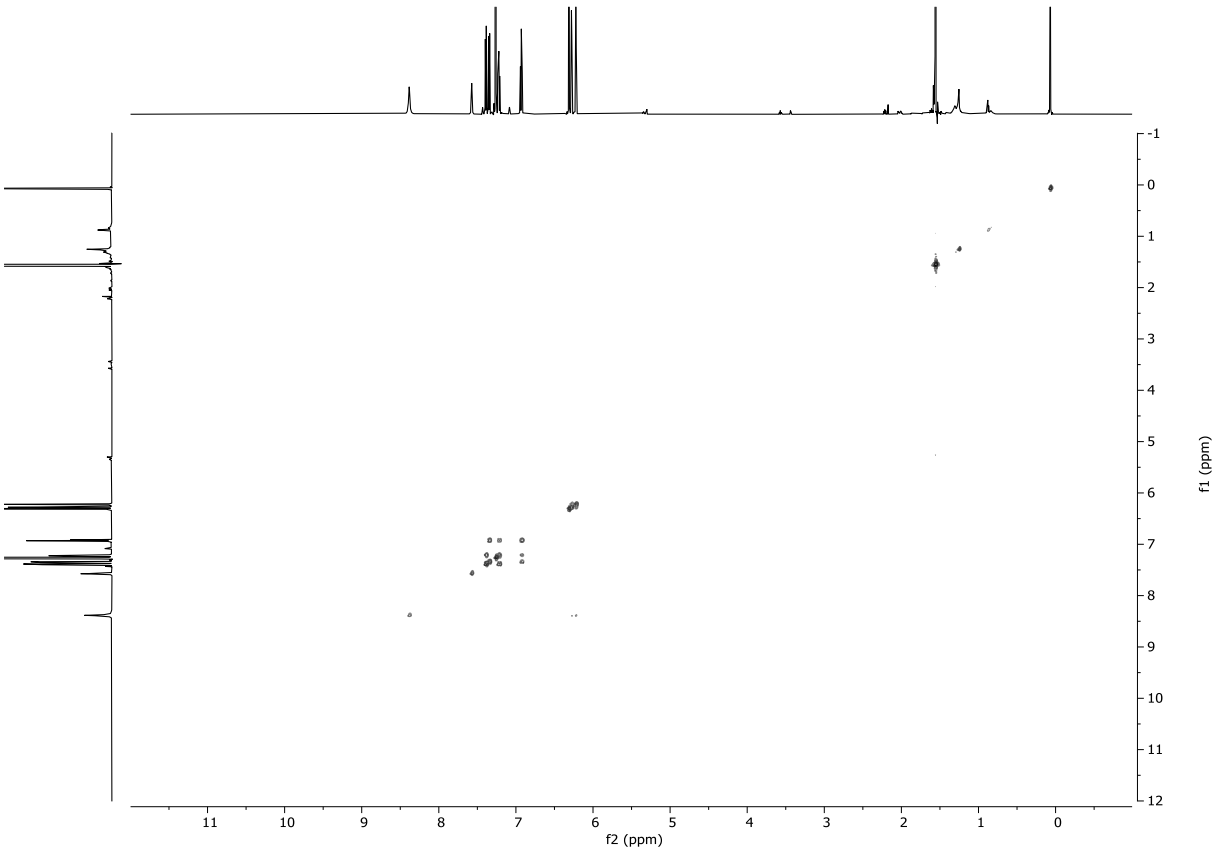

Figure S25. ^{1}H-^{1}H COSY spectrum of **1a** (600 MHz, $CDCl_3$, 293 K).

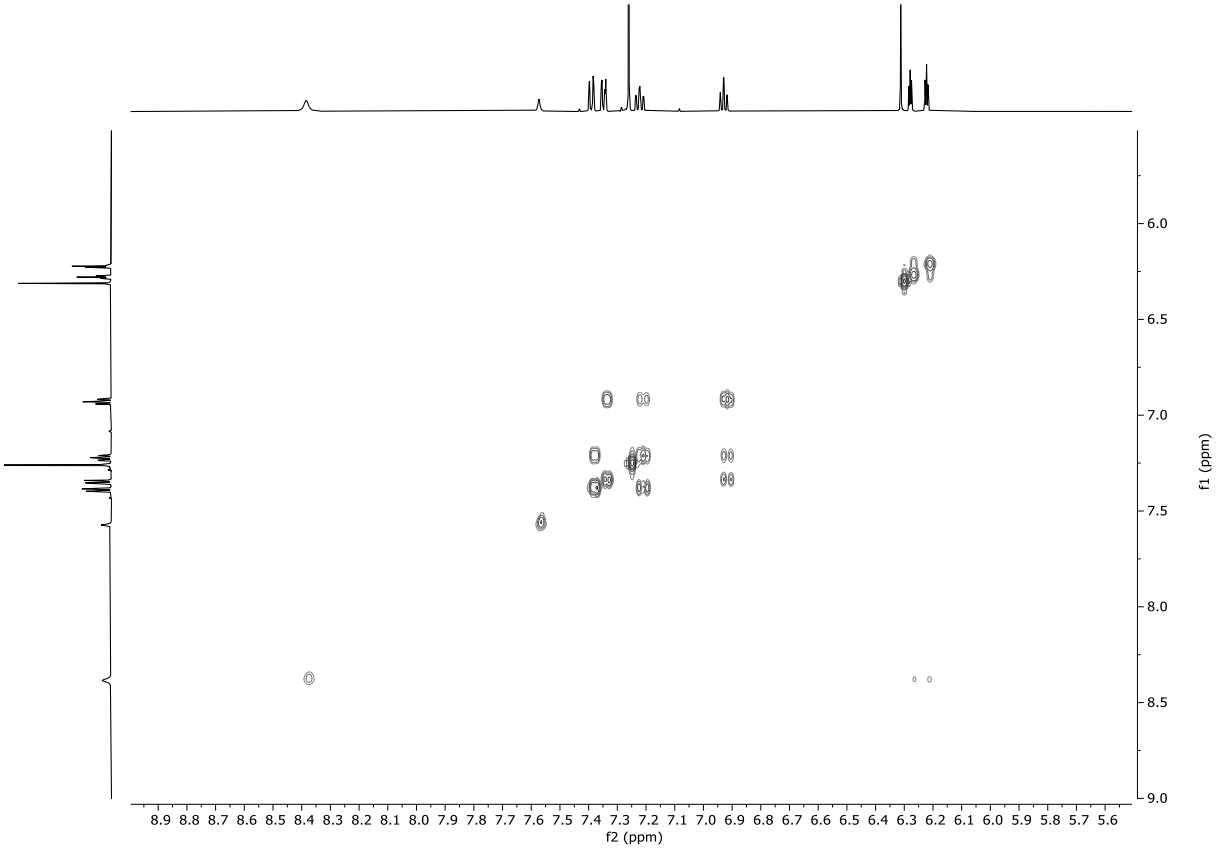

Figure S26. ^{1}H-^{1}H COSY spectrum of **1a** (600 MHz, $CDCl_3$, 293 K, 5.5 – 9.0 ppm region).

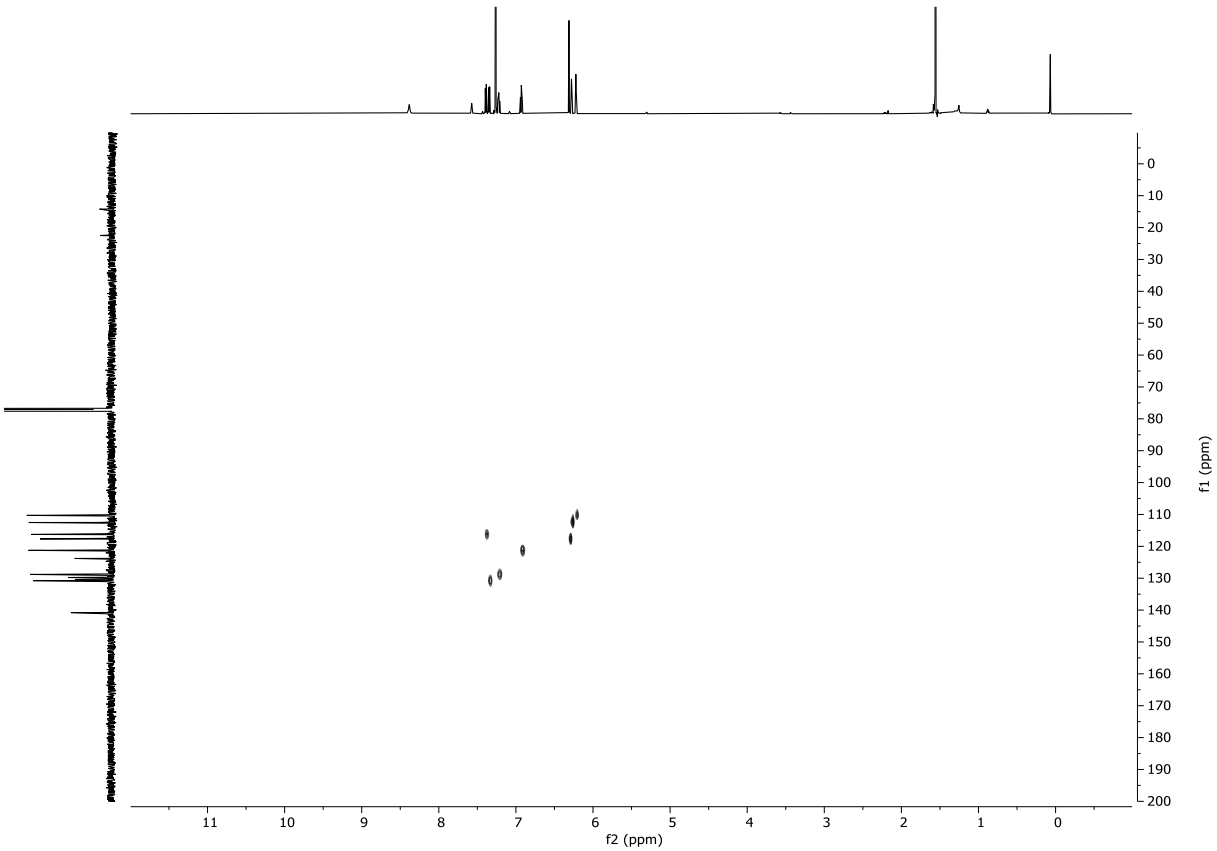

Figure S27. ^{1}H-^{13}C HSQC spectrum of **1a** (600 MHz, $CDCl_3$, 293 K).

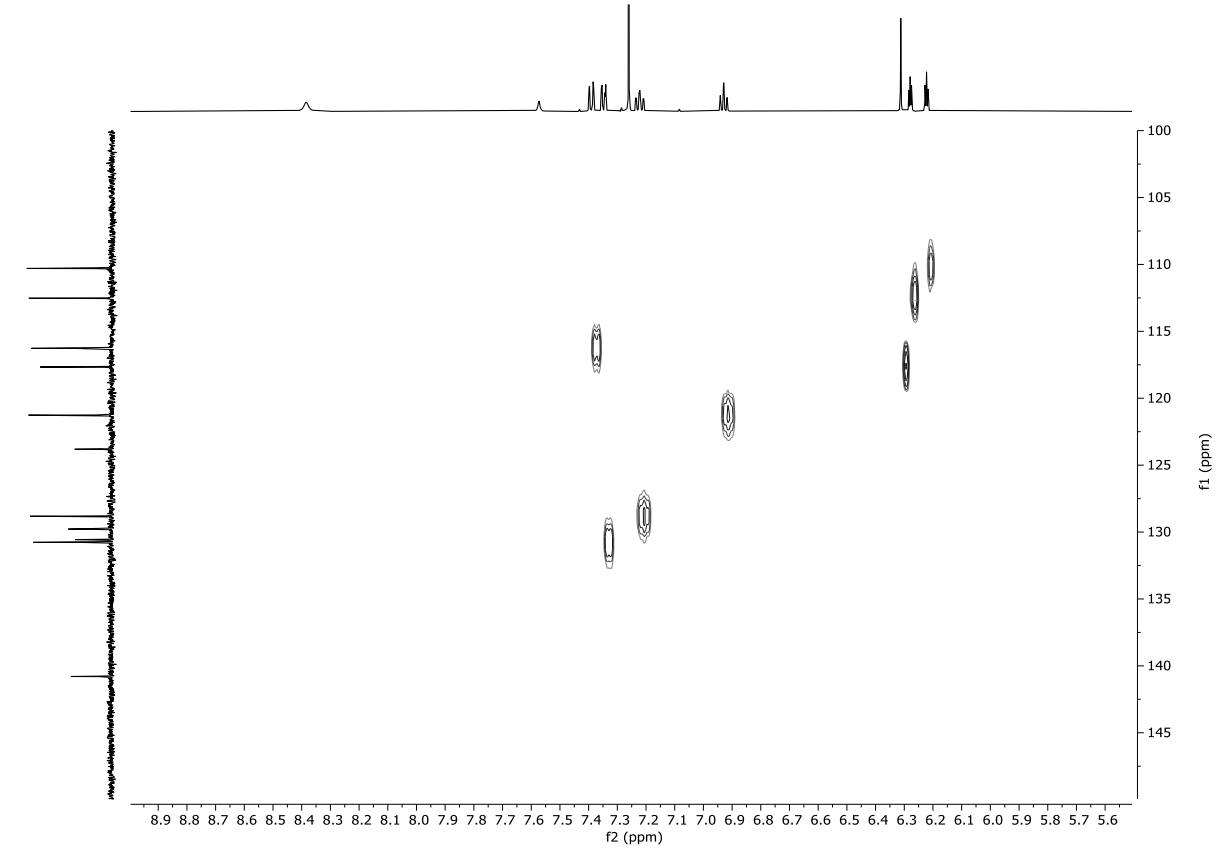

Figure S28. ^{1}H-^{13}C HSQC spectrum of **1a** (600 MHz, $CDCl_3$, 293 K, 5.5 – 9.0 & 100 – 150 ppm region).

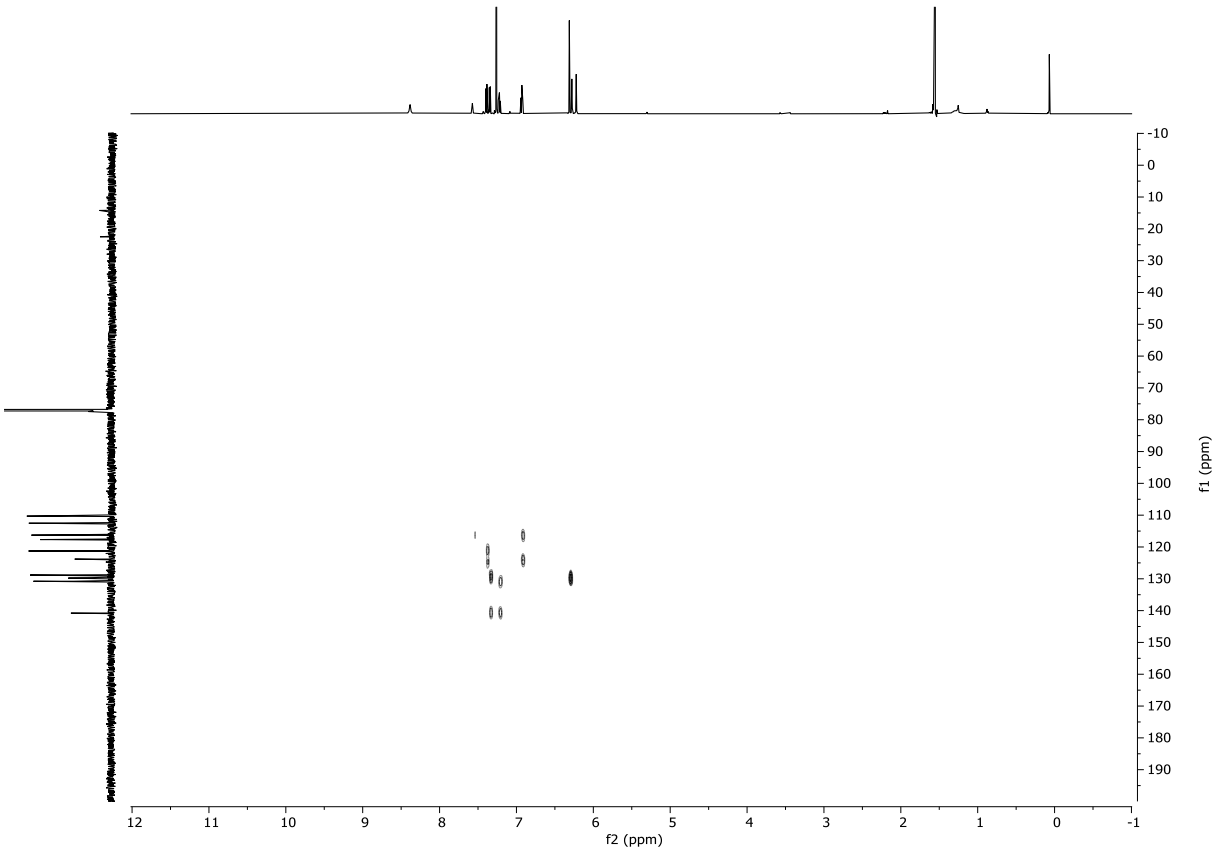

Figure S29. ^{1}H-^{13}C HMBC spectrum of **1a** (600 MHz, $CDCl_3$, 293 K).

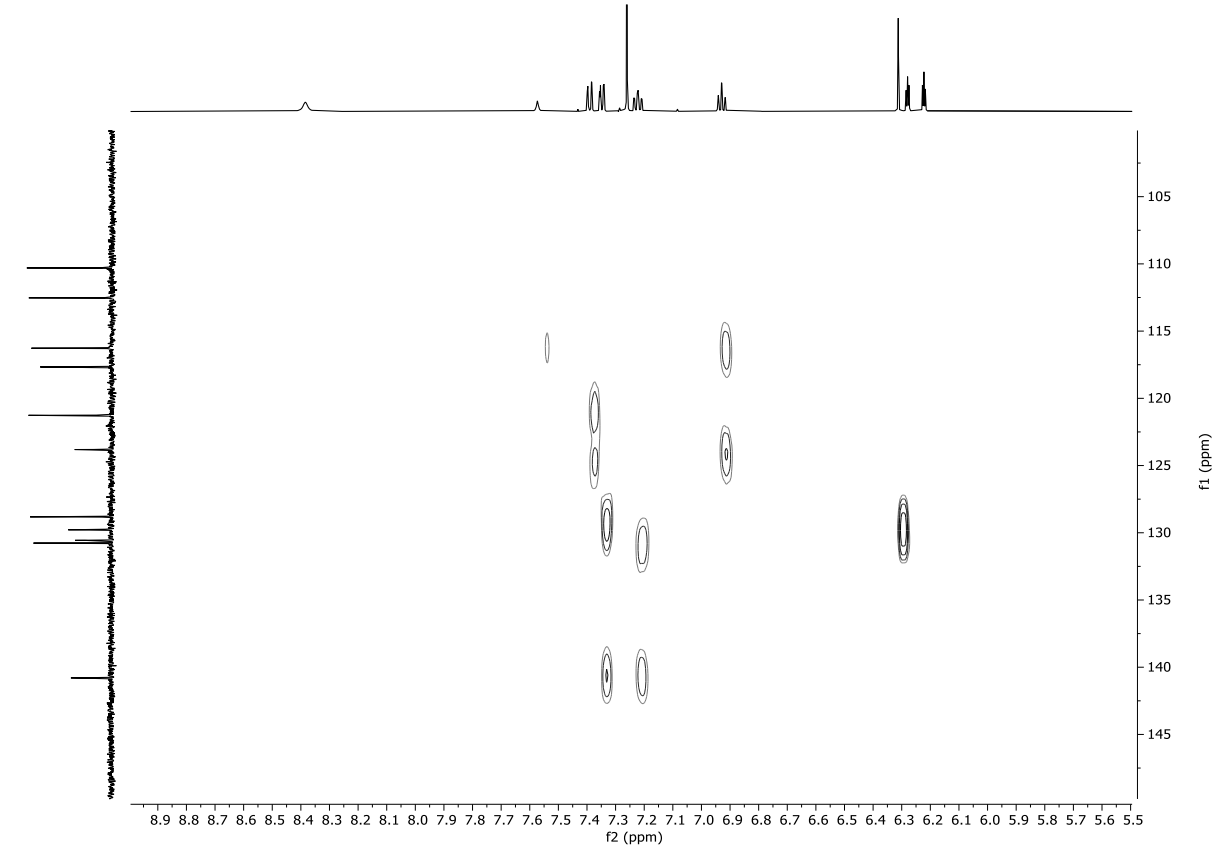

Figure S30. ^{1}H-^{13}C HMBC spectrum of **1a** (600 MHz, $CDCl_3$, 293 K, 5.5 – 9.0 & 100 – 150 ppm region).

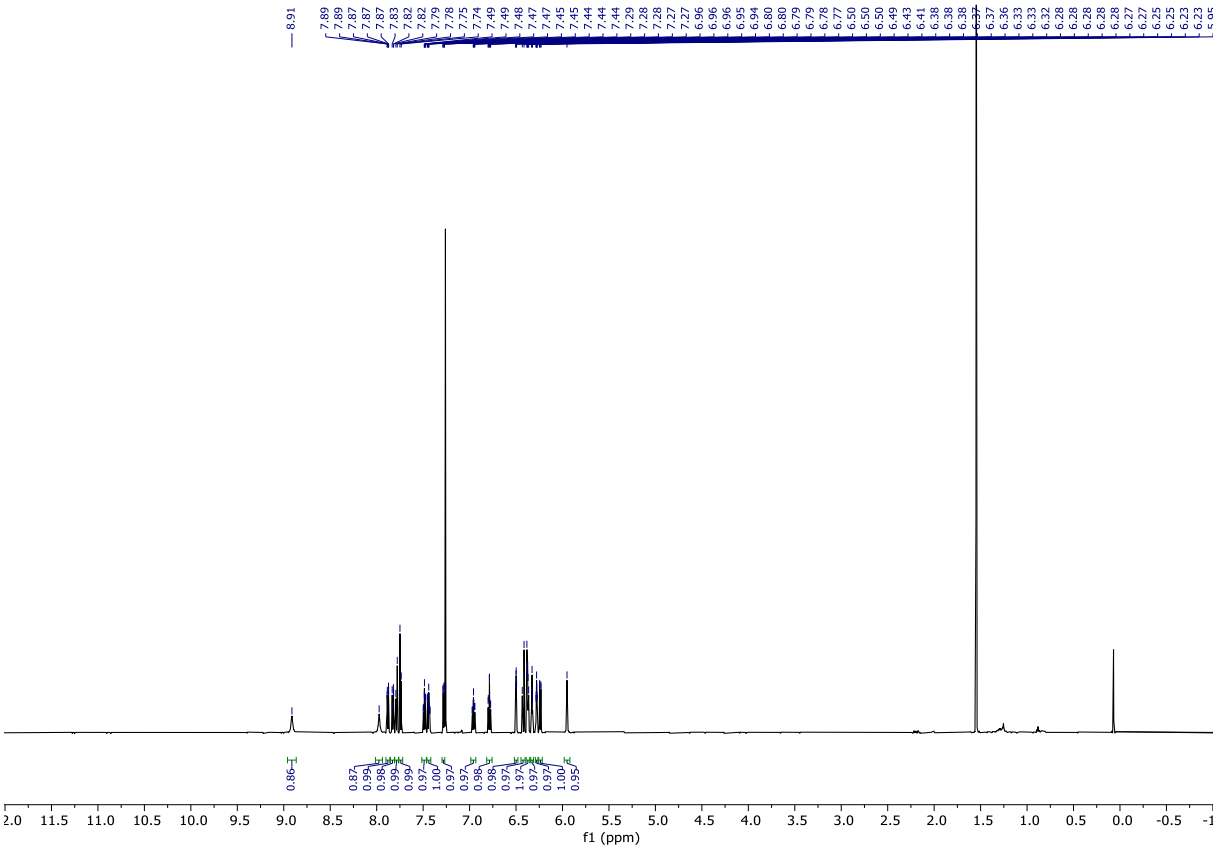

Figure S31. ^{1}H NMR spectrum of **1b** (600 MHz, $CDCl_3$, 293 K).

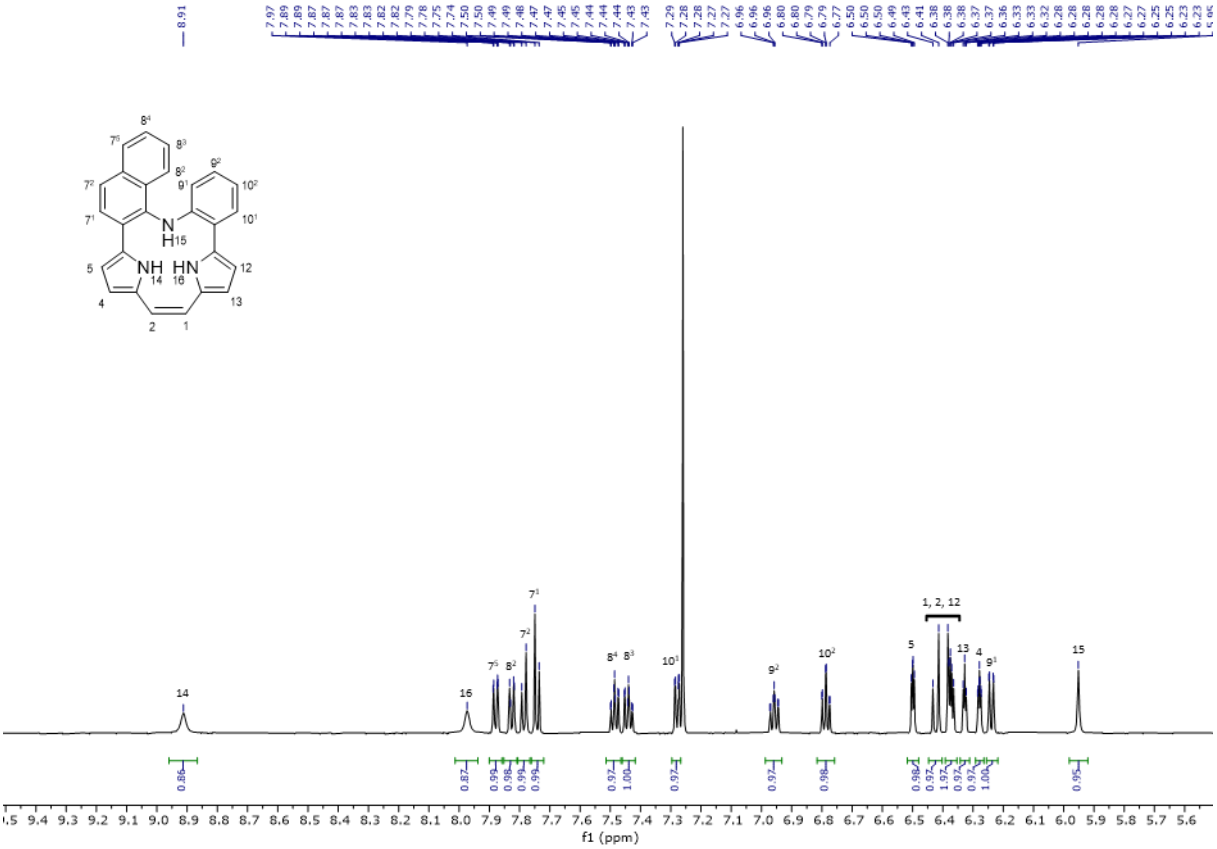

Figure S32. ^{1}H NMR spectrum of **1b** (600 MHz, $CDCl_3$, 293 K, 5.5 – 9.5 ppm region).

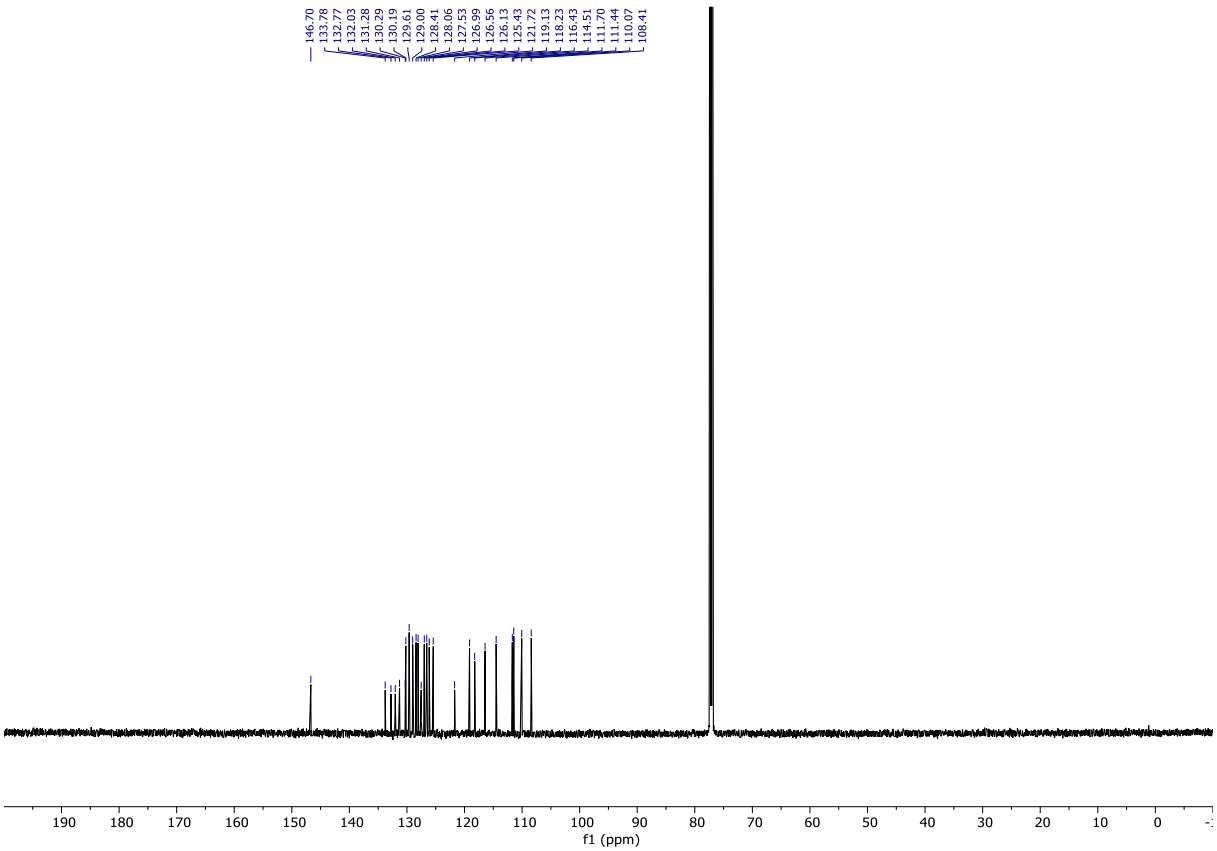

Figure S33. ^{13}C NMR spectrum of **1b** (151 MHz, CDCl3, 293 K).

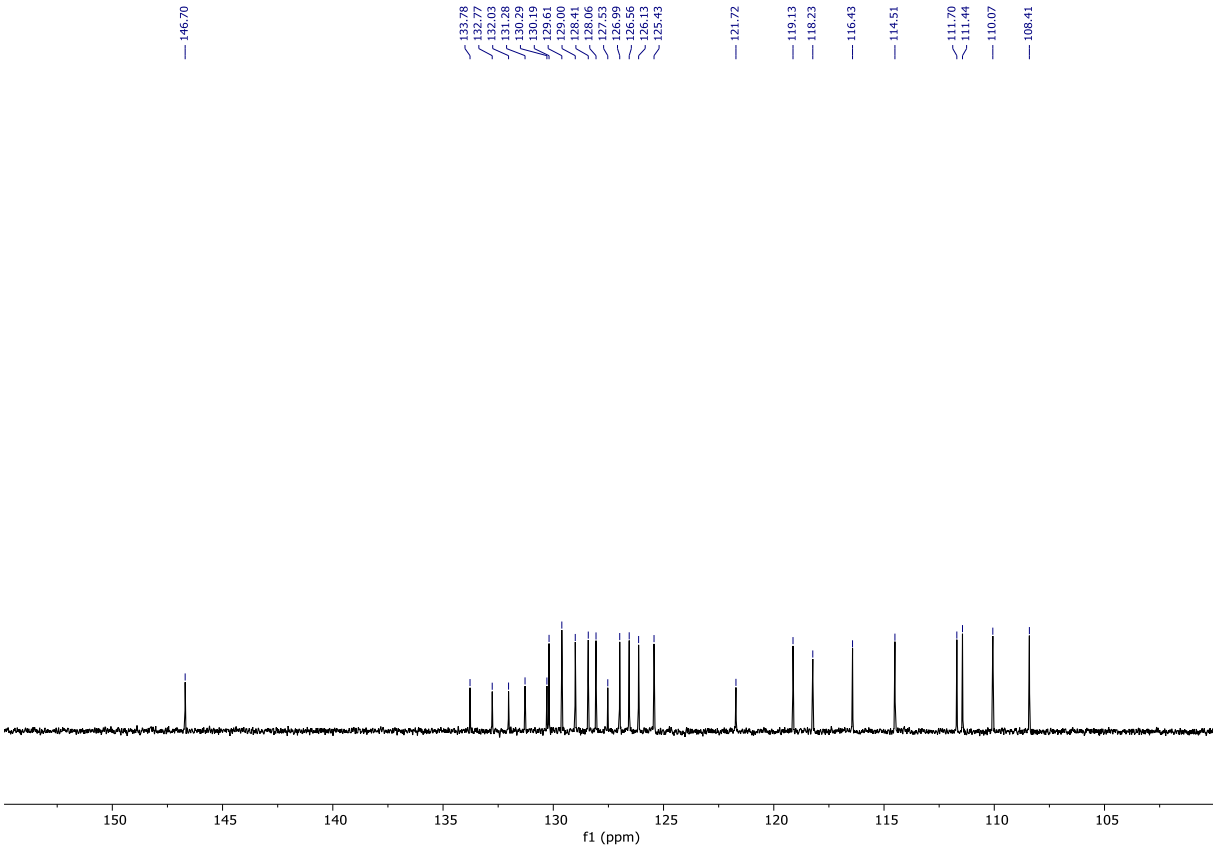

Figure S34. ^{13}C NMR spectrum of **1b** (151 MHz, CDCl3, 293 K, 100 – 155 ppm region).

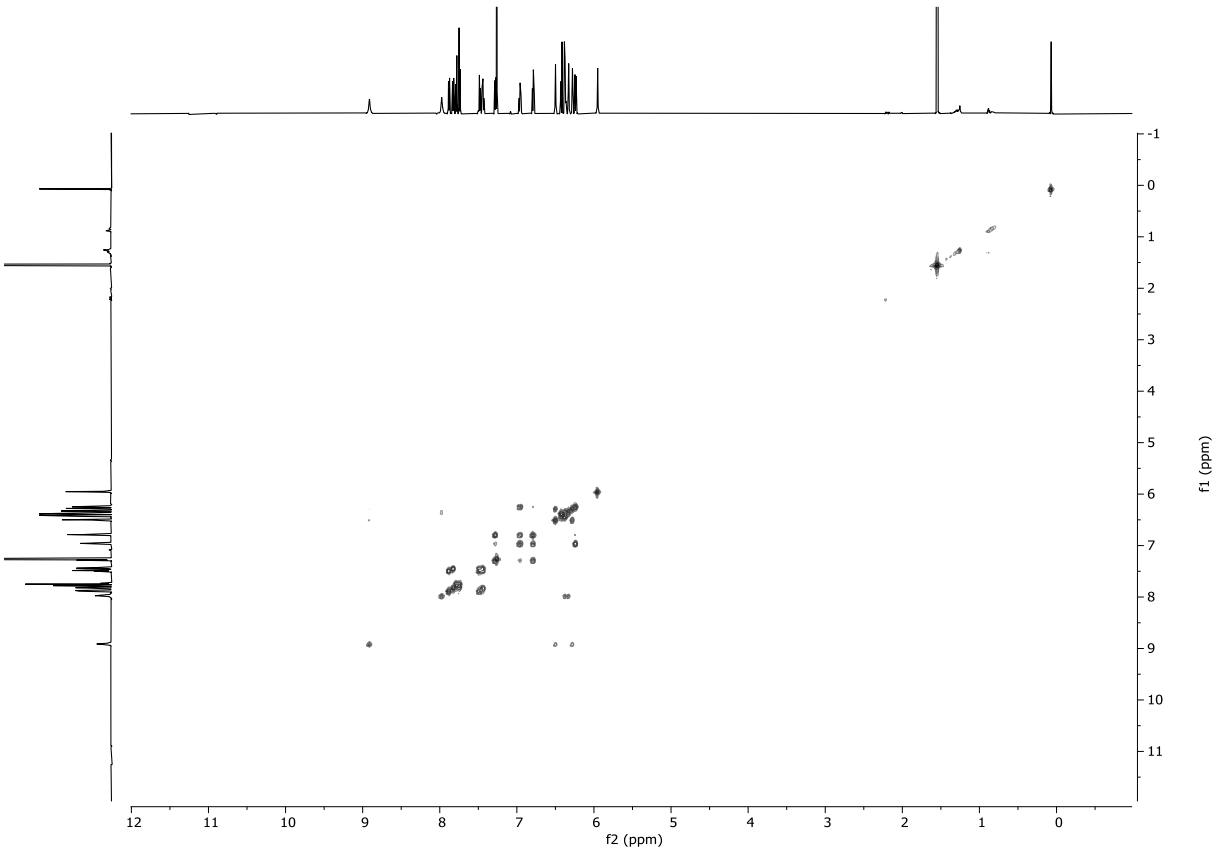

Figure S35. ^{1}H-^{1}H COSY spectrum of **1b** (600 MHz, $CDCl_3$, 293 K).

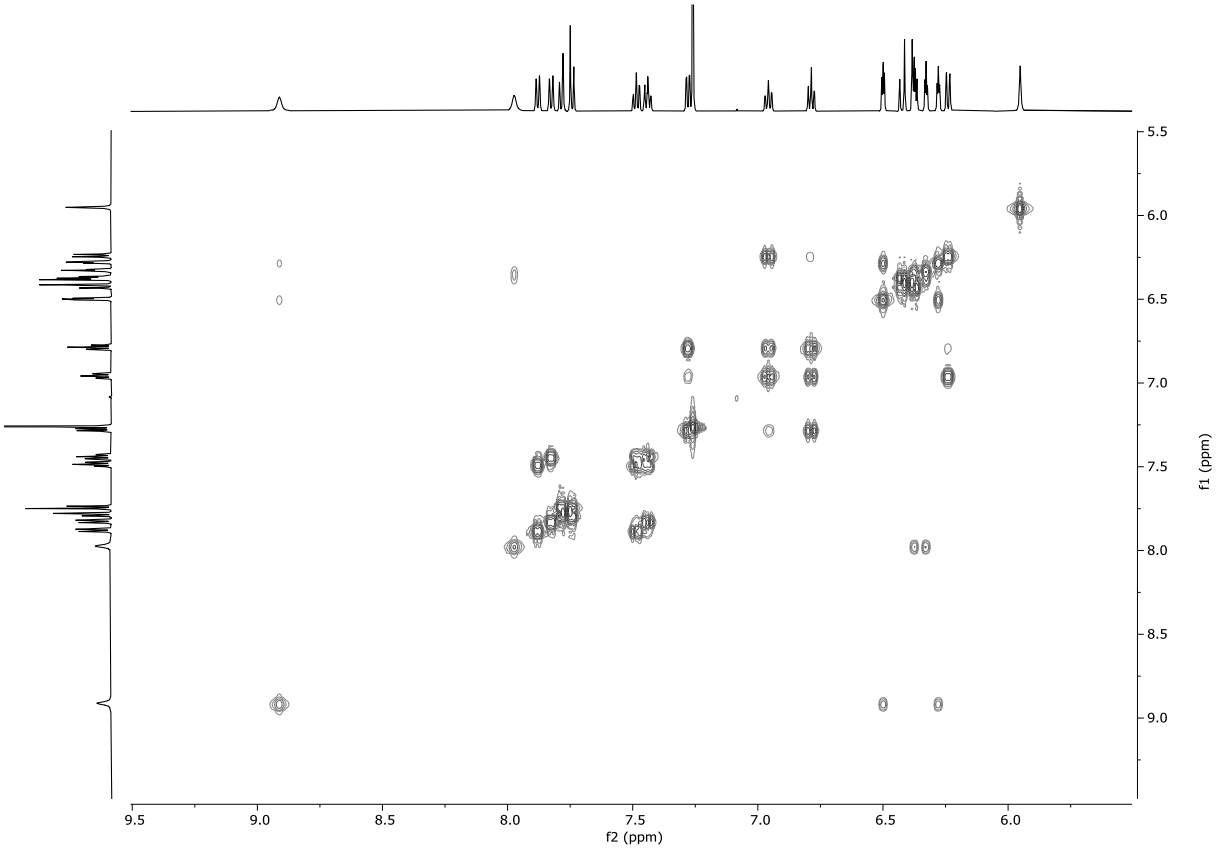

Figure S36. ^{1}H-^{1}H COSY spectrum of **1b** (600 MHz, $CDCl_3$, 293 K, 5.5 – 9.5 ppm region).

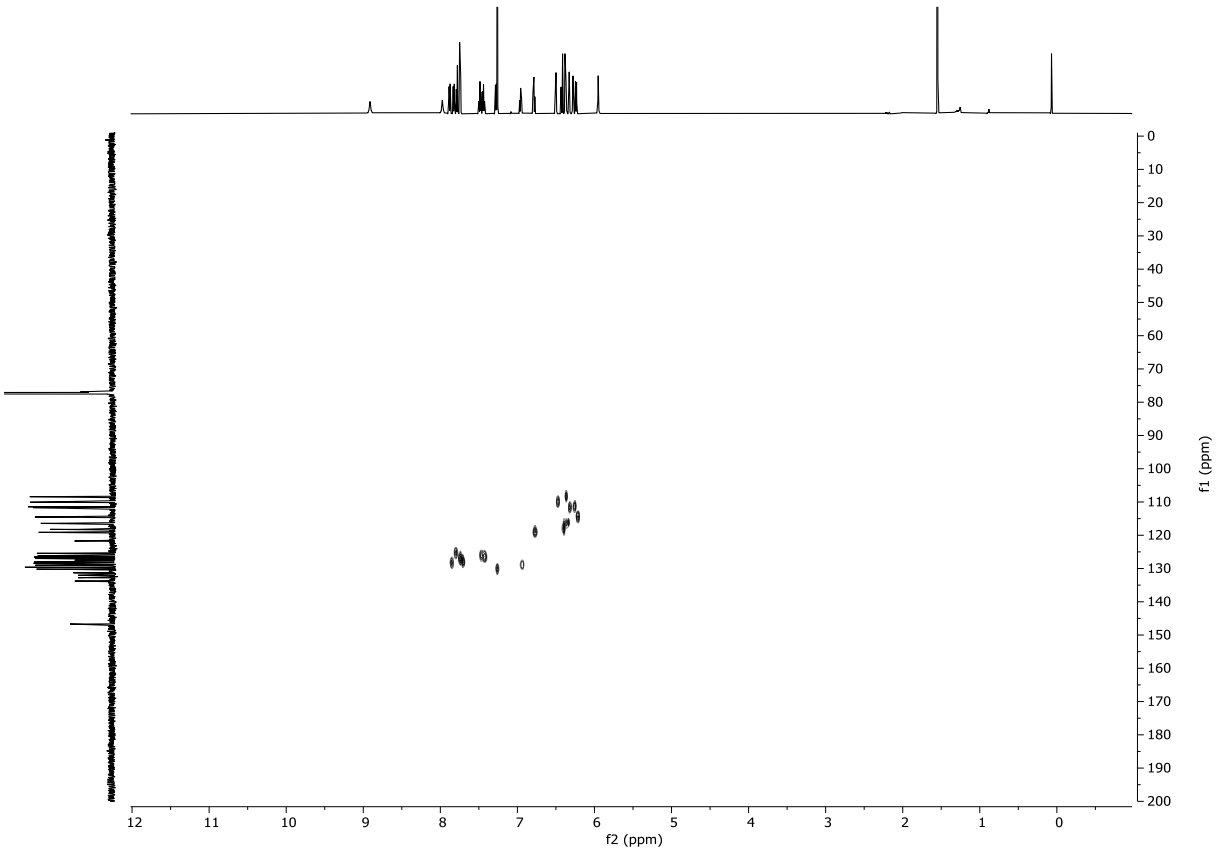

Figure S37. ^{1}H-^{13}C HSQC spectrum of **1b** (600 MHz, $CDCl_3$, 293 K).

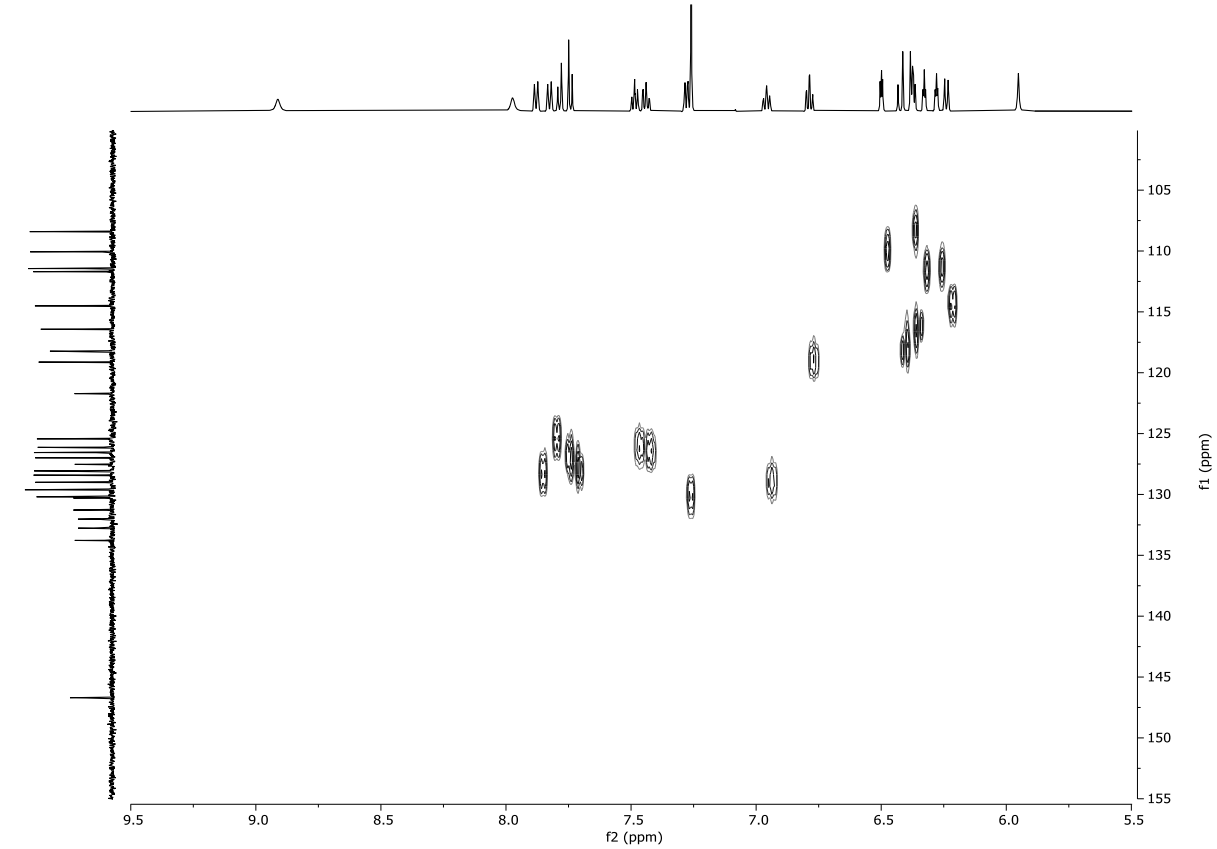

Figure S38. ^{1}H-^{13}C HSQC spectrum of **1b** (600 MHz, $CDCl_3$, 293 K, 5.5 – 9.5 & 100 – 155 ppm region).

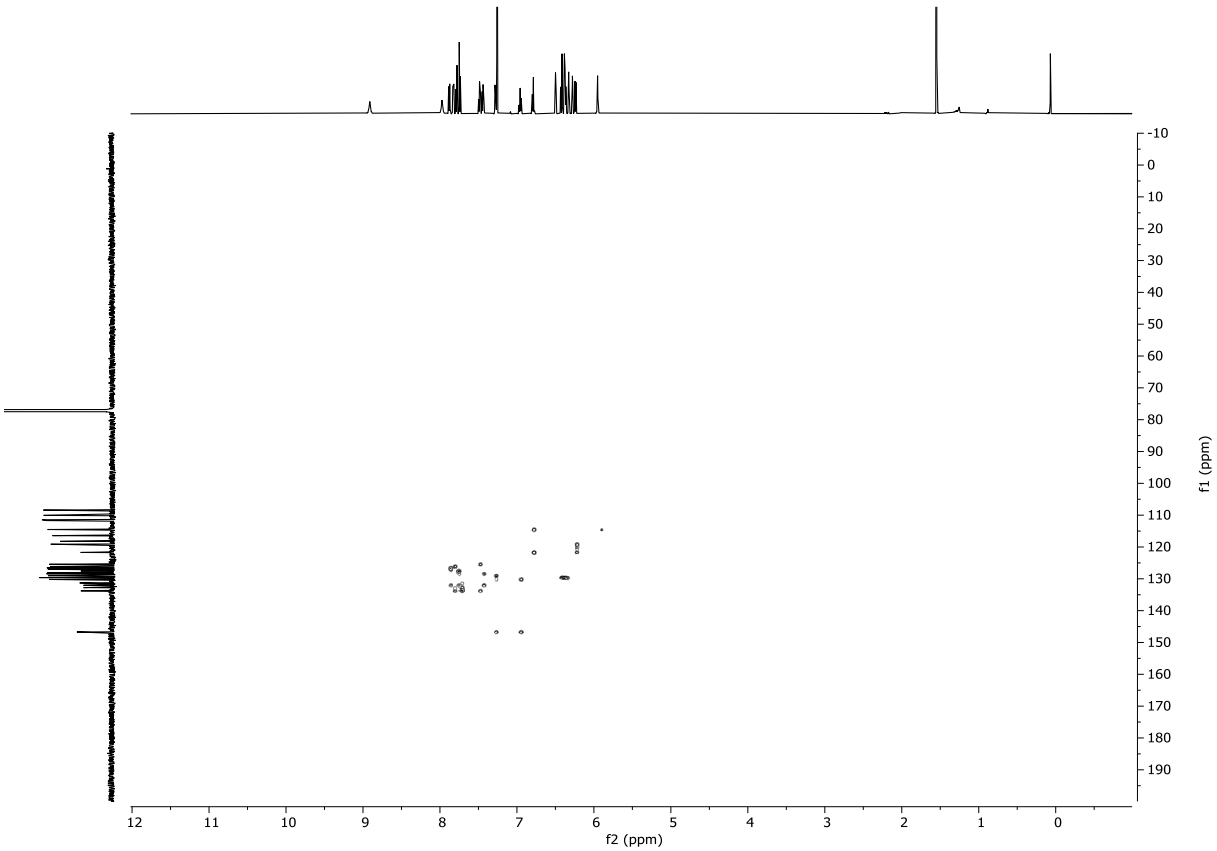

Figure S39. ^{1}H-^{13}C HMBC spectrum of **1b** (600 MHz, $CDCl_3$, 293 K).

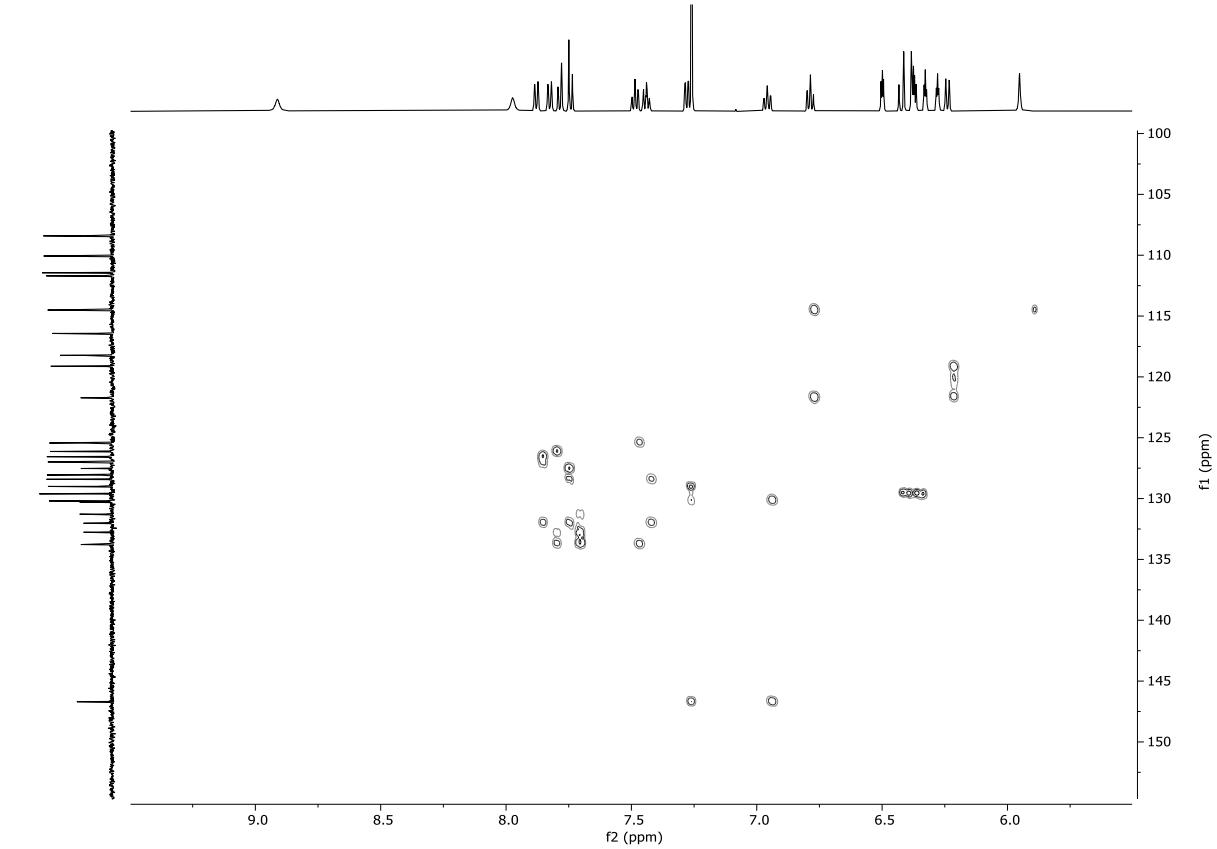

Figure S40. ^{1}H-^{13}C HMBC spectrum of **1b** (600 MHz, $CDCl_3$, 293 K, 5.5 – 9.5 & 100 – 155 ppm region).

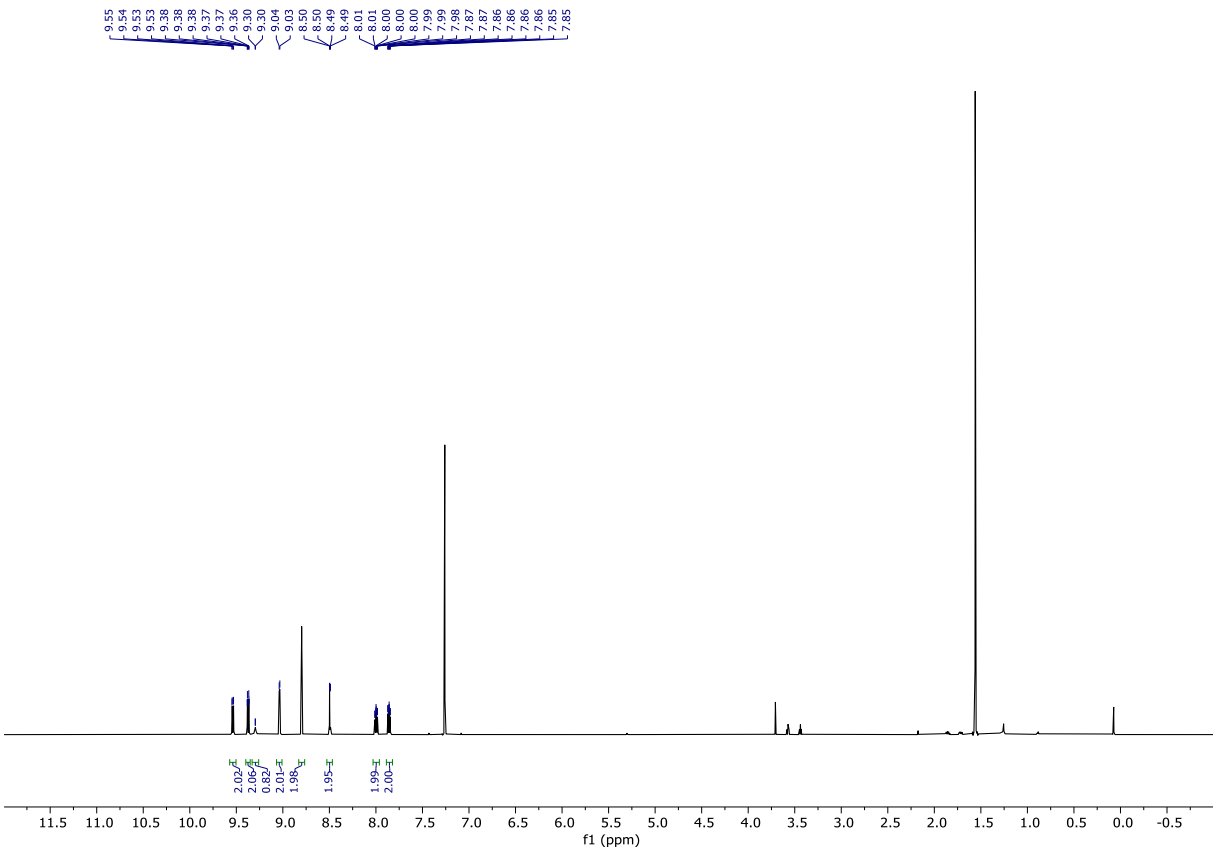

Figure S41. ^{1}H NMR spectrum of **3a** (600 MHz, $CDCl_3$, 293 K).

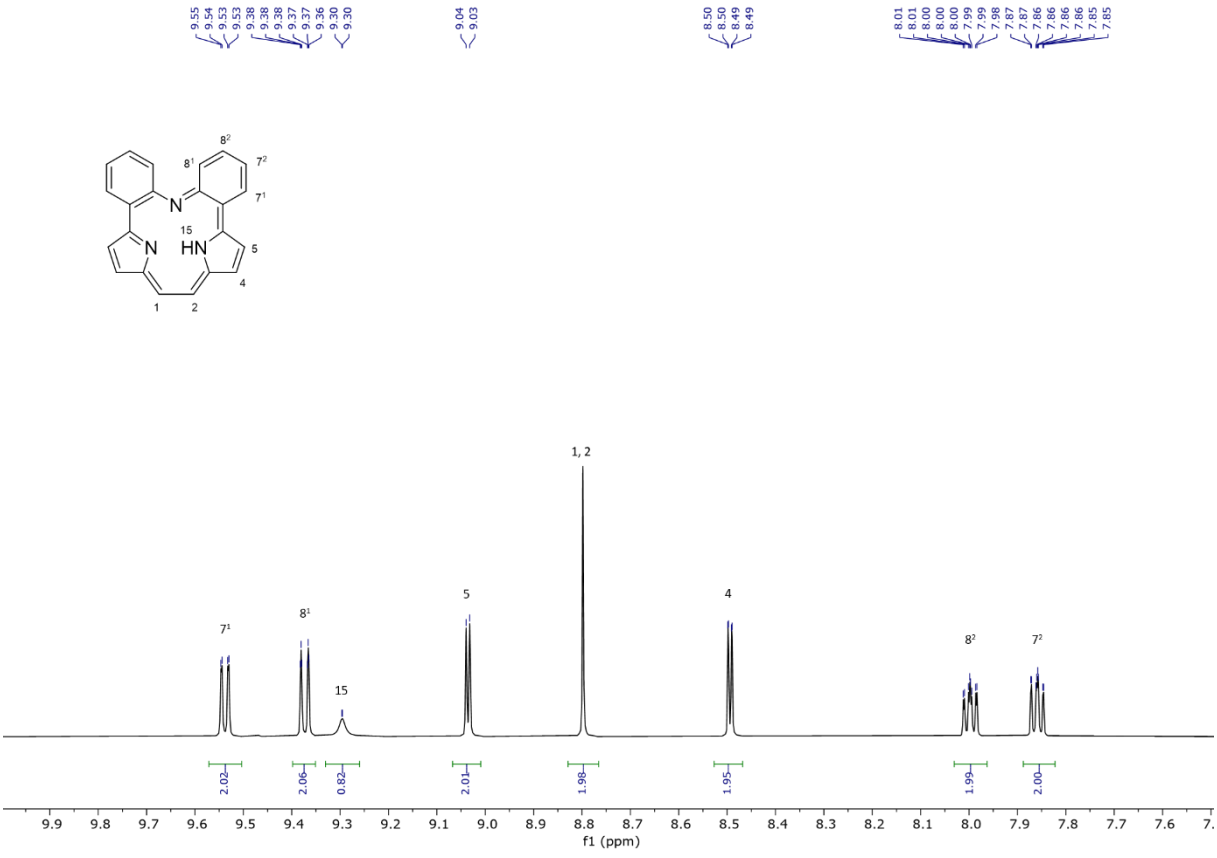

Figure S42. ^{1}H NMR spectrum of **3a** (600 MHz, $CDCl_3$, 293 K, 7.5 – 10.0 ppm region).

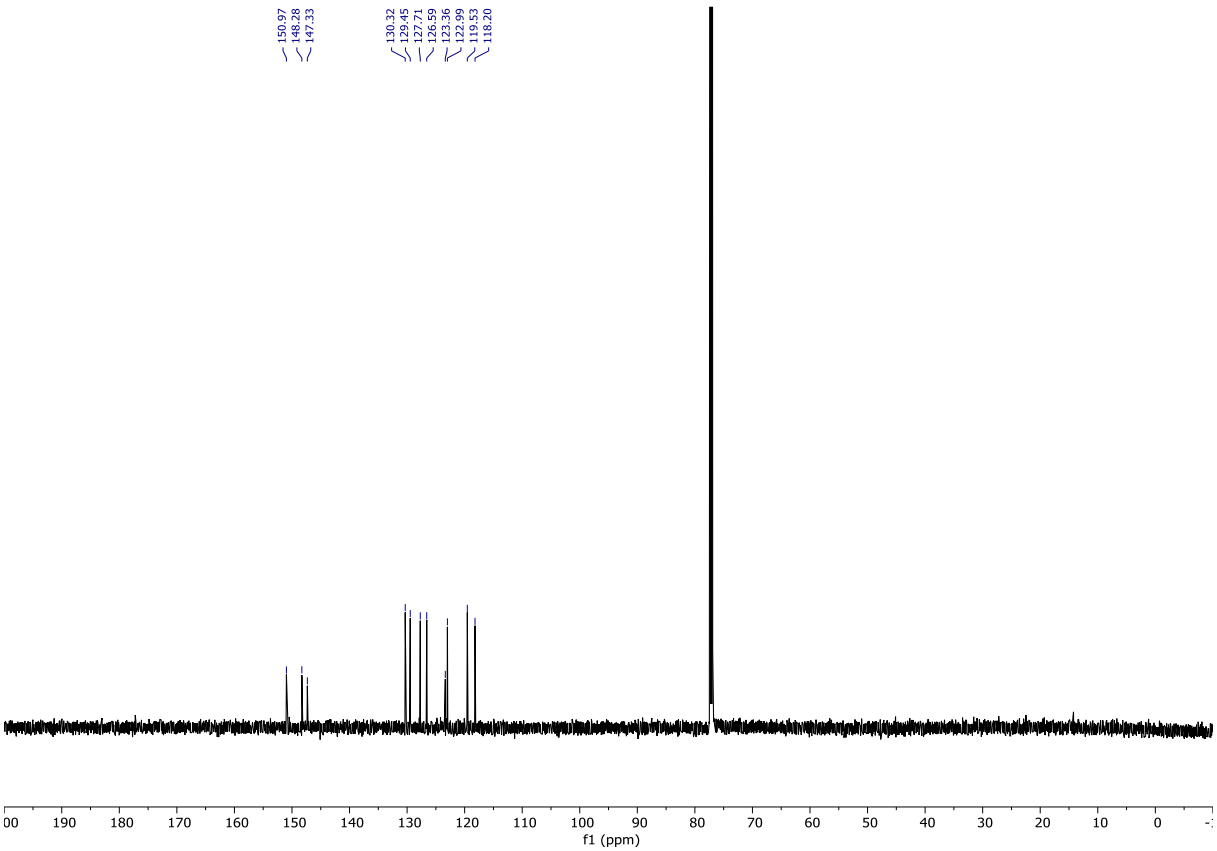

Figure S43. ^{13}C NMR spectrum of **3a** (151 MHz, $CDCl_3$, 293 K).

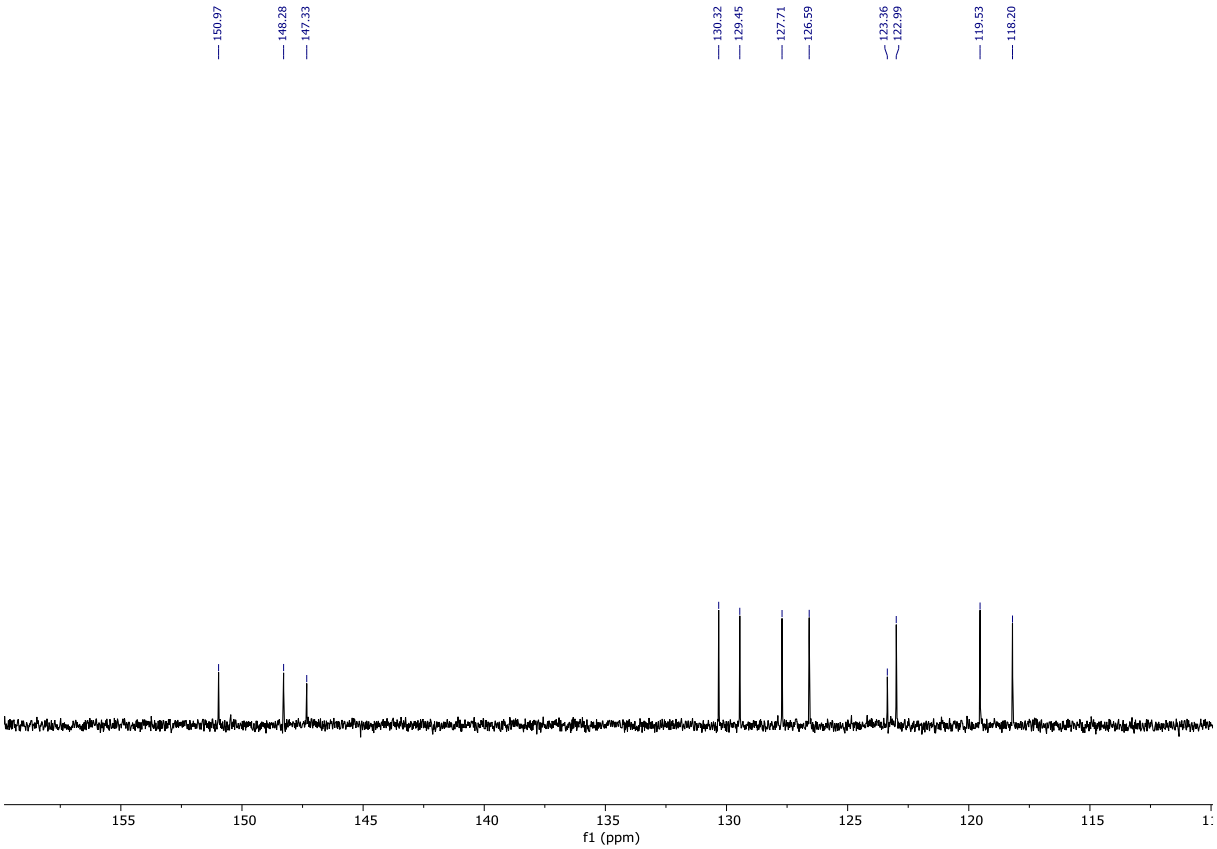

Figure S44. ^{13}C NMR spectrum of **3a** (151 MHz, $CDCl_3$, 293 K, 110 – 160 ppm region).

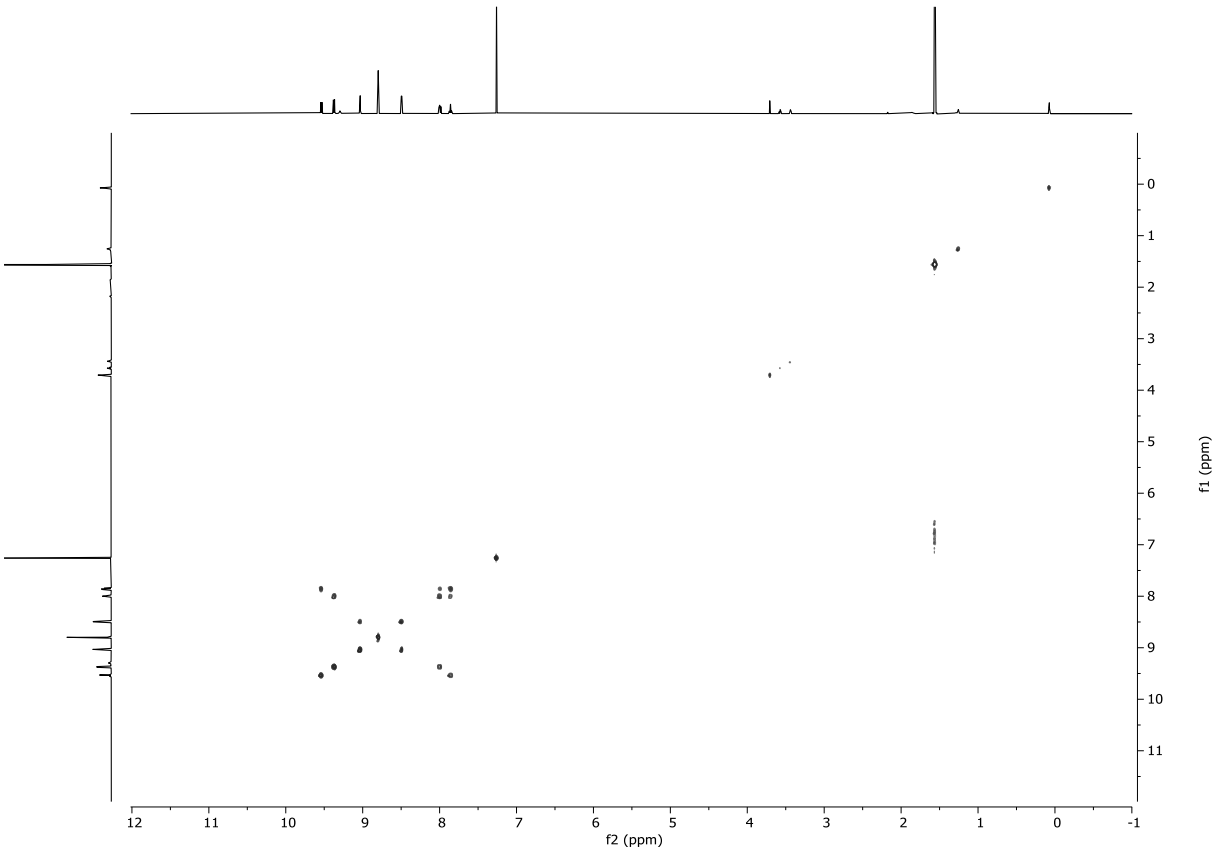

Figure S45. ^{1}H-^{1}H COSY spectrum of **3a** (600 MHz, $CDCl_3$, 293 K).

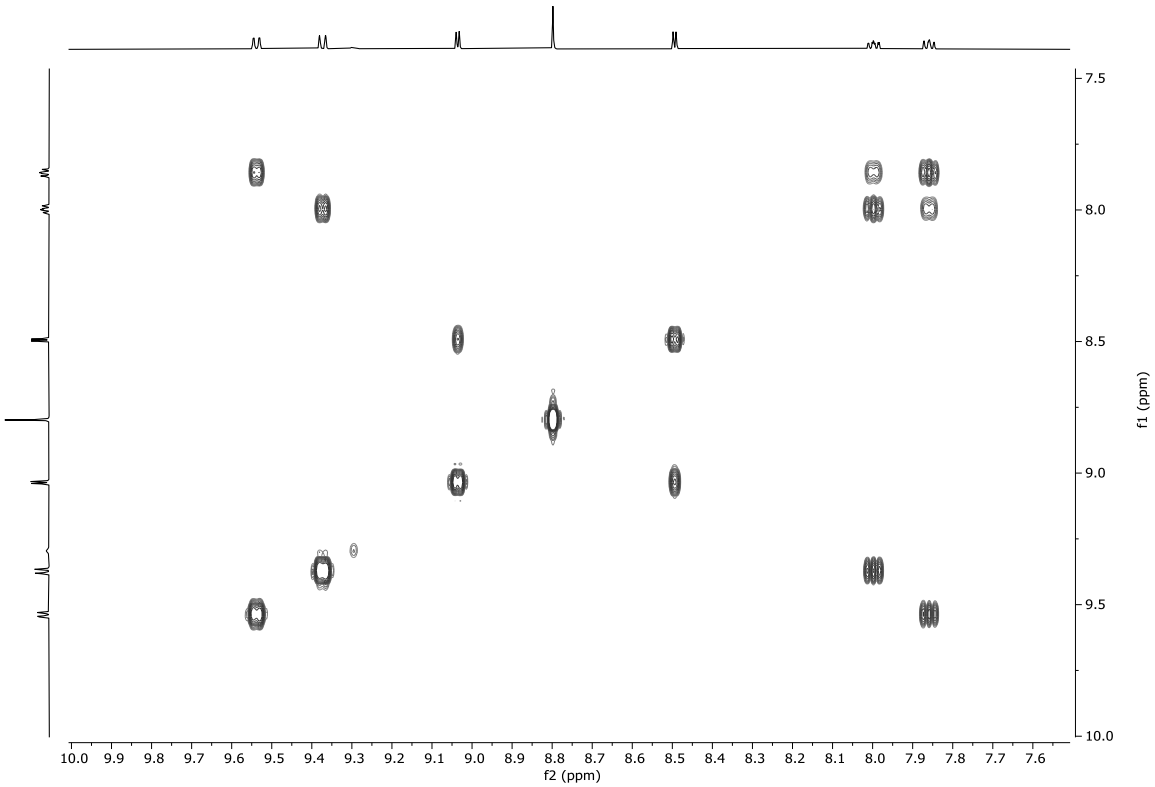

Figure S46. ^{1}H-^{1}H COSY spectrum of **3a** (600 MHz, $CDCl_3$, 293 K, 7.5 – 10.0 ppm region).

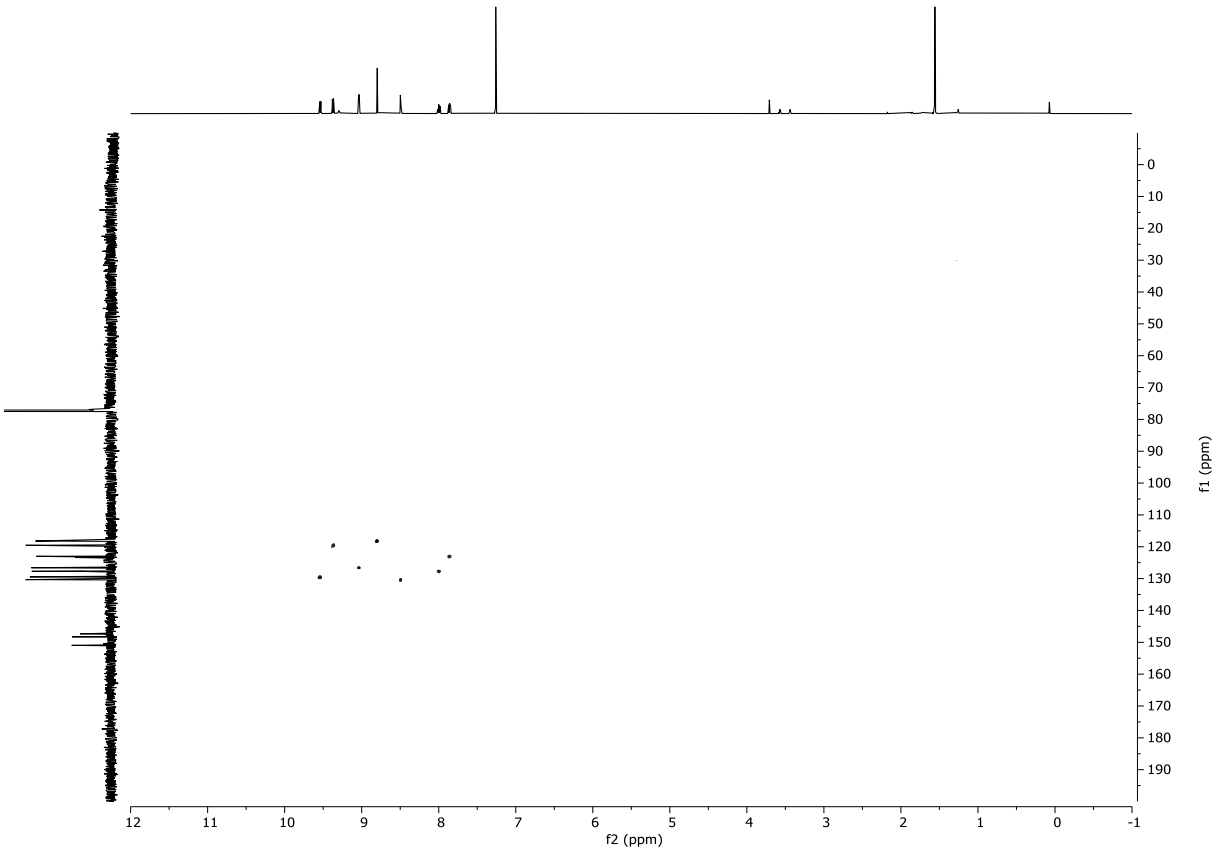

Figure S47. ^{1}H-^{13}C HSQC spectrum of **3a** (600 MHz, $CDCl_3$, 293 K).

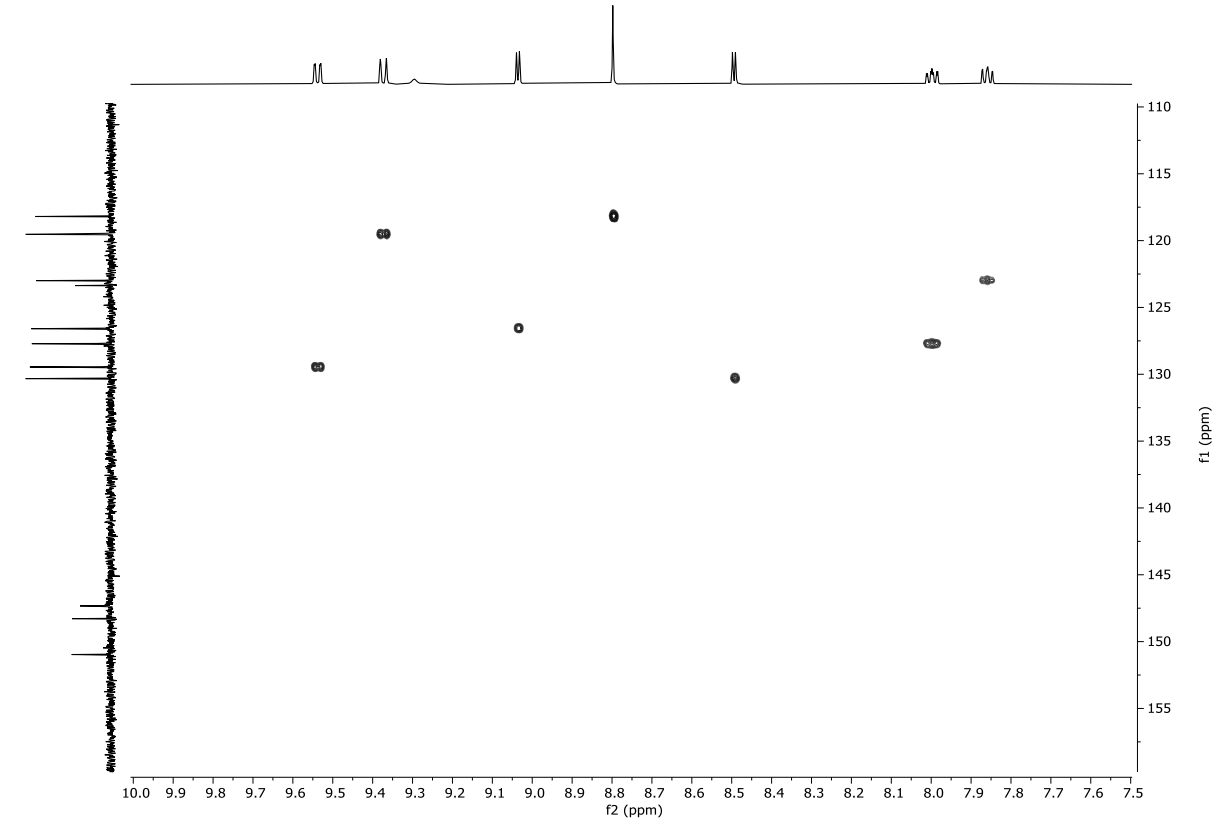

Figure S48. ^{1}H-^{13}C HSQC spectrum of **3a** (600 MHz, $CDCl_3$, 293 K, 7.5 – 10.0 & 110 – 160 ppm region).

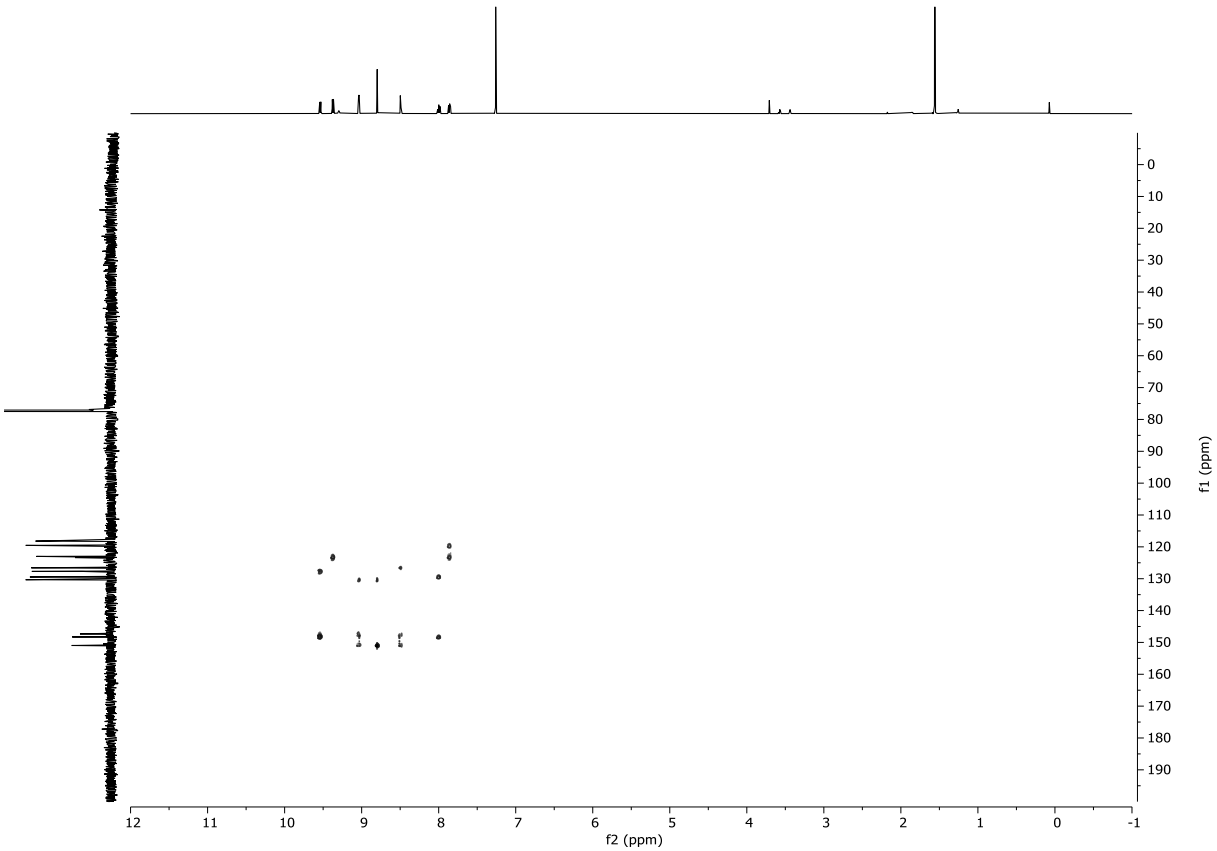

Figure S49. ^{1}H-^{13}C HMBC spectrum of **3a** (600 MHz, $CDCl_3$, 293 K).

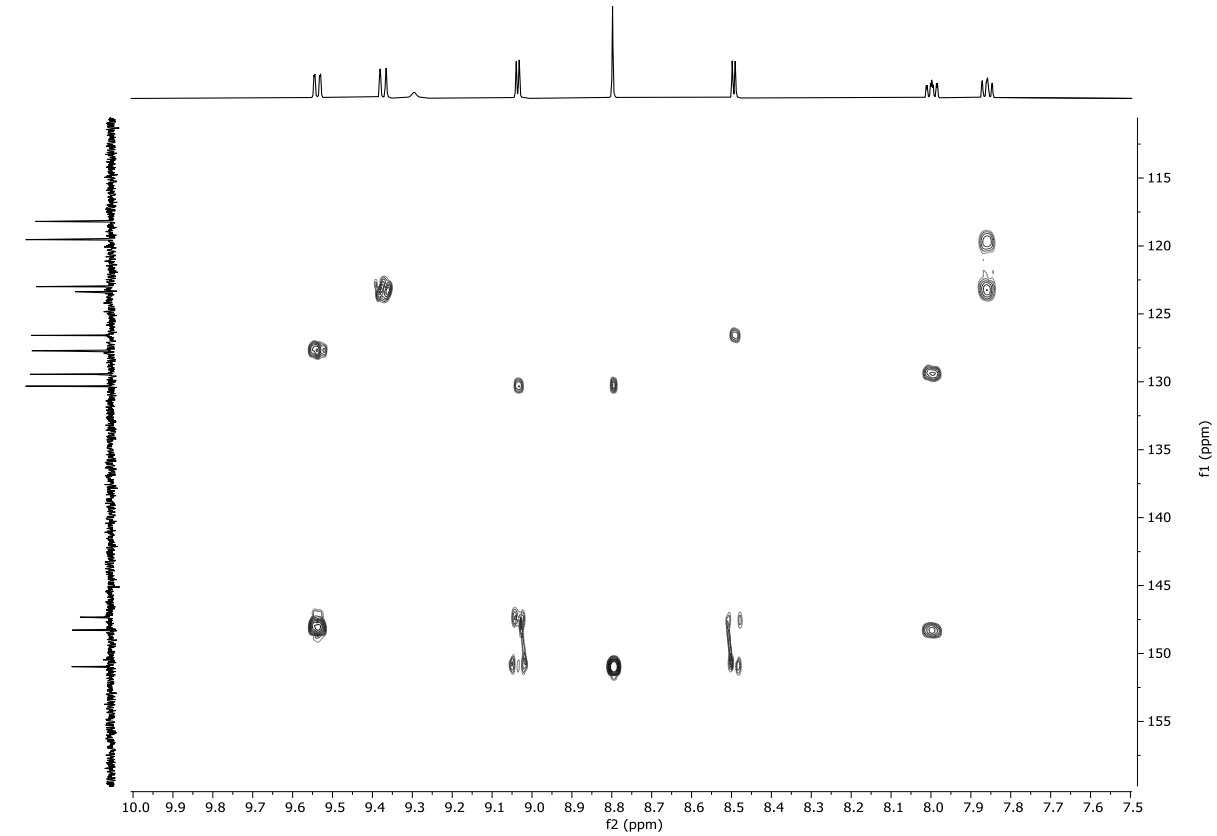

Figure S50. ^{1}H-^{13}C HMBC spectrum of **3a** (600 MHz, $CDCl_3$, 293 K, 7.5 – 10.0 & 110 – 160 ppm region).

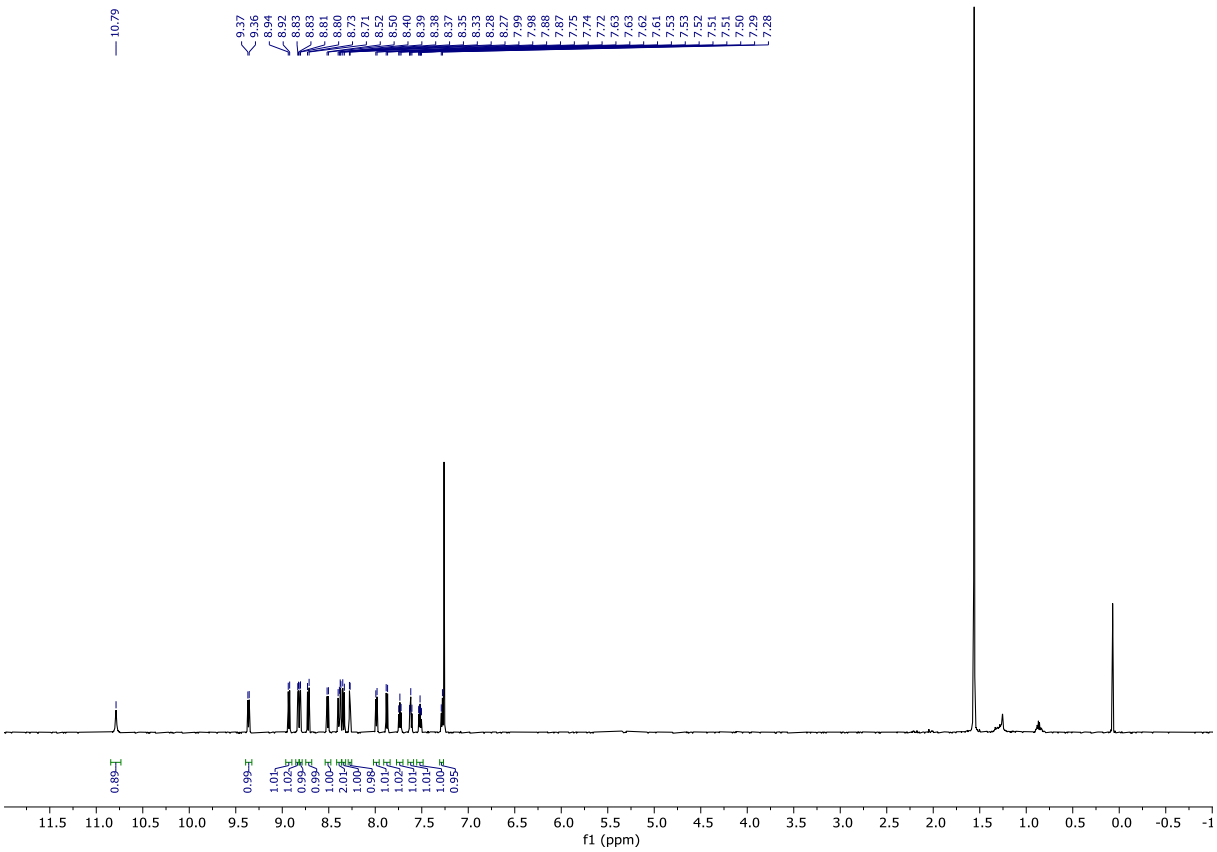

Figure S51. ^{1}H NMR spectrum of **3b** (600 MHz, $CDCl_3$, 293 K).

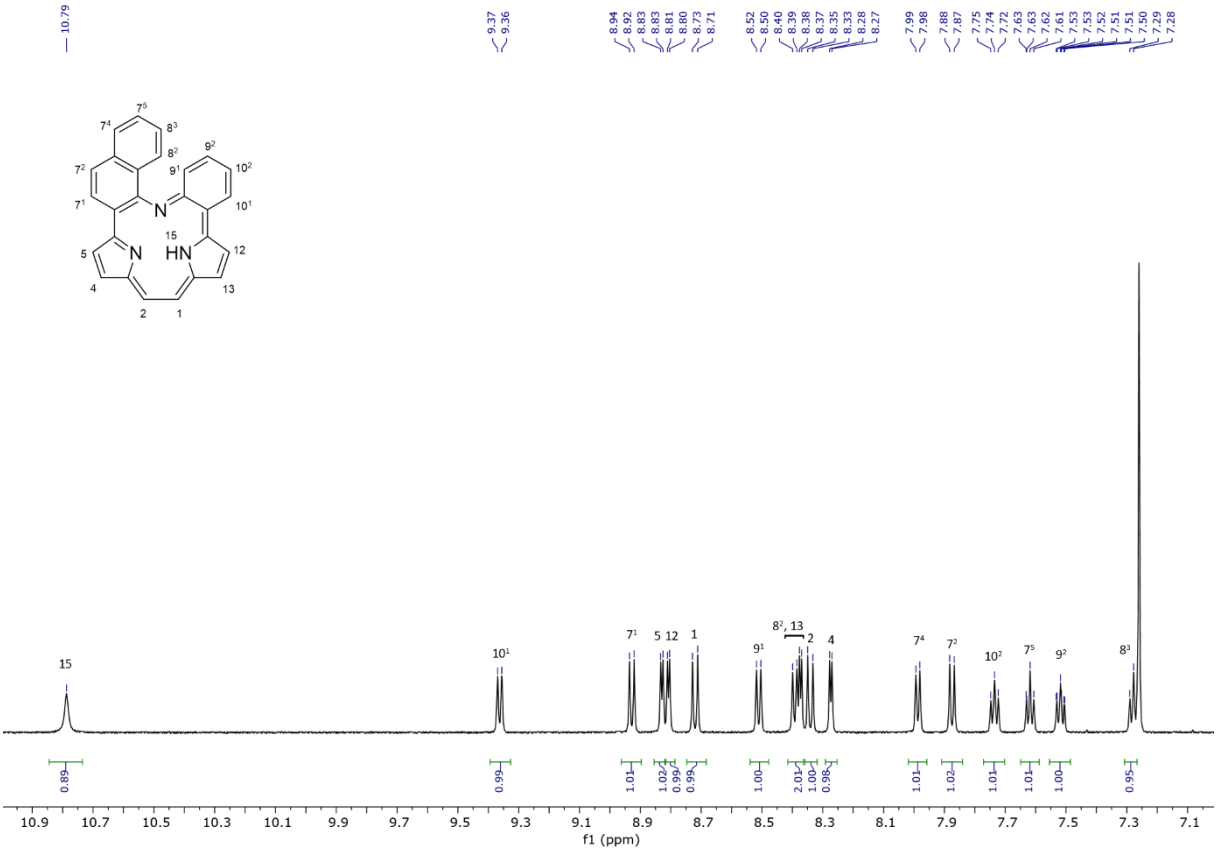

Figure S52. ^{1}H NMR spectrum of **3b** (600 MHz, $CDCl_3$, 293 K, 7.0 – 11.0 ppm region).

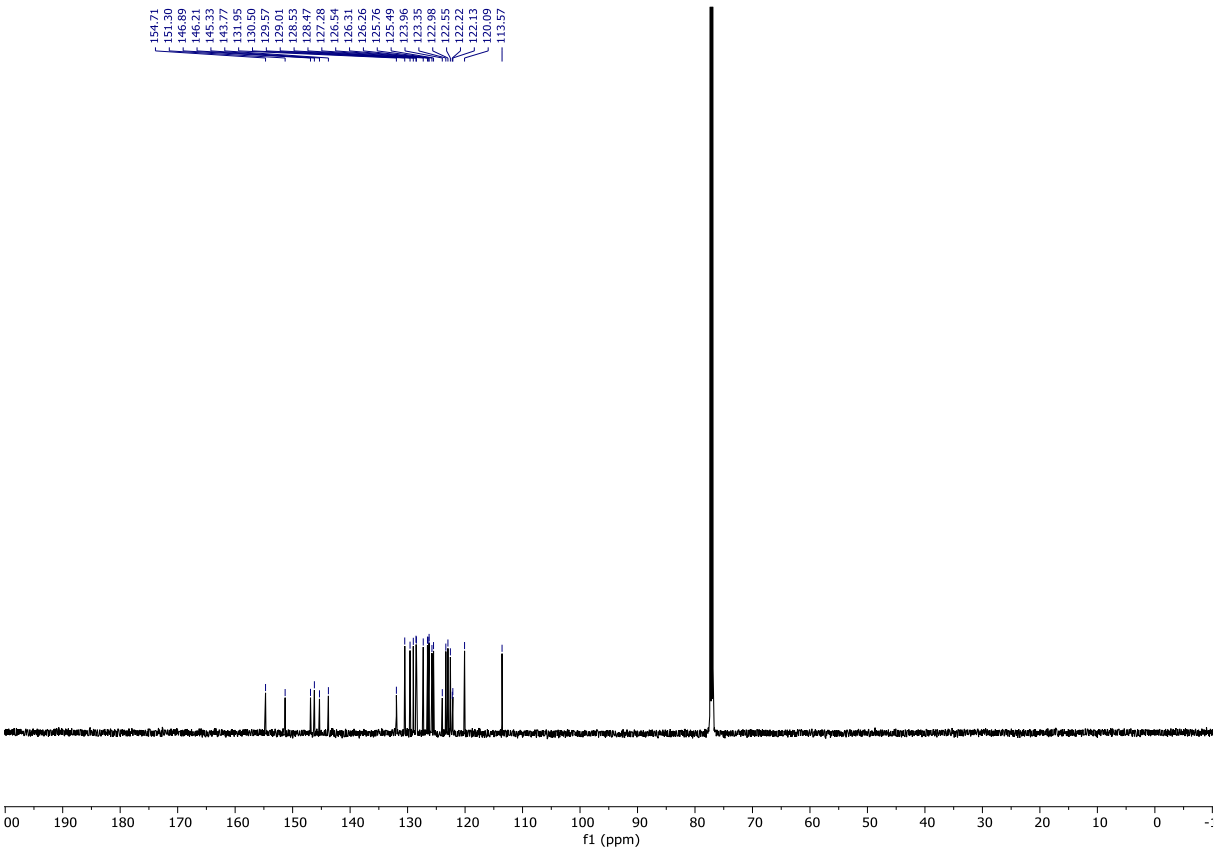

Figure S53. ^{13}C NMR spectrum of **3b** (151 MHz, $CDCl_3$, 293 K).

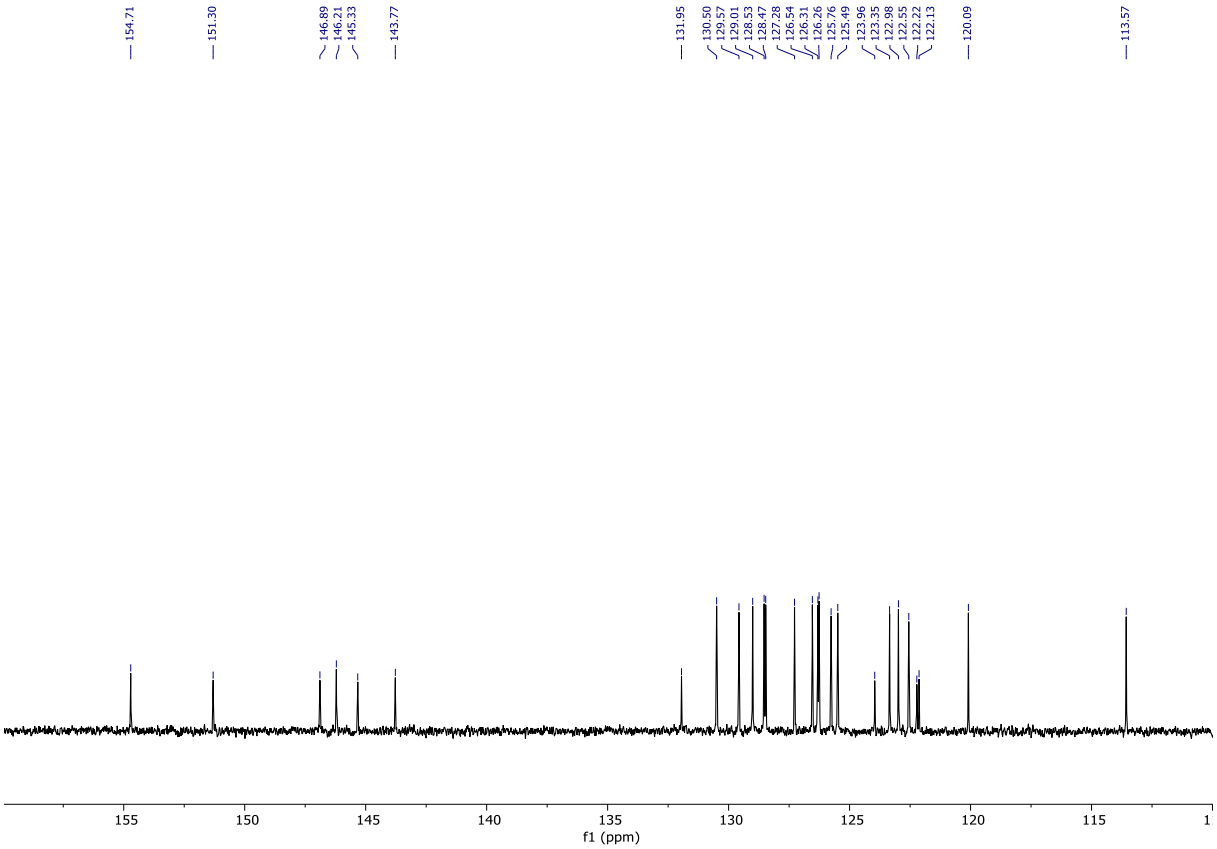

Figure S54. ^{13}C NMR spectrum of **3b** (151 MHz, $CDCl_3$, 293 K, 110 – 160 ppm region).

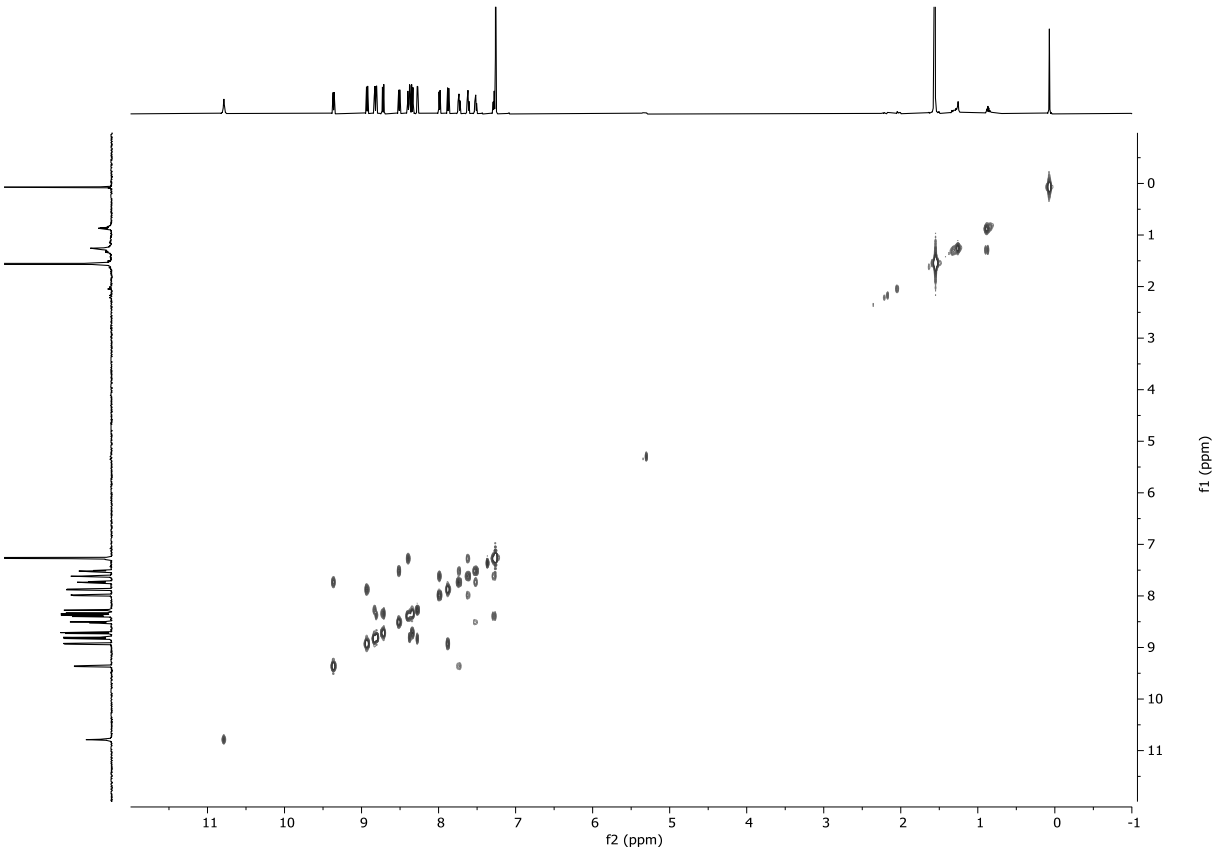

Figure S55. ^{1}H-^{1}H COSY spectrum of **3b** (600 MHz, $CDCl_3$, 293 K).

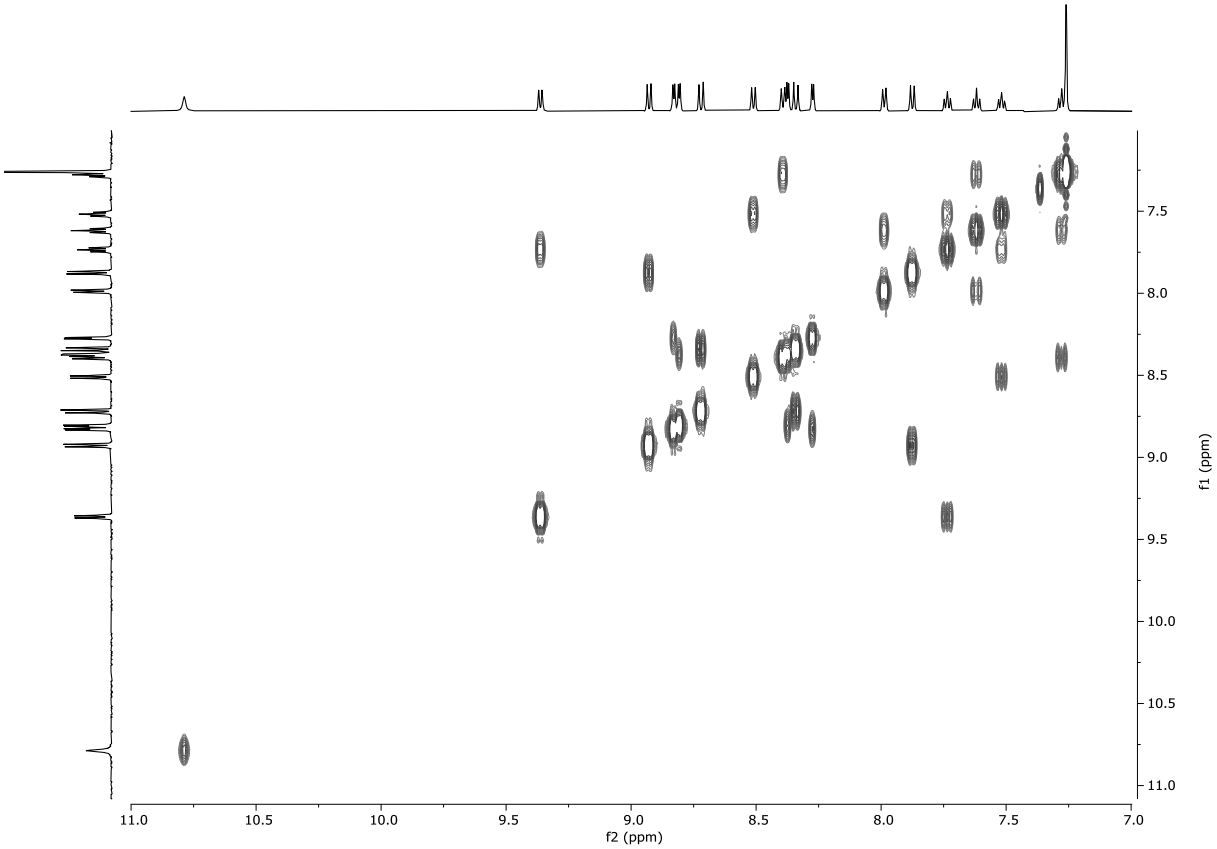

Figure S56. ^{1}H-^{1}H COSY spectrum of **3b** (600 MHz, $CDCl_3$, 293 K, 7.0 – 11.0 ppm region).

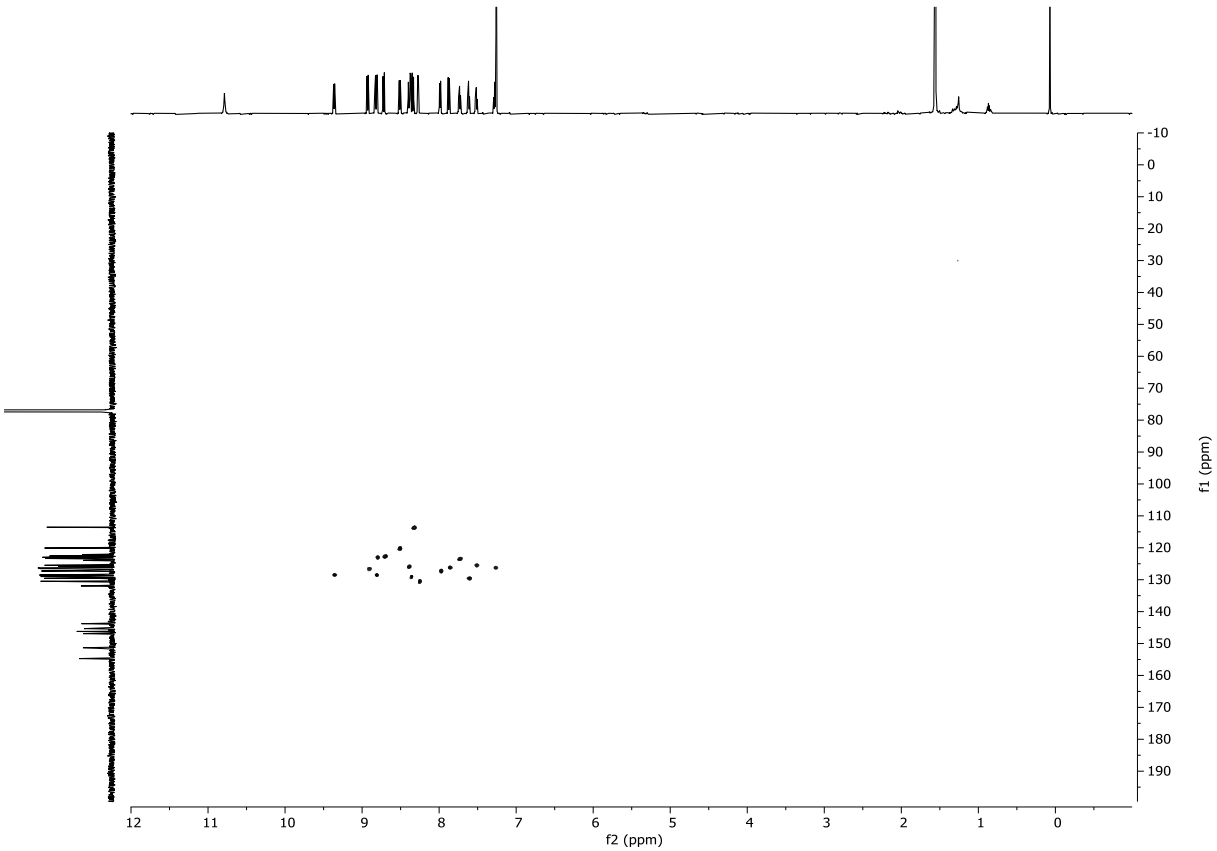

Figure S57. ^{1}H-^{13}C HSQC spectrum of **3b** (600 MHz, $CDCl_3$, 293 K).

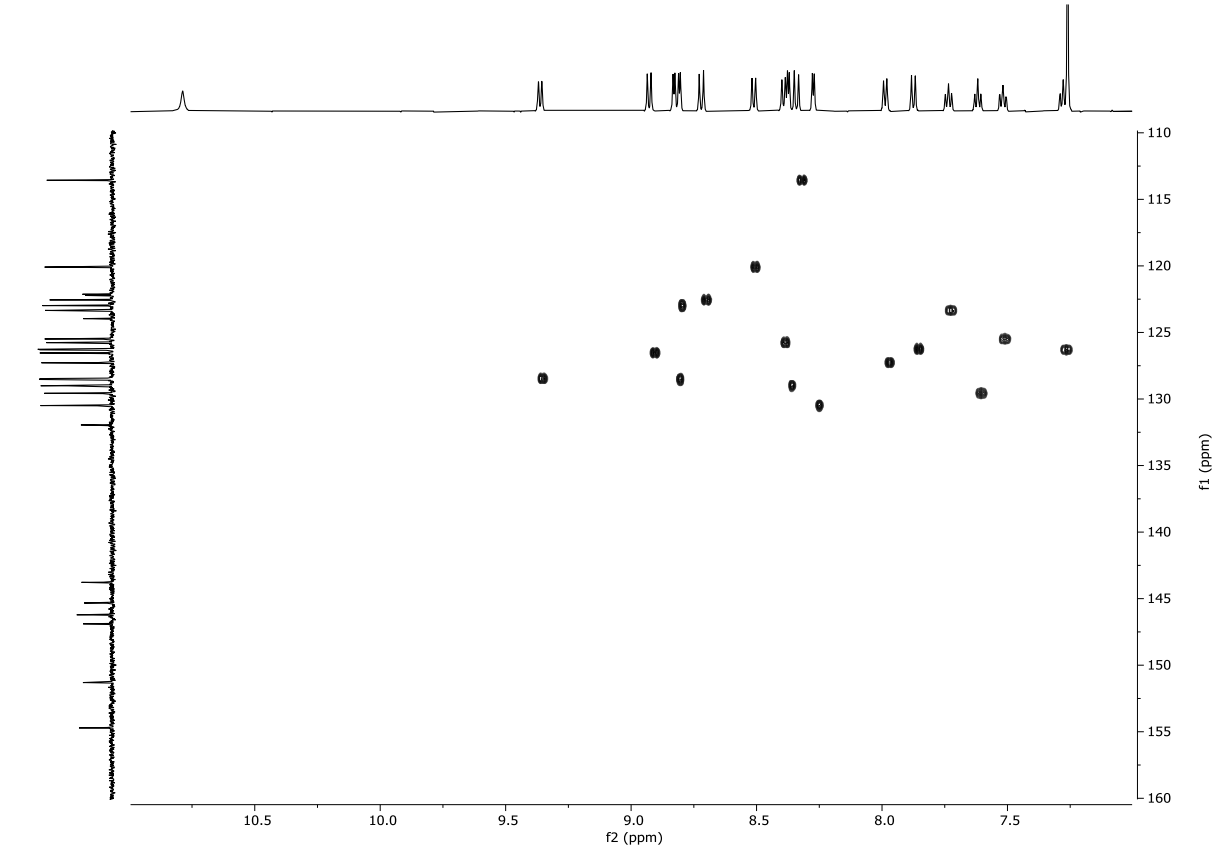

Figure S58. ^{1}H-^{13}C HSQC spectrum of **3b** (600 MHz, $CDCl_3$, 293 K, 7.0 – 11.0 & 110 – 160 ppm region).

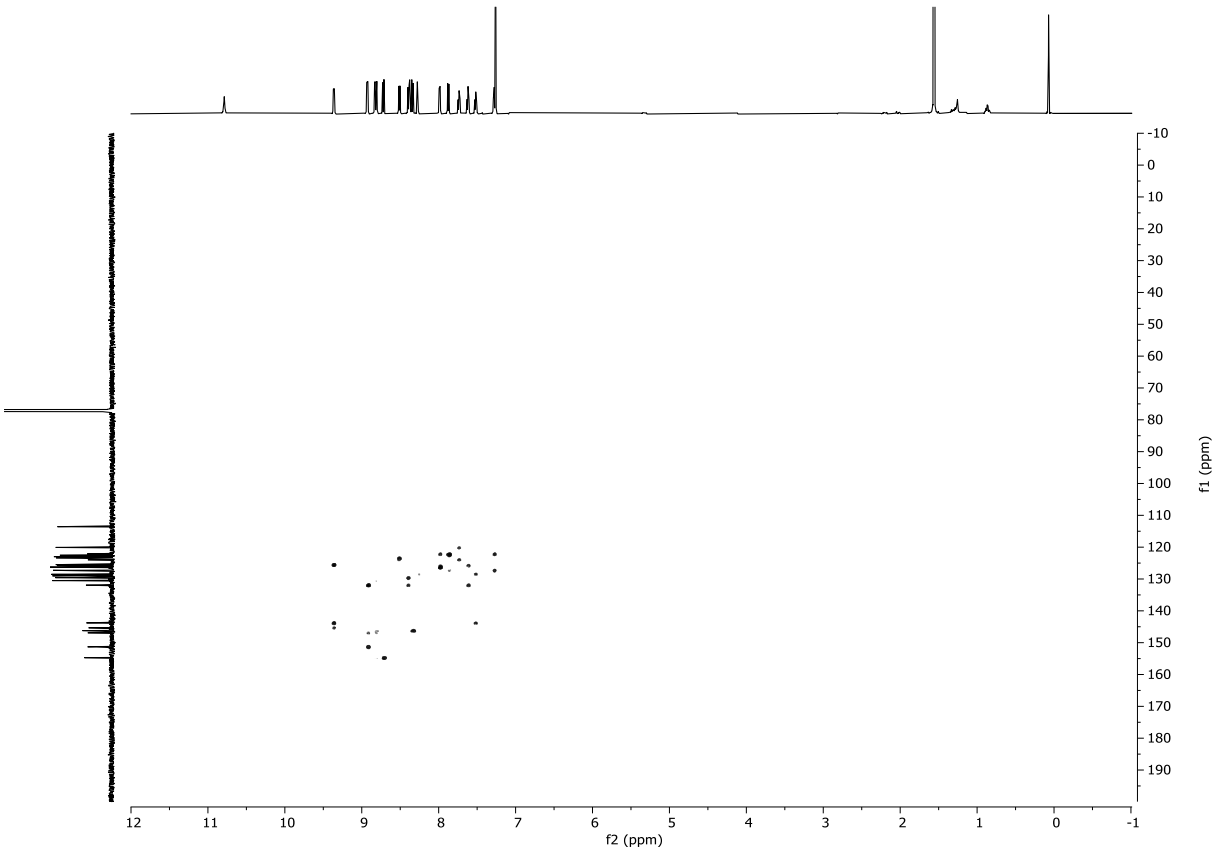

Figure S59. ^{1}H-^{13}C HMBC spectrum of **3b** (600 MHz, $CDCl_3$, 293 K).

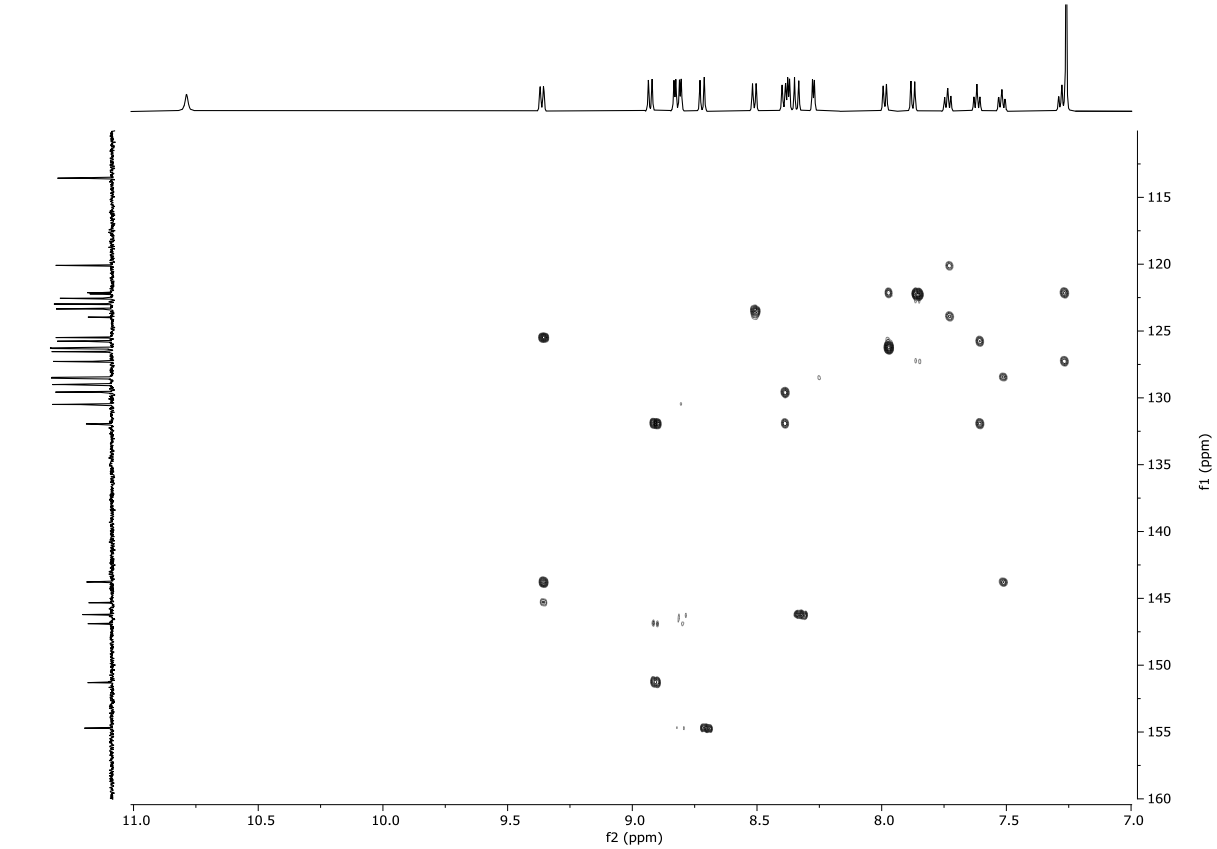

Figure S60. ^{1}H-^{13}C HMBC spectrum of **3b** (600 MHz, $CDCl_3$, 293 K, 7.0 – 11.0 & 110 – 160 ppm region).

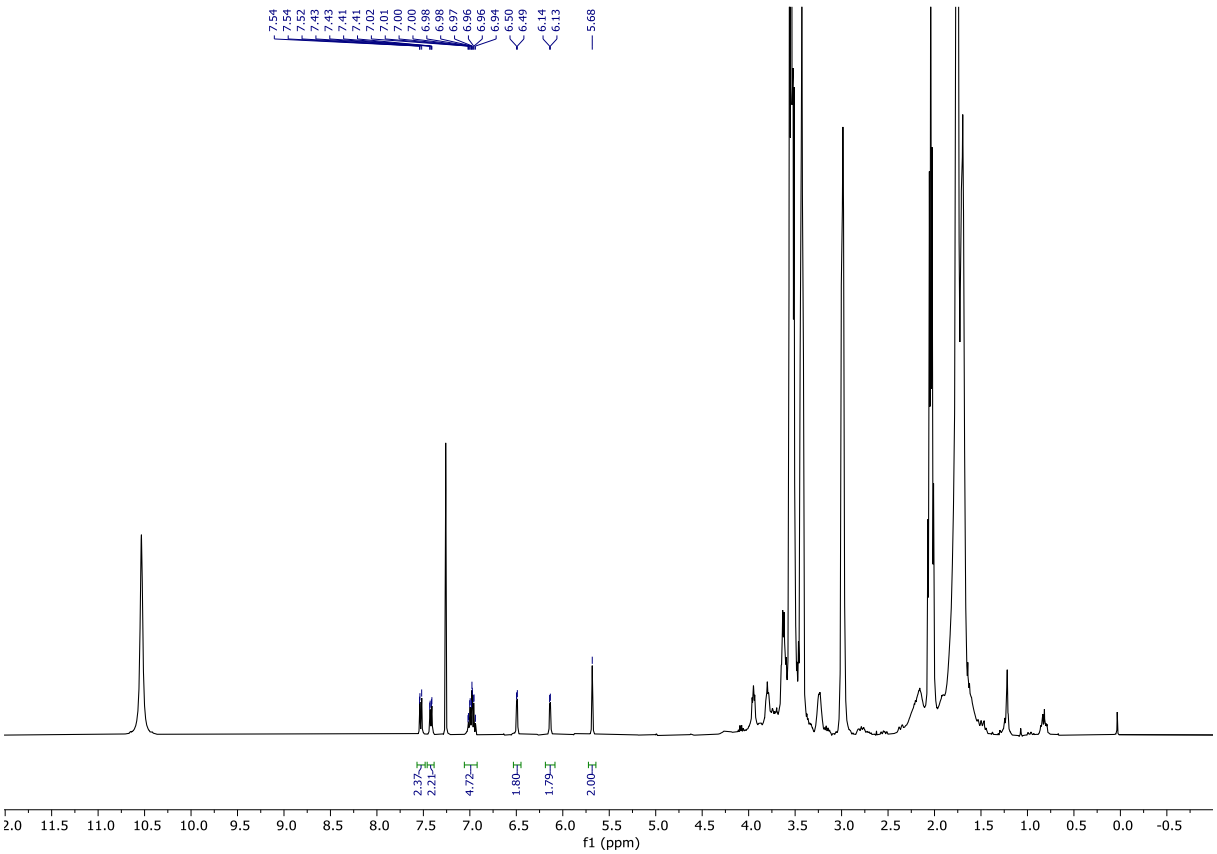

Figure S61. ^{1}H NMR spectrum of **8a** (400 MHz, $CDCl_3$, 293 K).

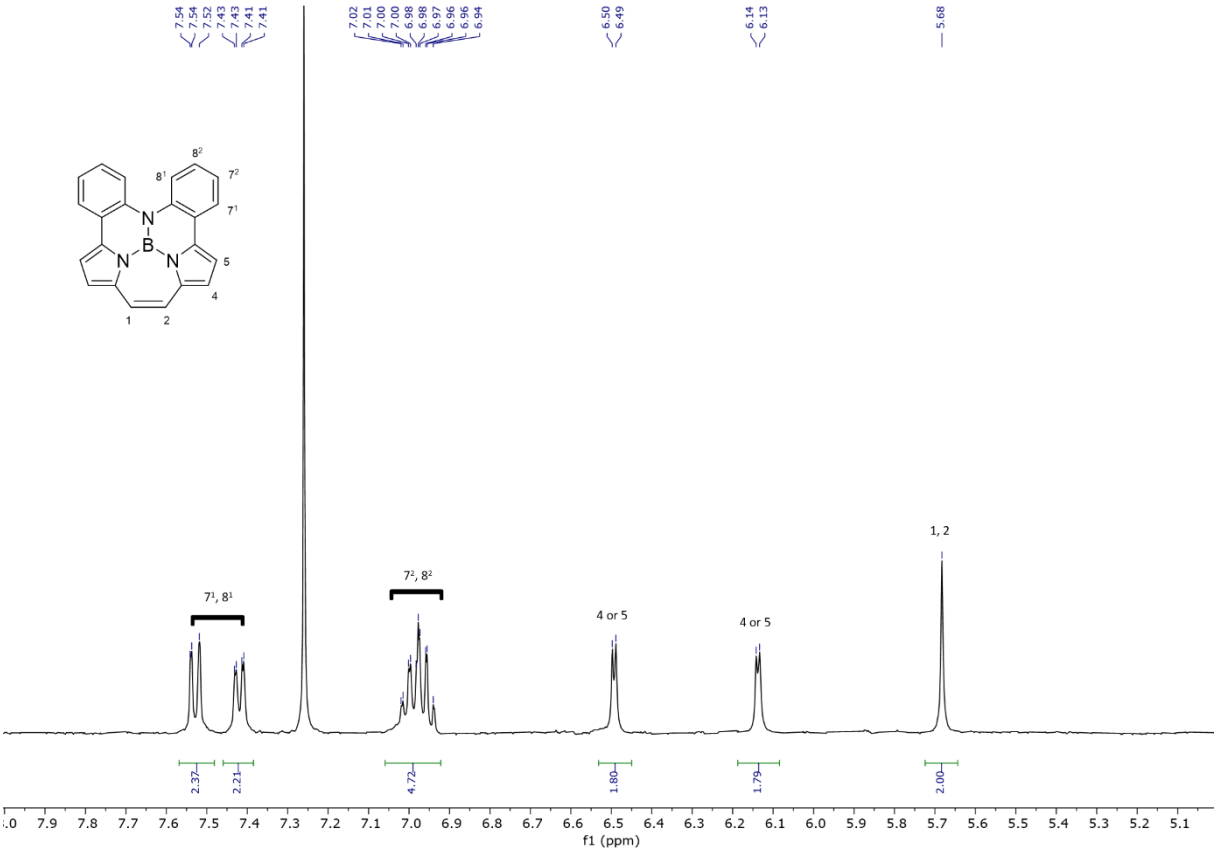

Figure S62. ^{1}H NMR spectrum of **8a** (400 MHz, $CDCl_3$, 293 K, 5.0 – 8.0 ppm region).

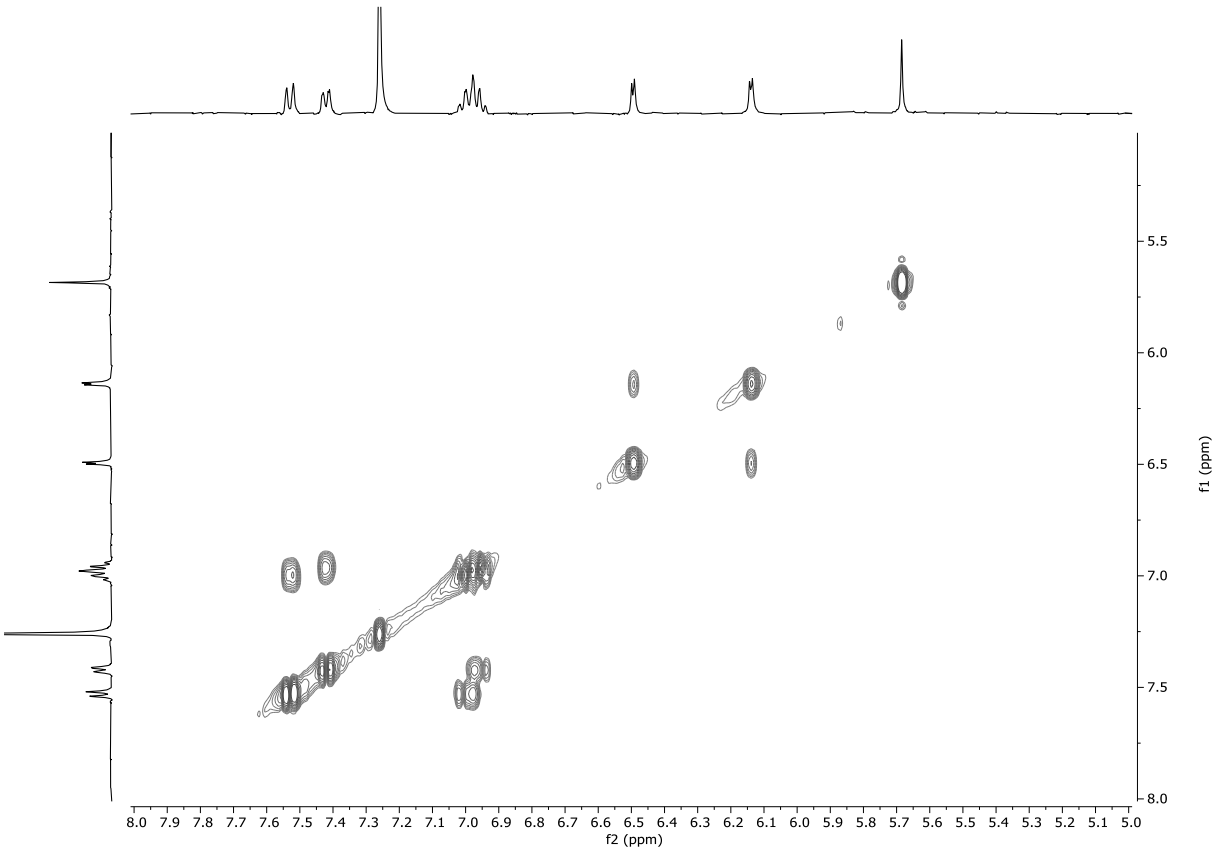

Figure S63. ^{1}H-^{1}H COSY spectrum of **8a** (400 MHz, $CDCl_3$, 293 K, 5.0 – 8.0 ppm region).

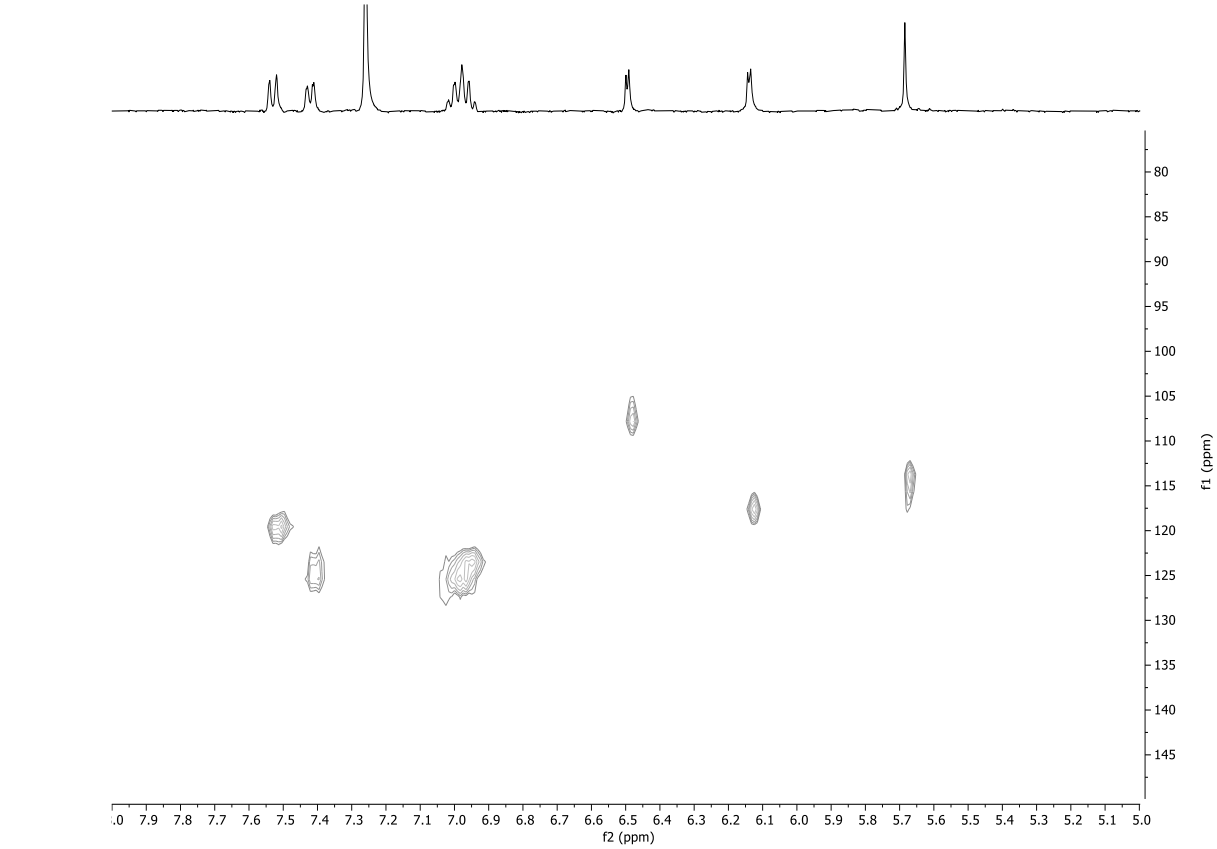

Figure S64. ^{1}H-^{13}C HMBC spectrum of **8a** (400 MHz, $CDCl_3$, 293 K, 5.0 – 8.0 & 75 – 150 ppm region).

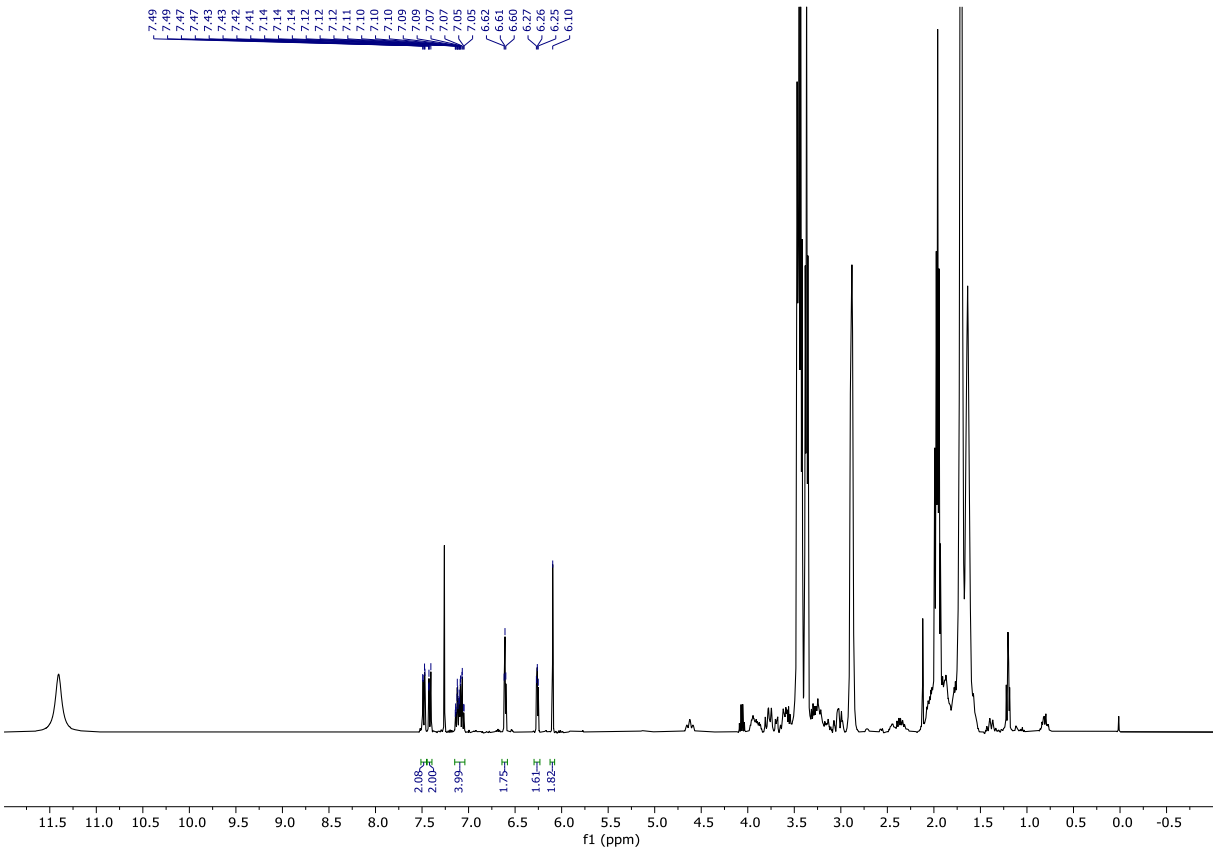

Figure S65. ^{1}H NMR spectrum of **S1** (400 MHz, $CDCl_3$, 293 K).

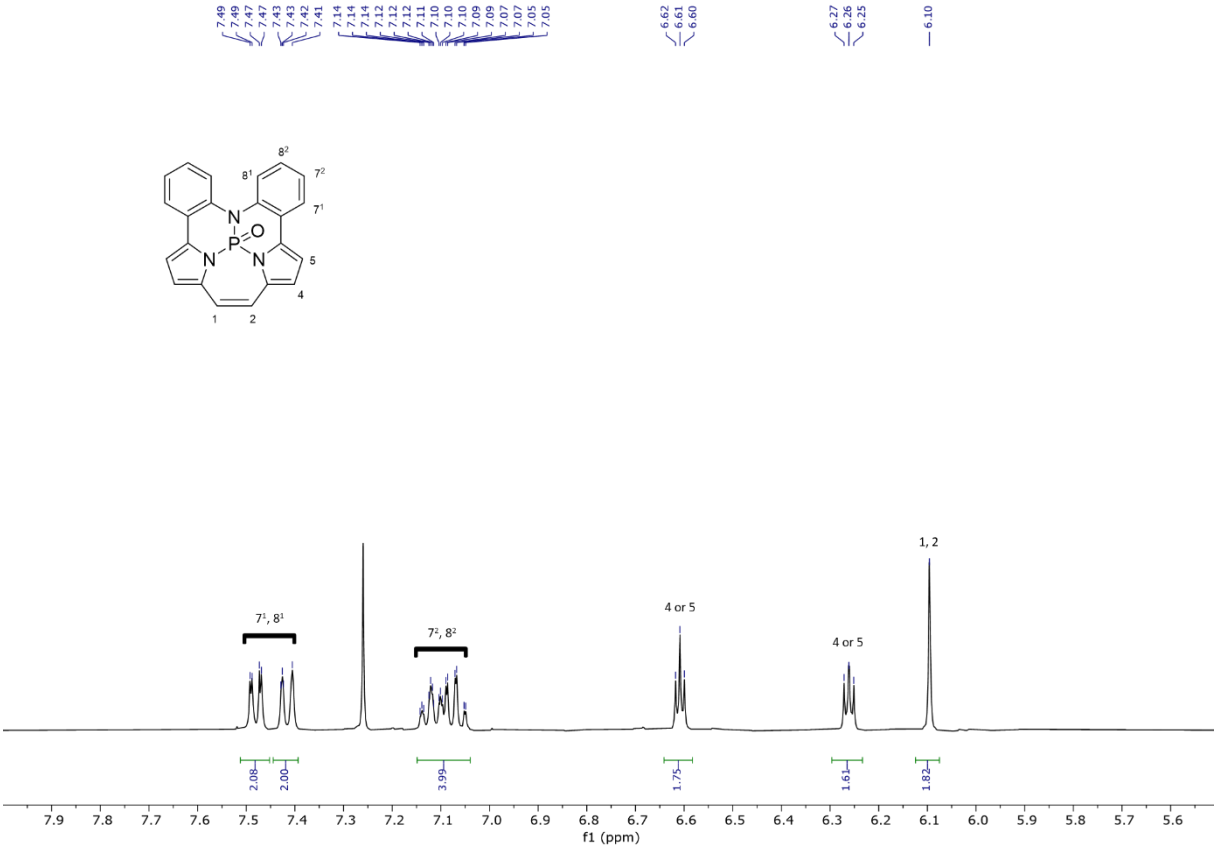

Figure S66. ^{1}H NMR spectrum of **S1** (400 MHz, $CDCl_3$, 293 K, 5.5 – 8.0 ppm region).

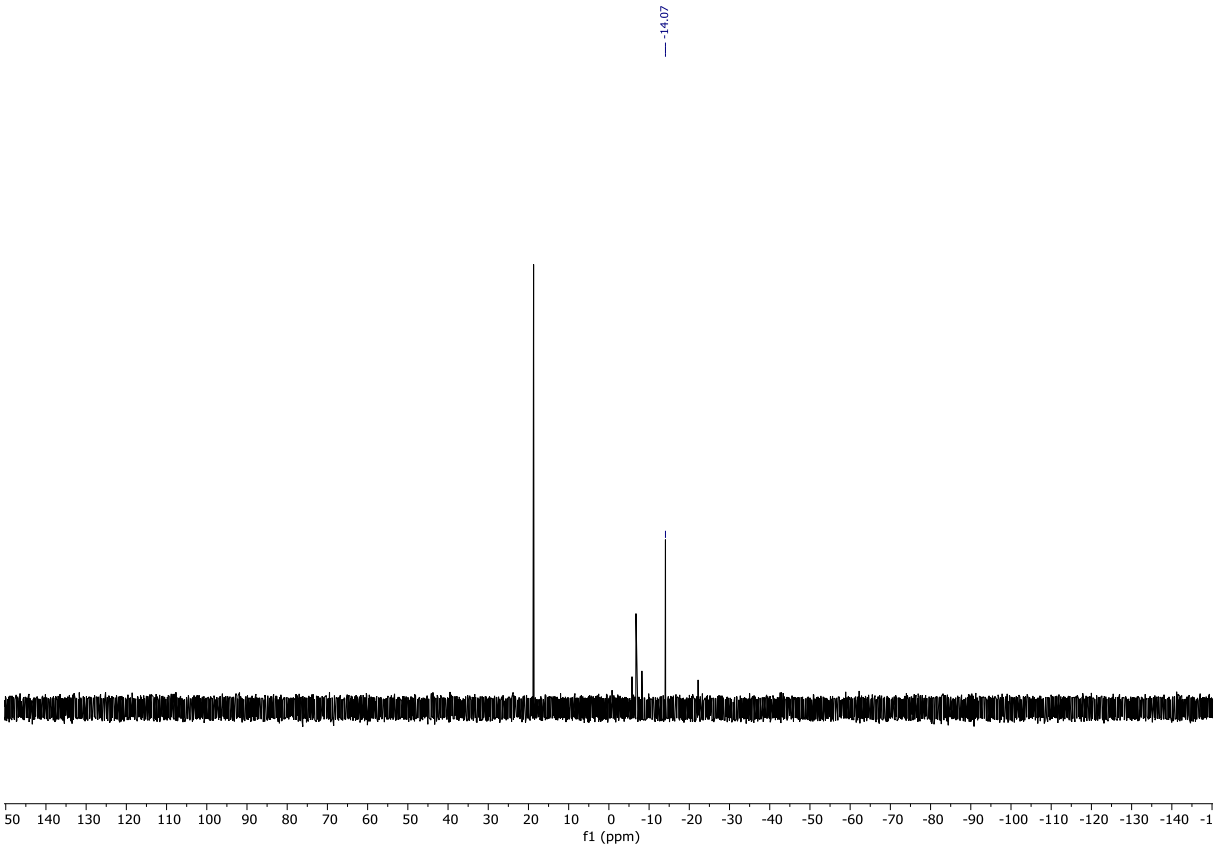

Figure S67. ^{31}P NMR spectrum of **S1** (162 MHz, $CDCl_3$, 293 K).

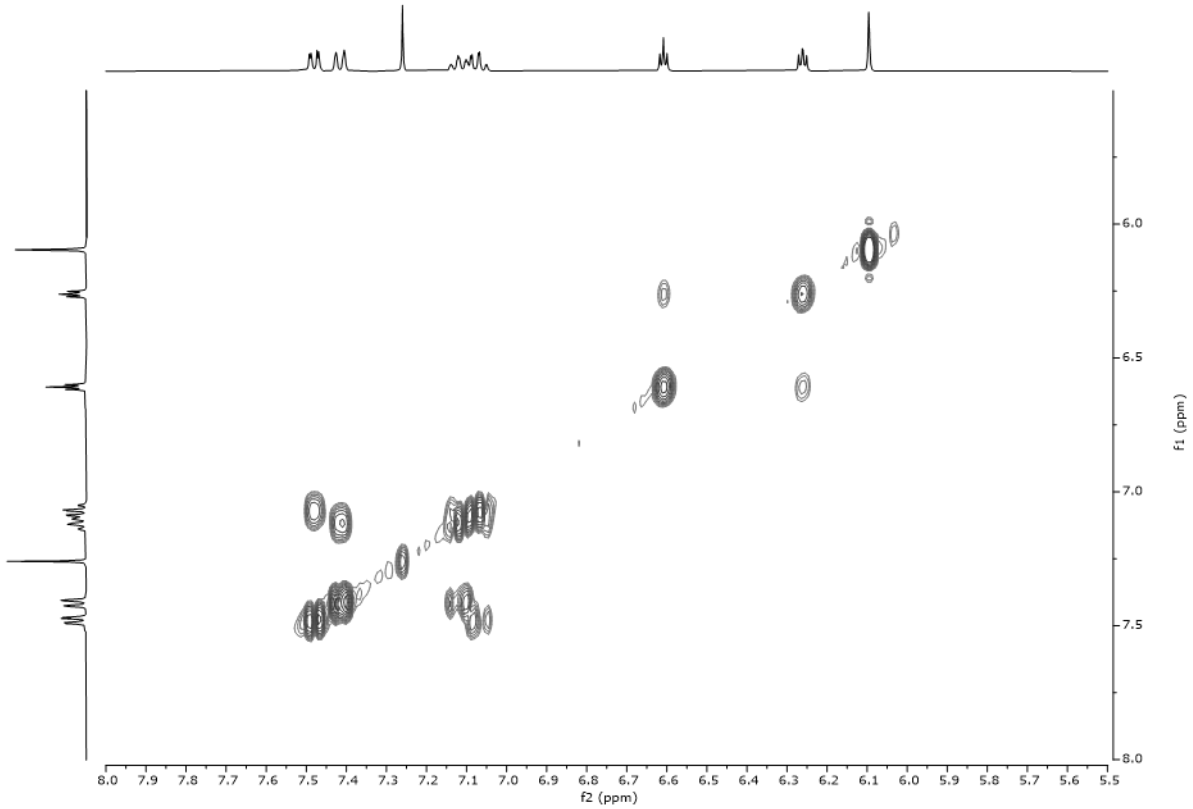

Figure S68. ^{1}H-^{1}H COSY spectrum of **S1** (400 MHz, $CDCl_3$, 293 K, 5.5 – 8.0 ppm region).

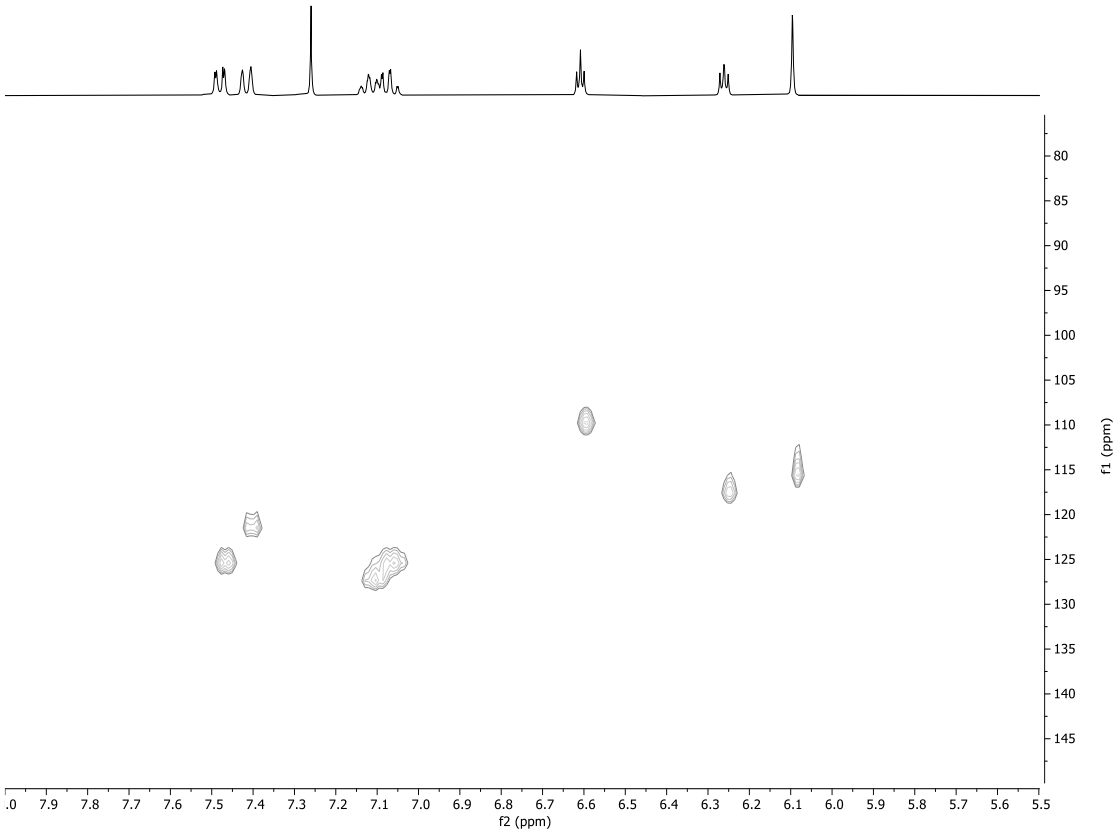

Figure S69. ^{1}H-^{13}C HMBC spectrum of **S1** (400 MHz, $CDCl_3$, 293 K, 5.5 – 8.0 & 75 – 150 ppm region).

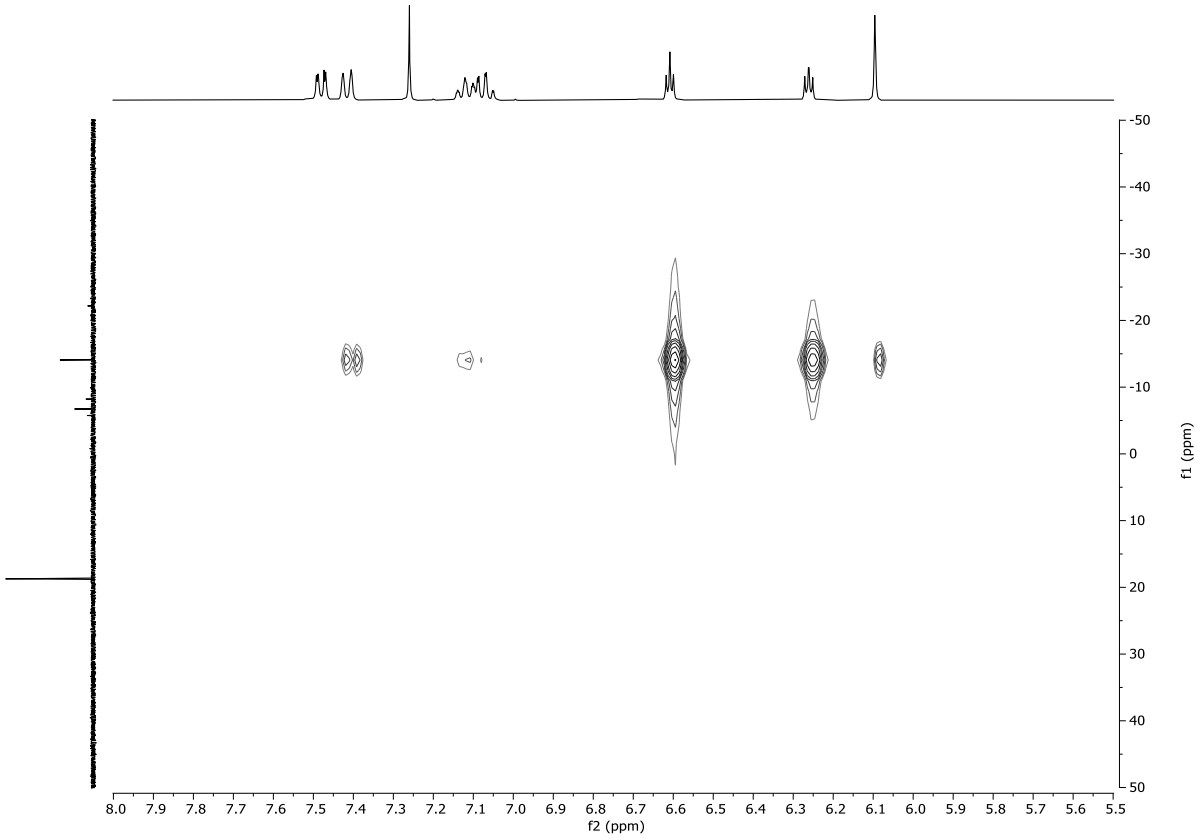

Figure S70. ^{1}H-^{31}P HMBC spectrum of **S1** (400 MHz, $CDCl_3$, 293 K, 5.5 – 8.0 & -50 – 50 ppm region).

4. MS Spectra

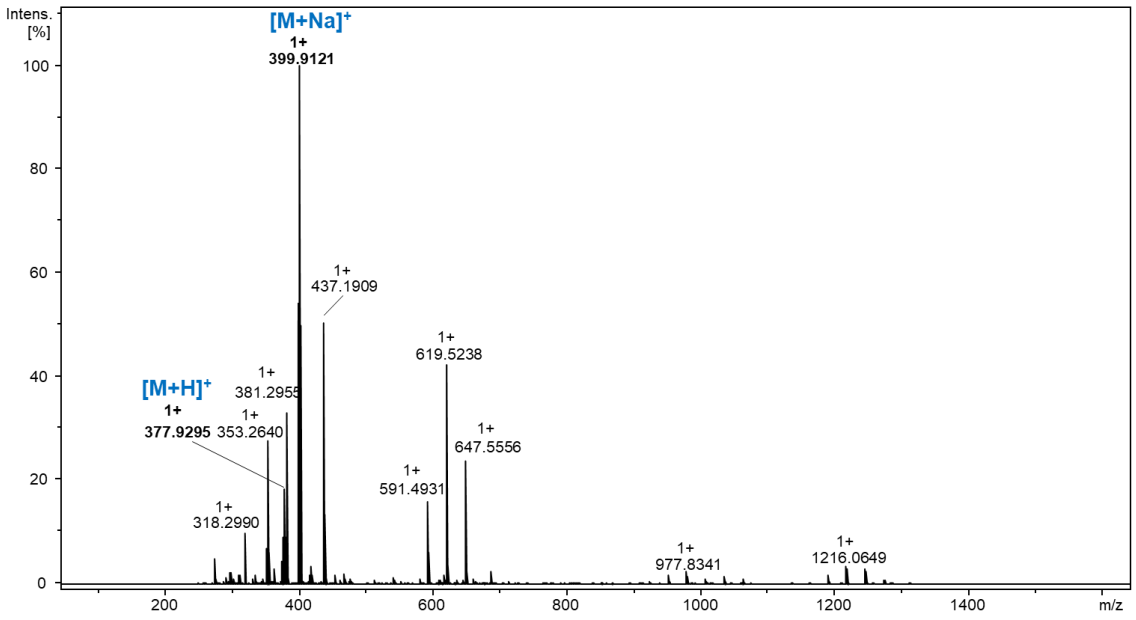

Figure S71. HRMS spectrum of **6b** (ESI ionization). Visible noise due to poor ESI ionization.

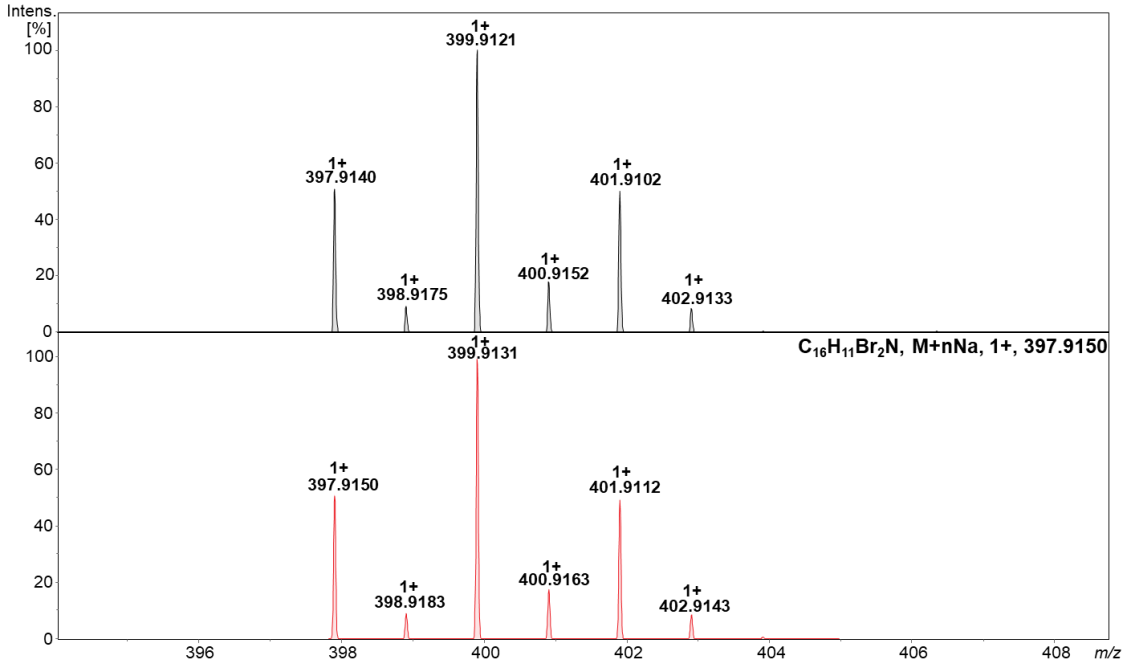

Figure S72. HRMS spectrum of **6b** – [M+Na]+ region zoom (top) and calculated isotopic pattern (bottom).

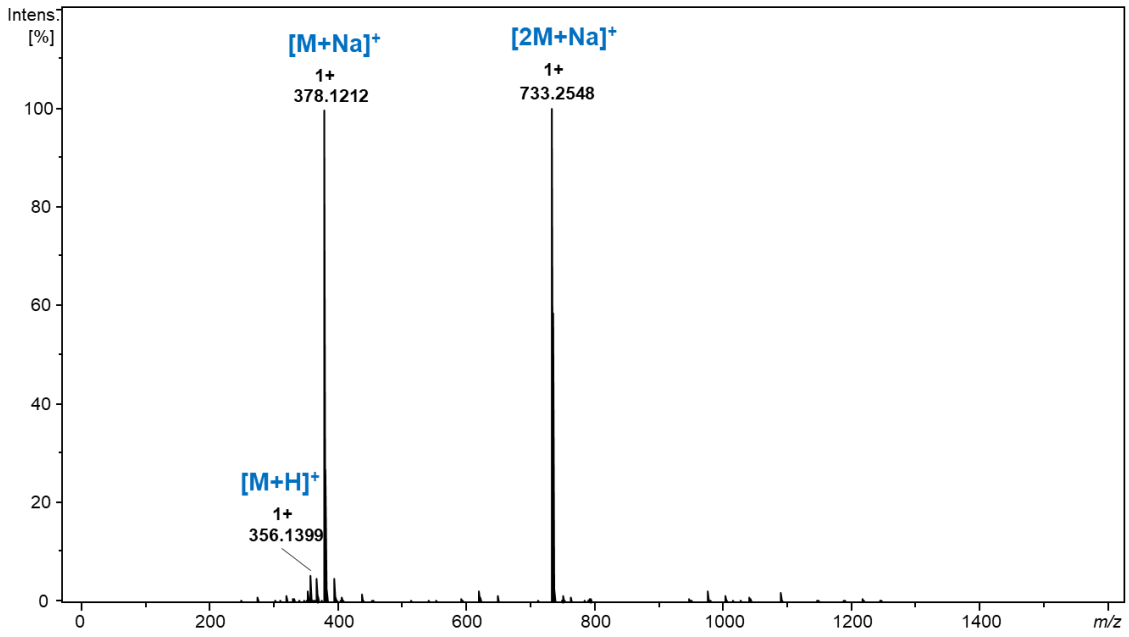

Figure S73. HRMS spectrum of **7a** (ESI ionization).

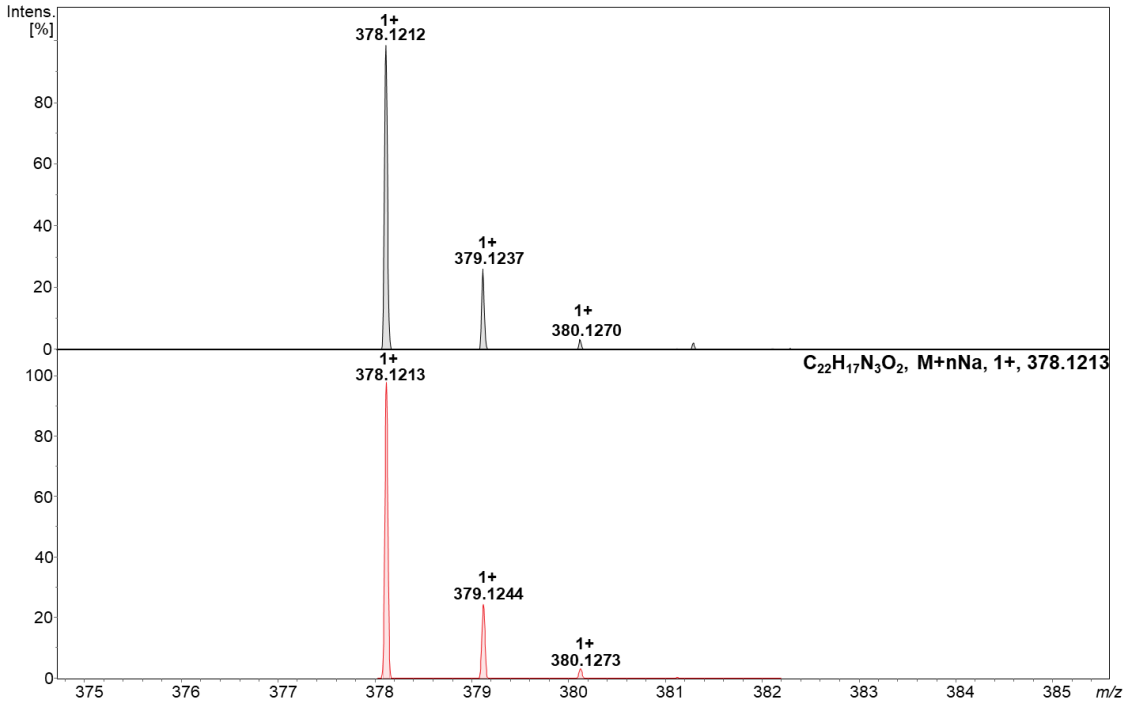

Figure S74. HRMS spectrum of **7a** – [M+Na]+ region zoom (top) and calculated isotopic pattern (bottom).

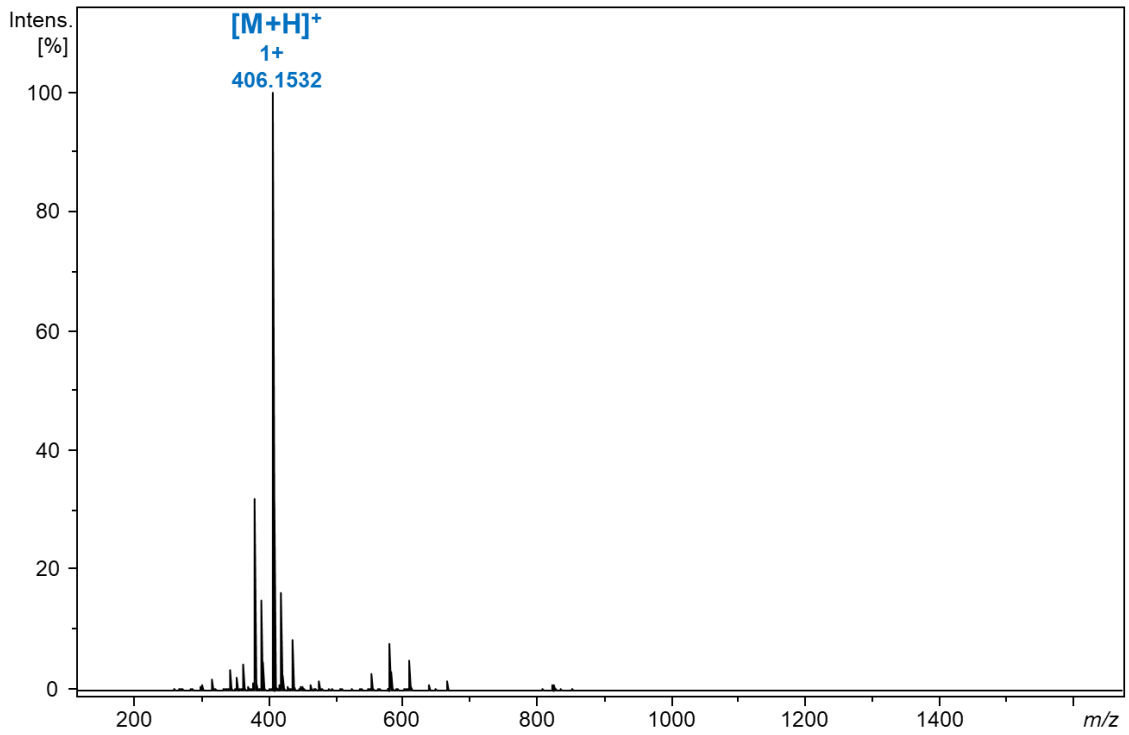

Figure S75. HRMS spectrum of **7b** (APCI ionization).

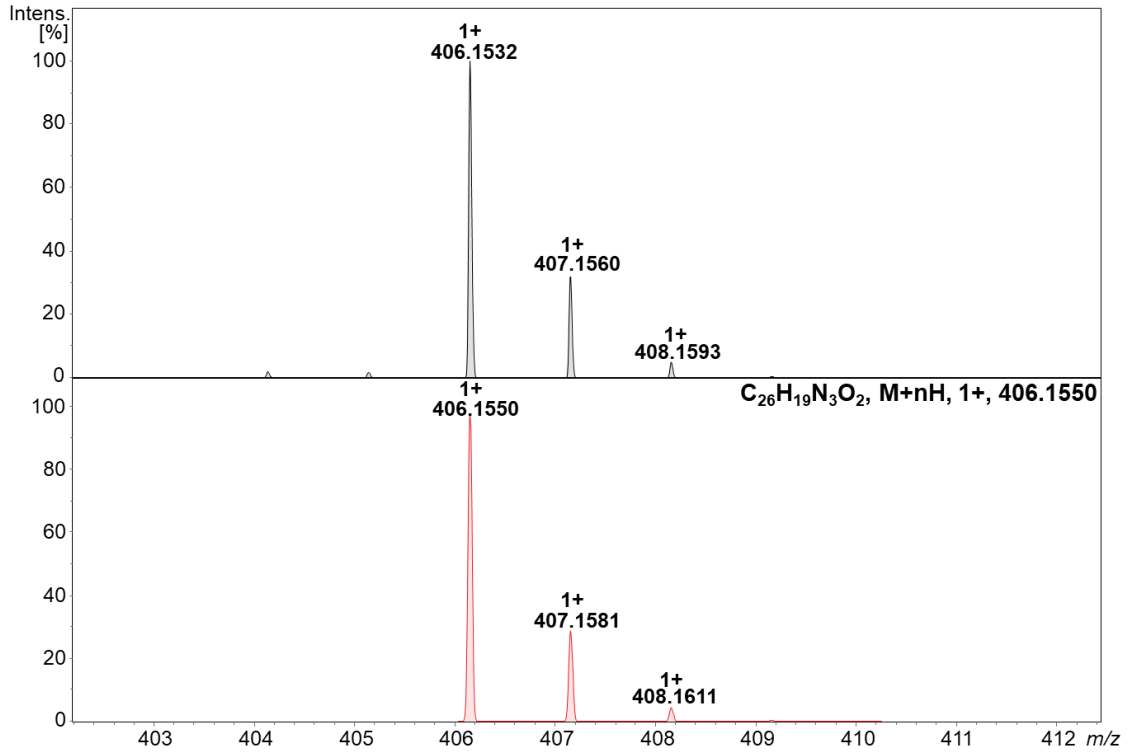

Figure S76. HRMS spectrum of **7b** – [M+H]+ region zoom (top) and calculated isotopic pattern (bottom).

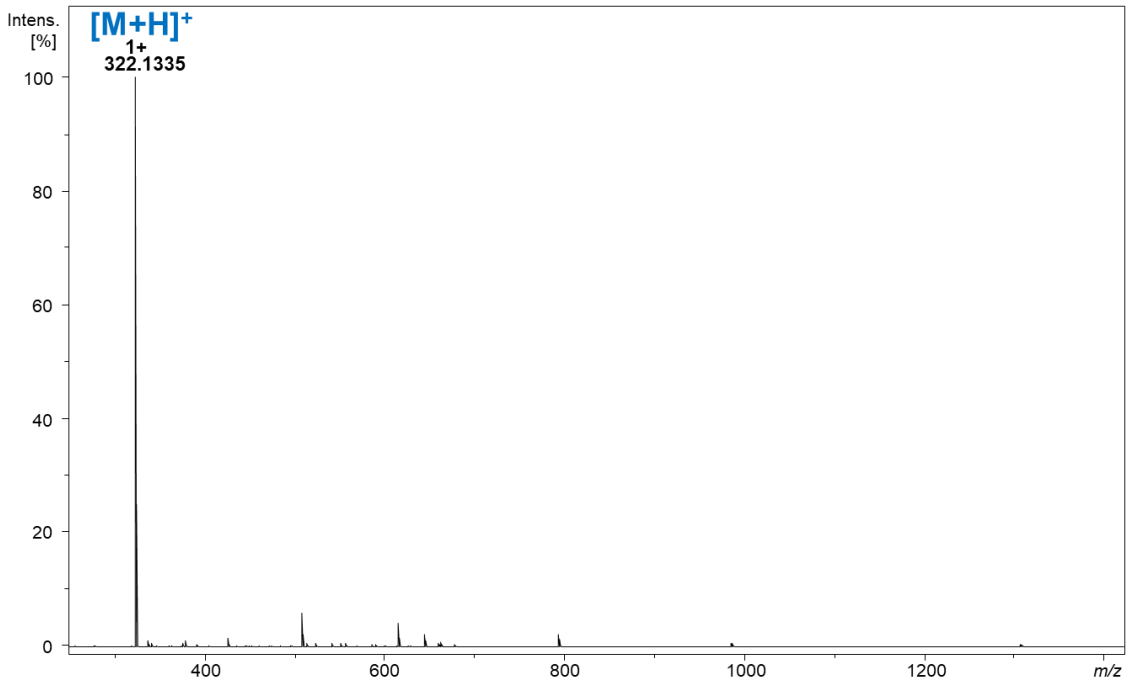

Figure S77. HRMS spectrum of **3a** (ESI ionization).

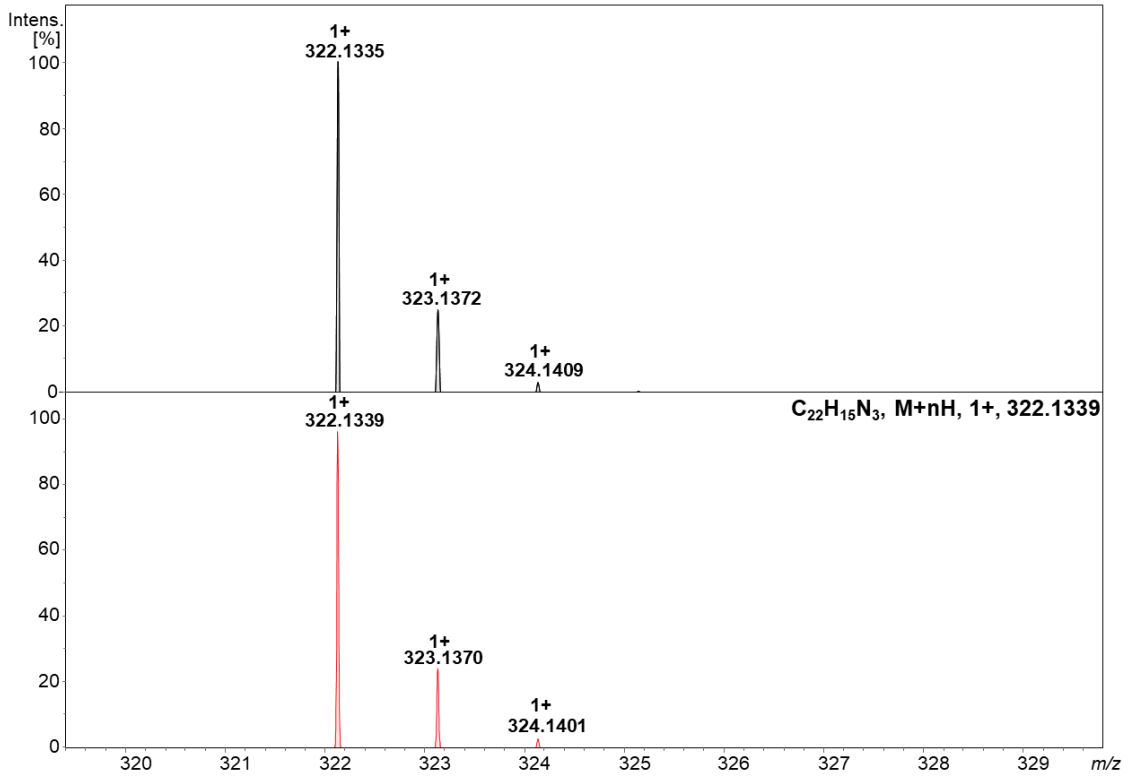

Figure S78. HRMS spectrum of **3a** – [M+H]+ region zoom (top) and calculated isotopic pattern (bottom).

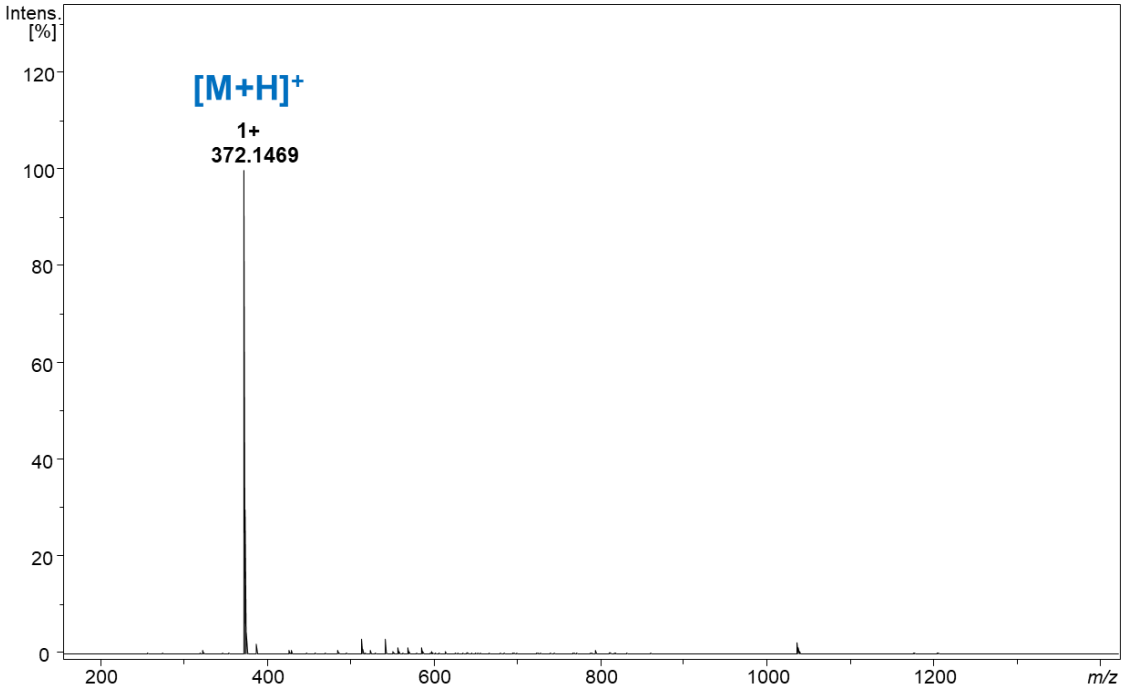

Figure S79. HRMS spectrum of **3b** (ESI ionization).

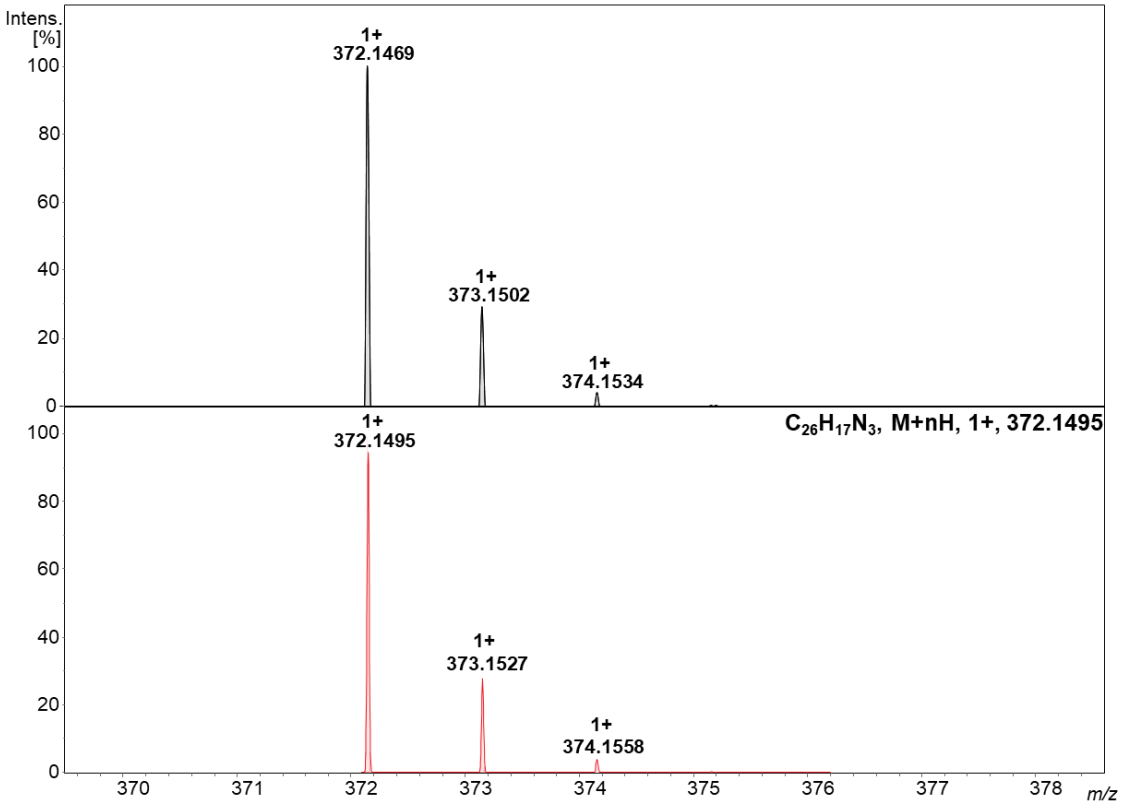

Figure S80. HRMS spectrum of **3b** – [M+H]+ region zoom (top) and calculated isotopic pattern (bottom).

5. UV-Vis Spectra

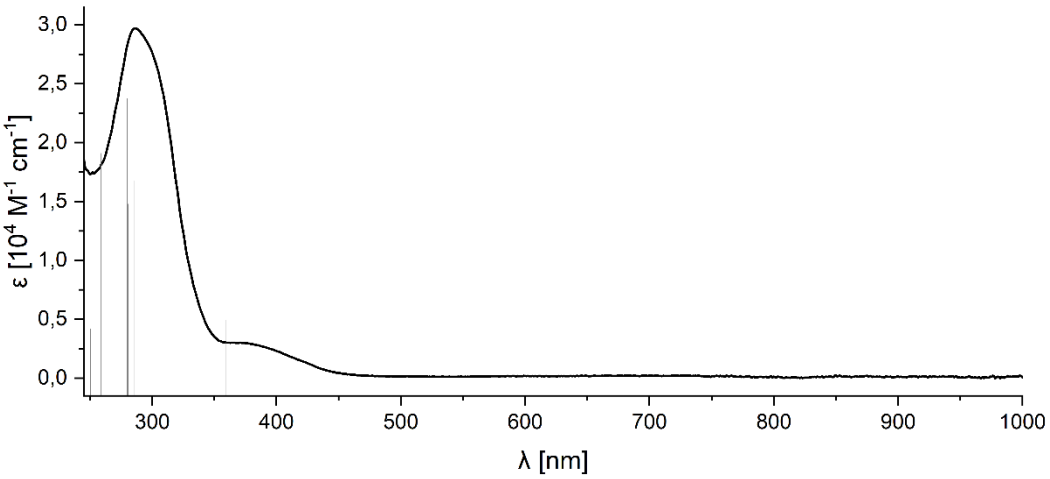

Figure S81. UV-Vis spectrum of **1a** ($CHCl_3$, 293 K) with calculated (TD-DFT, CAM-B3LYP/6-311G(d,p), PCM = chloroform, GD3BJ empirical dispersion correction) electronic transitions (vertical lines).

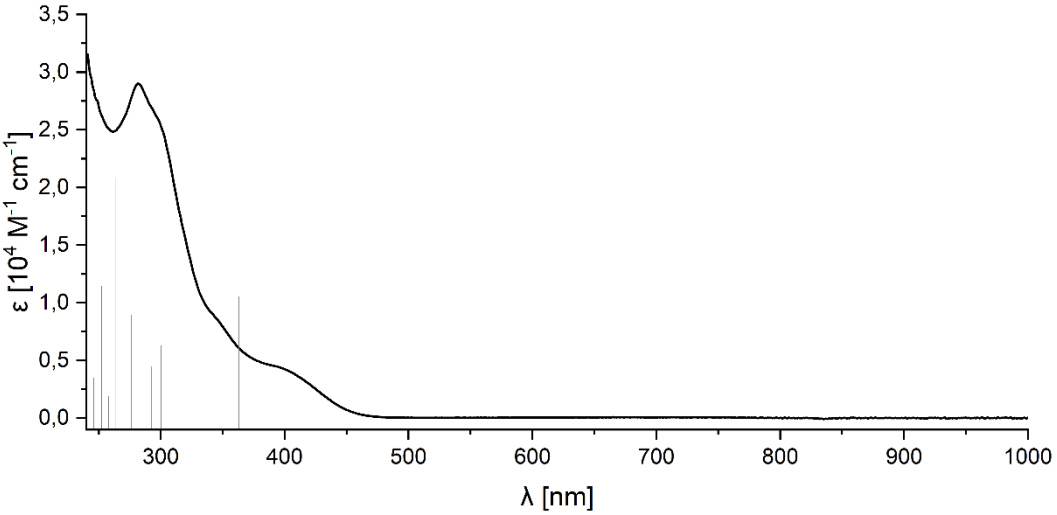

Figure S82. UV-Vis spectrum of **1b** ($CHCl_3$, 293 K) with calculated (TD-DFT, CAM-B3LYP/6-311G(d,p), PCM = chloroform, GD3BJ empirical dispersion correction) electronic transitions (vertical lines).

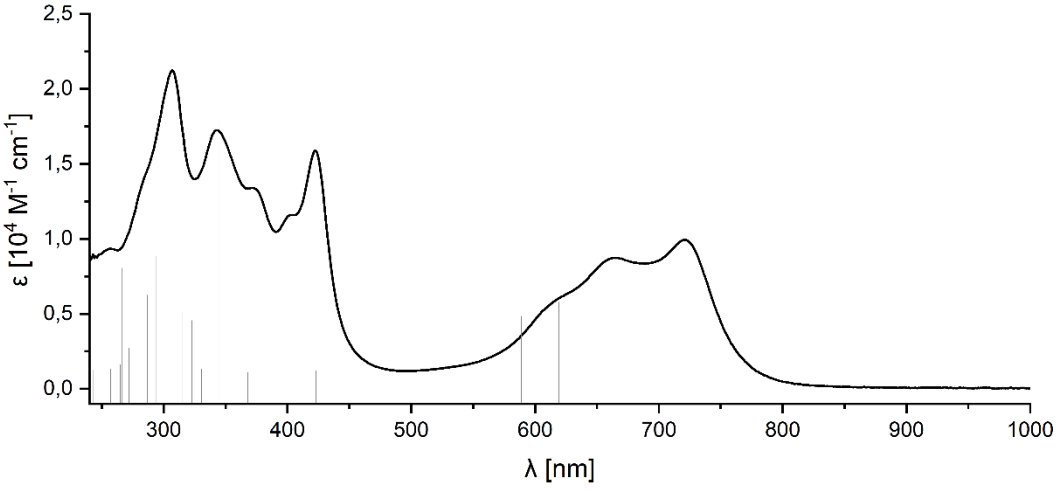

Figure S83. UV-Vis spectrum of **3a** ($CHCl_3$, 293 K) with calculated (TD-DFT, CAM-B3LYP/6-311G(d,p), PCM = chloroform, GD3BJ empirical dispersion correction) electronic transitions (vertical lines).

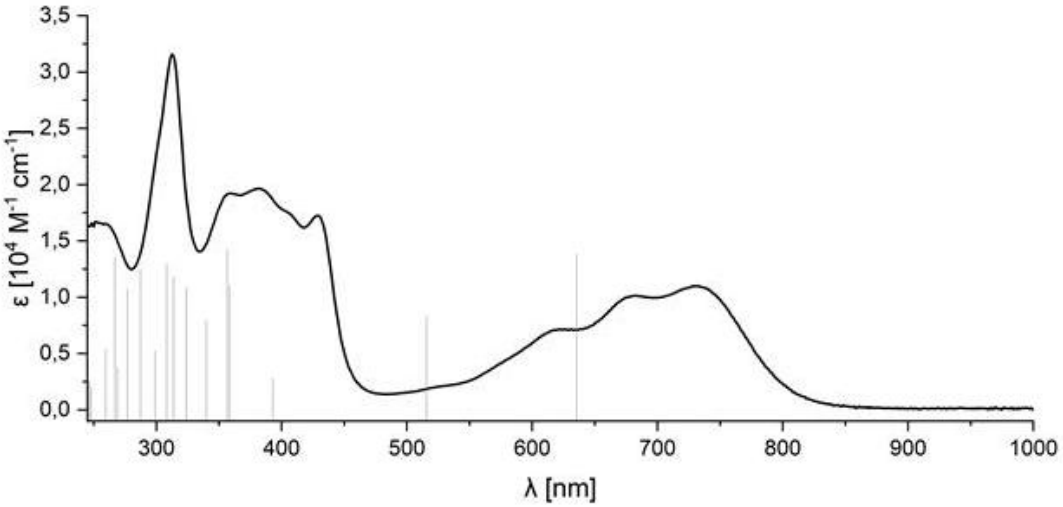

Figure S84. UV-Vis spectrum of **3b** ($CHCl_3$, 293 K) with calculated (TD-DFT, CAM-B3LYP/6-311G(d,p), PCM = chloroform, GD3BJ empirical dispersion correction) electronic transitions (vertical lines).

6. EPR Spectra

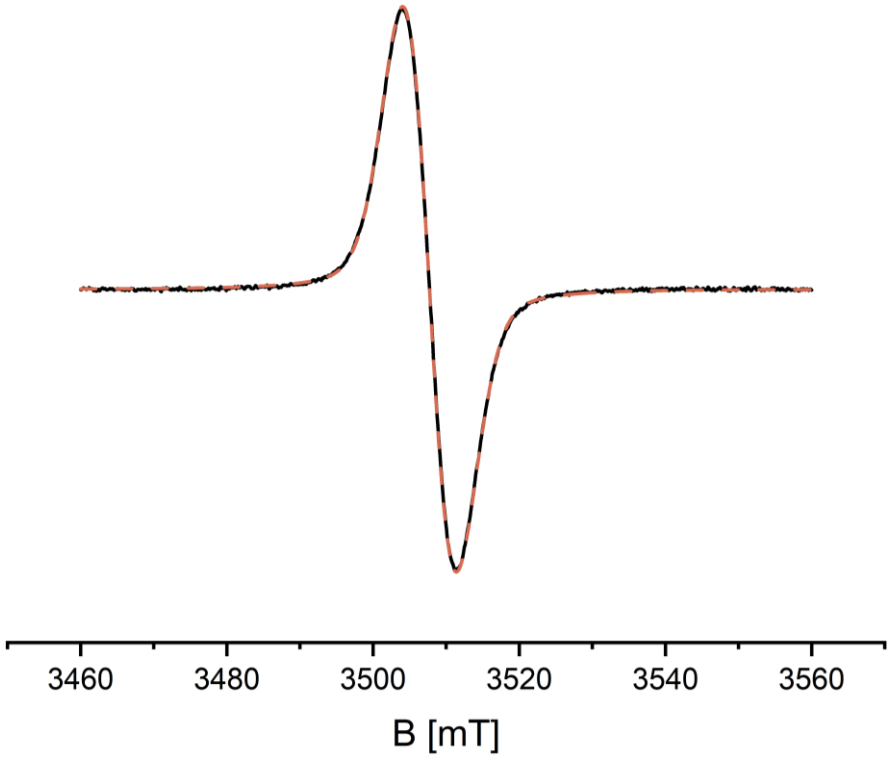

Figure S85. EPR spectrum of **2a** (benzene, 293 K) – experimental (solid black) and simulation (dashed red).

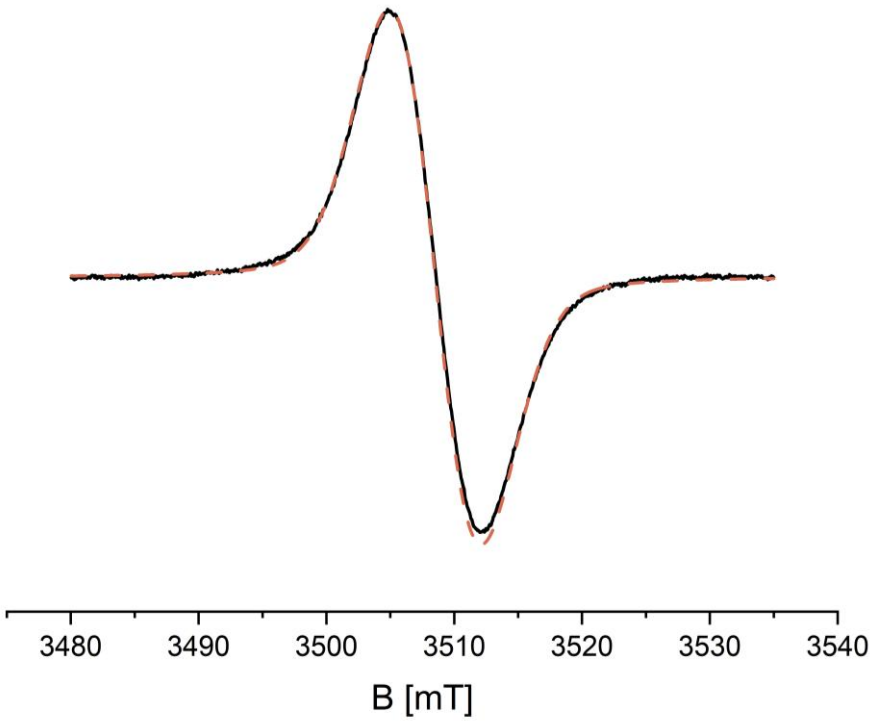

Figure S86. EPR spectrum of **2b** (benzene, 293 K) – experimental (solid black) and simulation (dashed red).

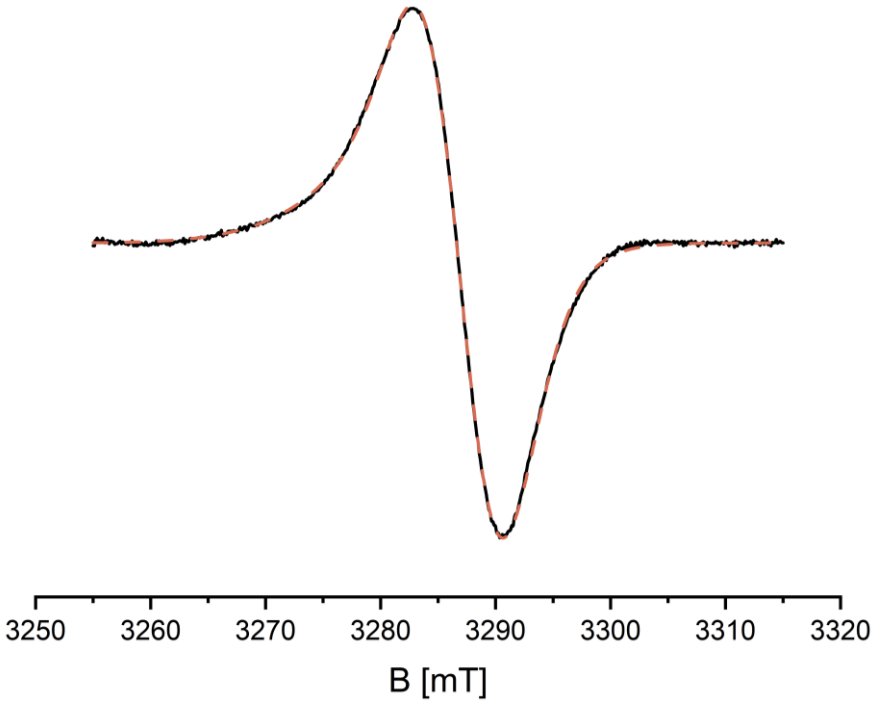

Figure S87. EPR spectrum of **9a** ($CHCl_3$, 120 K) – experimental (solid black) and simulation (dashed red).

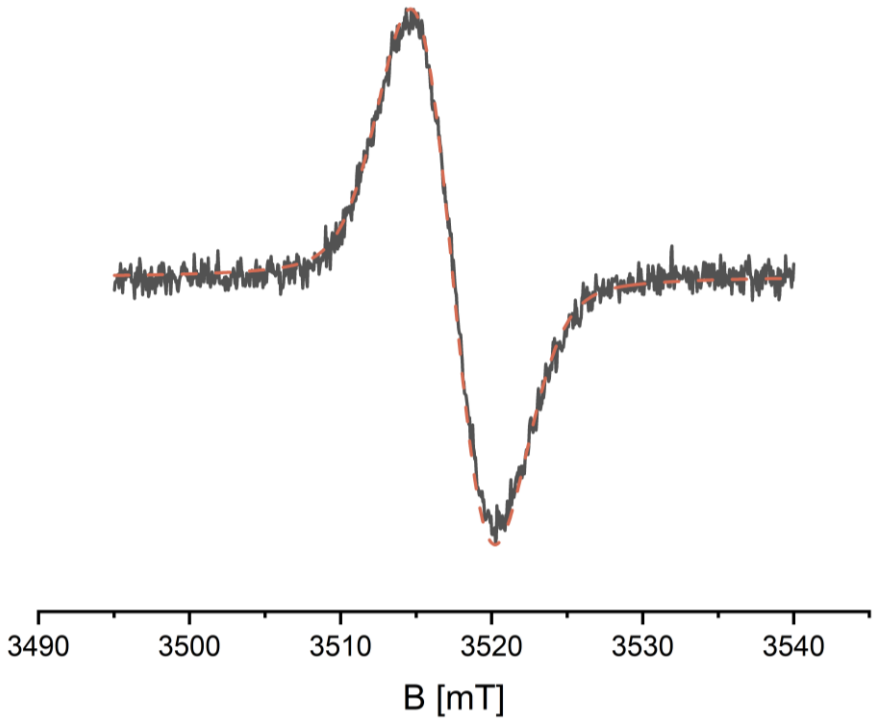

Figure S88. EPR spectrum of **S2** ($CHCl_3$, 293 K) – experimental (solid black) and simulation (dashed red).

7. Cyclic Voltammograms

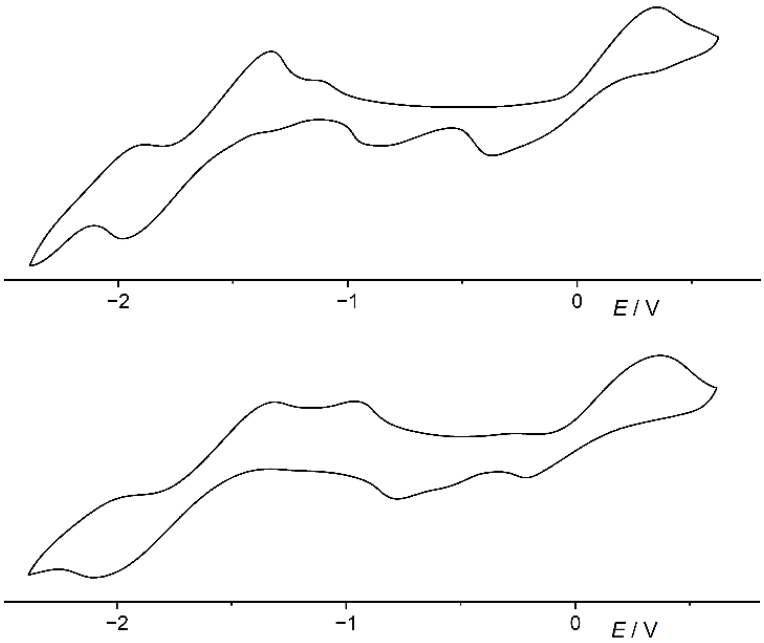

Figure S89. Cyclic voltammetry of **3a** and **3b**. Conditions: DCM, Bu_4NBF_4, GC working electrode, 293 K, calibrated to Fc/Fc^+.

8. X-Ray Crystallography Data

Identification code	**1b**
Empirical formula	$C_{26}H_{19}N_3$
CCDC number	**2477813**
Formula weight	373.44
Temperature [K]	100(1)
Wavelength [Å]	0.71073
Crystal system, space group	orthorhombic, *Pca2₁*
Unit cell dimensions [Å] and [°]	a = 12.3366(4) α = 90 b = 19.8244(6) β = 90 c = 7.4816(2) γ = 90
Volume [Å^3]	1829.74(9)
Z, Calculated density [Mg·m^{-3}]	4, 1.356
Absorption coefficient [mm^{-1}]	0.081
F(000)	784.0
Crystal size [mm]	0.20 × 0.05 × 0.03
2Θ range for data collection [°]	4.11 to 51.35
Limiting indices	-15 ≤ h ≤ 15 -24 ≤ k ≤ 24 -9 ≤ l ≤ 8
Reflections collected/unique	45762/3461 (R_{int} = 0.1091)
Completeness [%] to theta [°]	100.0 to 25.68
Absorption correction	multi-scan
Max. and min. transmission	0.745/0.701
Refinement method	Full-matrix least-squares on F^2
Data/restraints/parameters	3461/1/268
Goodness-of-fit on F^2	1.047
Final R indices [I>2σ(I)]	R_1 = 0.0307, wR_2 = 0.0670
R indices (all data)	R_1 = 0.0368, wR_2 = 0.0691
Largest diff. peak and hole [eÅ^{-3}]	0.12/-0.17

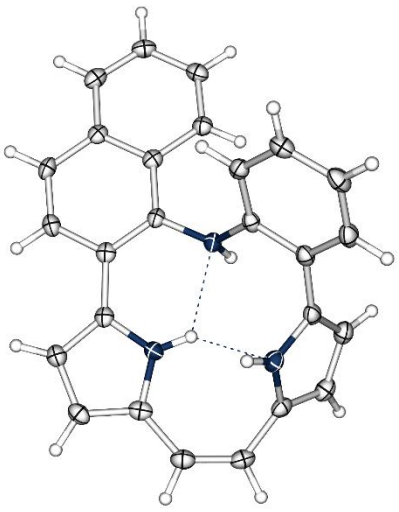

Figure S90. Crystal structure of **1b** with thermal ellipsoids at 50% of probability.

Identification code	**3b**
Empirical formula	$C_{26}H_{17}N_3$
CCDC number	**2392444**
Formula weight	371.42
Temperature [K]	120(1)
Wavelength [Å]	0.71073
Crystal system, space group	monoclinic, $P2_1/n$
Unit cell dimensions [Å] and [°]	a = 5.9210(4) α = 90 b = 13.6349(8) β = 96.426(3) c = 22.0309(15) γ = 90
Volume [Å^3]	1767.4(2)
Z, Calculated density [Mg·m^{-3}]	4, 1.396
Absorption coefficient [mm^{-1}]	0.083
F(000)	776.0
Crystal size [mm]	0.40 × 0.05 × 0.03
2Θ range for data collection [°]	4.772 to 55.748
Limiting indices	-7 ≤ h ≤ 7 -17 ≤ k ≤ 17 -28 ≤ l ≤ 28
Reflections collected/unique	24221/4196 (R_{int} = 0.0555)
Completeness [%] to theta [°]	99.7 to 27.87
Absorption correction	multi-scan
Max. and min. transmission	0.746/0.702
Refinement method	Full-matrix least-squares on F^2
Data/restraints/parameters	4196/0/266
Goodness-of-fit on F^2	1.026
Final R indices [I>2σ(I)]	R_1 = 0.0436, wR_2 = 0.0961
R indices (all data)	R_1 = 0.0585, wR_2 = 0.1045
Largest diff. peak and hole [eÅ^{-3}]	0.26/-0.21

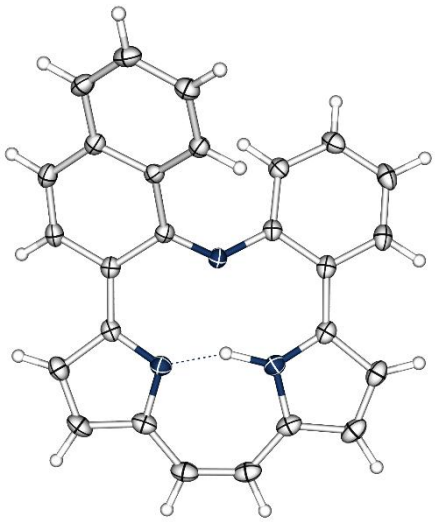

Figure S91. Crystal structure of **3b** with thermal ellipsoids at 50% of probability.

9. Theoretical Calculations

9.1. DFT Models

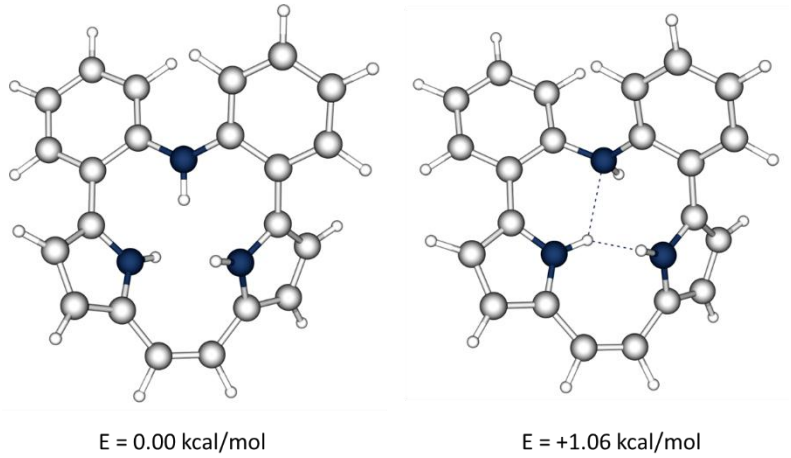

Figure S92. DFT models of **1a** tautomers (CAM-B3LYP/6-31G(d,p), PCM = chloroform, GD3BJ empirical dispersion correction).

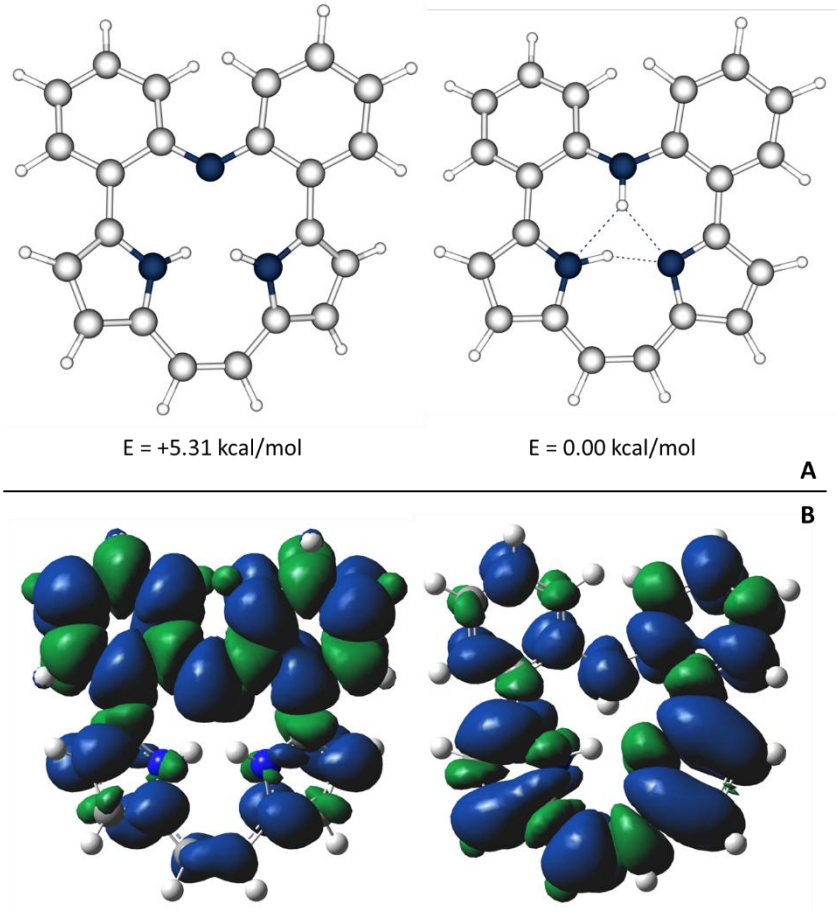

Figure S93. DFT models of **2a** tautomers (trace **A**) with spin density visualization (trace **B**) (CAM-B3LYP/6-31G(d,p), PCM = chloroform, GD3BJ empirical dispersion correction, iso-value 0.0004).

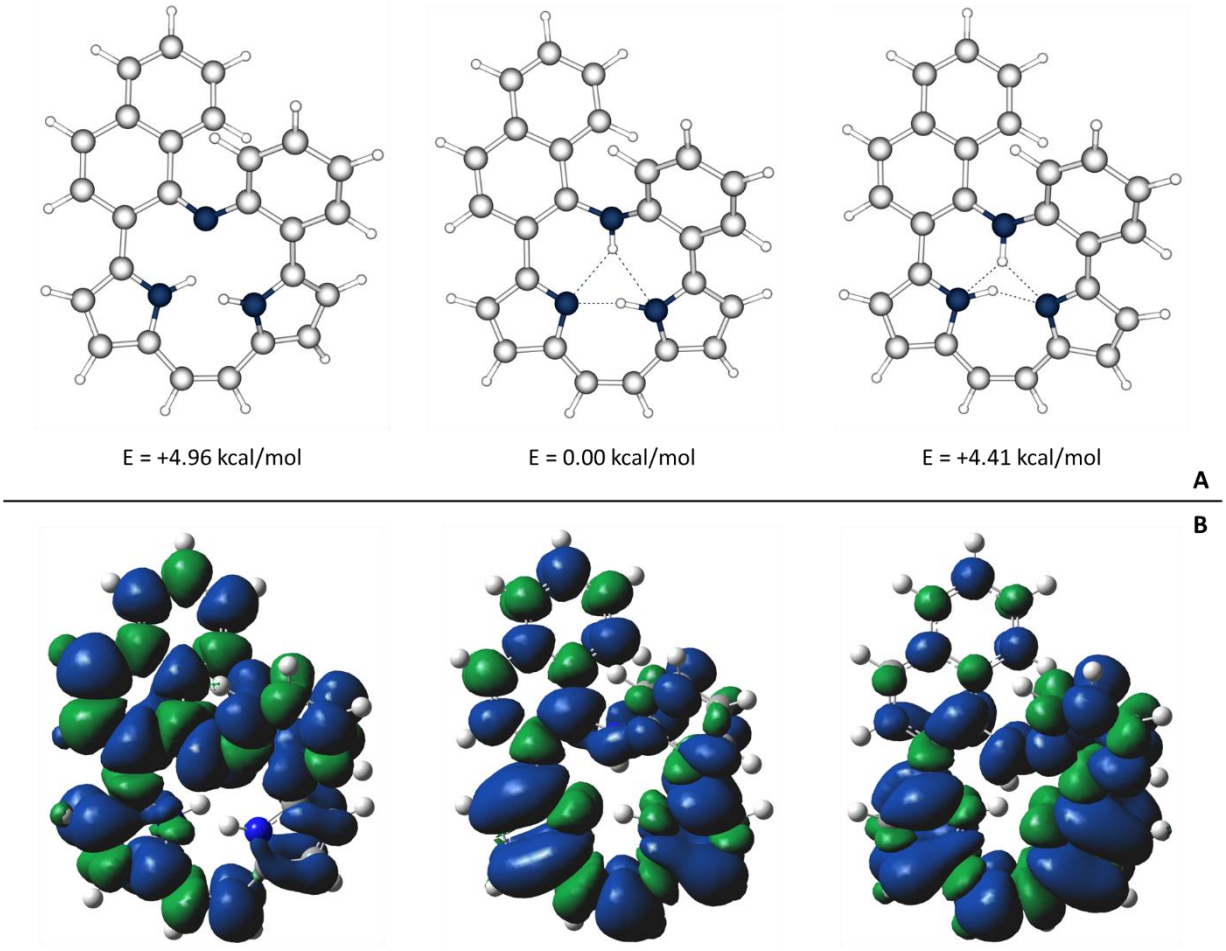

Figure S94. DFT models of **2b** tautomers (trace **A**) with spin density visualization (trace **B**) (CAM-B3LYP/6-31G(d,p), PCM = chloroform, GD3BJ empirical dispersion correction, iso-value 0.0004).

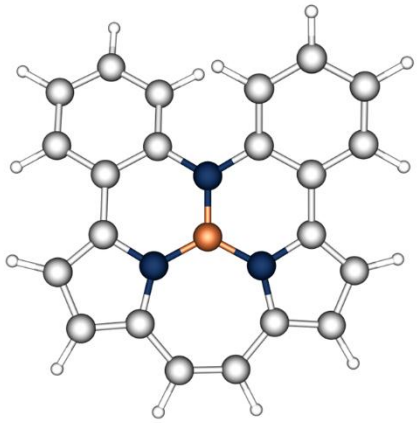

Figure S95. DFT model of **8a** (CAM-B3LYP/6-31G(d,p), PCM = chloroform, GD3BJ empirical dispersion correction).

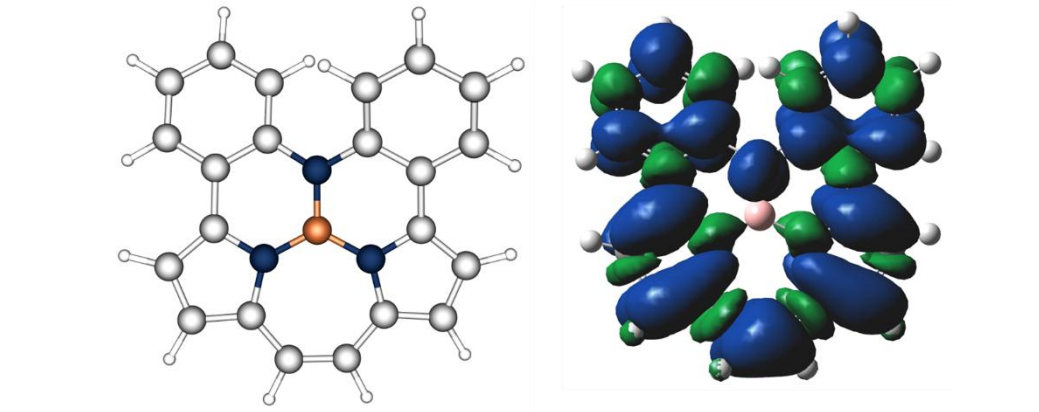

Figure S96. DFT model of **9a** with spin density visualization (CAM-B3LYP/6-31G(d,p), PCM = chloroform, GD3BJ empirical dispersion correction, iso-value 0.0004).

9.2. Frontier Orbitals

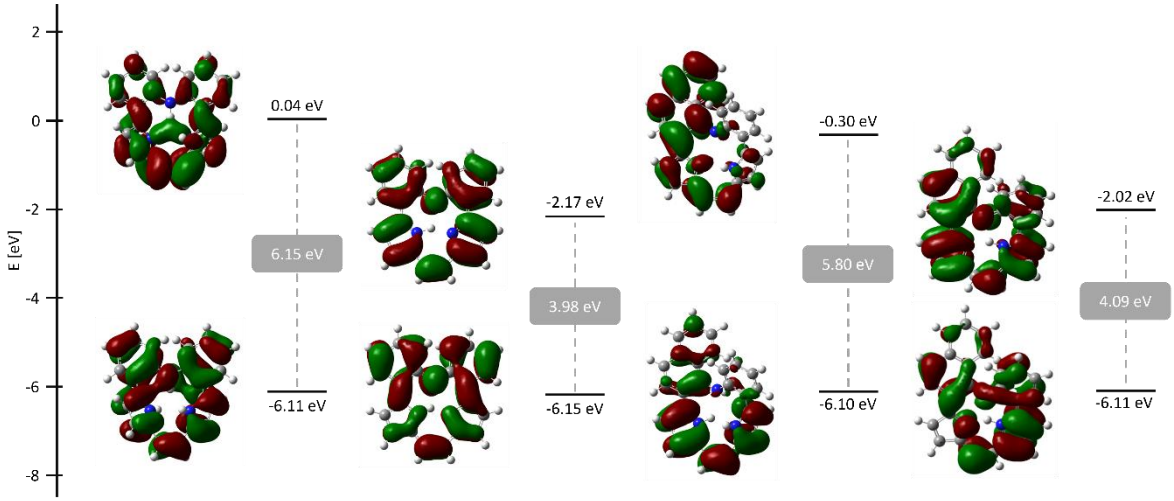

Figure S97. DFT model of HOMO and LUMO orbitals of **1a**, **3a**, **1b**, and **3b** (CAM-B3LYP/6-31G(d,p), PCM = chloroform, GD3BJ empirical dispersion correction, iso-value 0.02).

9.3. Cartesian Coordinates

Cartesian coordinates are available in the form of pdb files.

9.4. EPR Hyperfine Coupling Constants

Compound	Atom	Anisotropic Spin Dipole Couplings [Gauss]		
		Baa	*Bbb*	*Bcc*
2a (more stable tautomer)	N15	-0.450	0.222	0.228
	N16	-0.893	-0.868	1.761
	N17	-2.119	1.030	1.089
2a (less stable tautomer)	N15	-0.135	0.033	0.102
	N16	-7.257	-7.122	14.379
	N17	-0.135	0.033	0.102
5a	N15	-0.568	0.254	0.315
	N16	-0.737	-0.703	1.440
	N17	-0.568	0.254	0.315
	B	-0.348	0.095	0.253

Table S1. Hyperfine coupling constants for heteroatoms (CAM-B3LYP/EPR-II, PCM = chloroform).

9.5. Atoms in Molecules Analysis

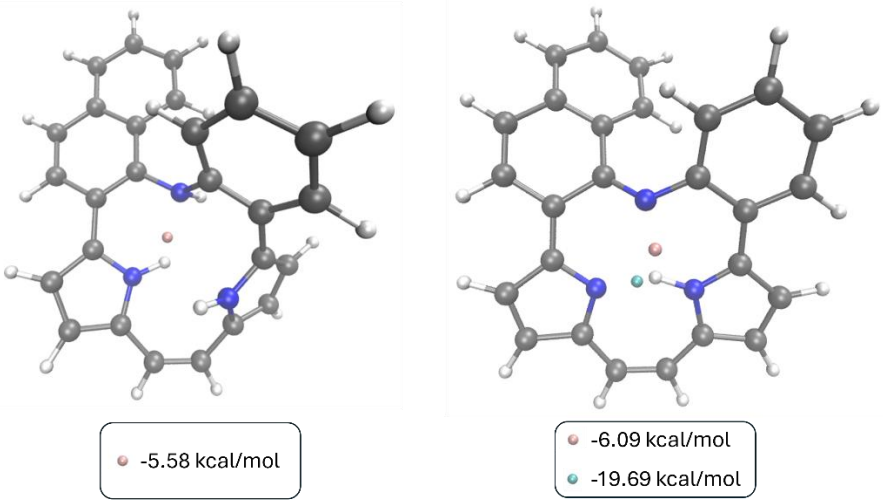

Figure S98. Critical points (3, -1) of hydrogen bonds within cavities of **1b** and **3b** (AIM, CAM-B3LYP/6-31G(d,p), PCM = chloroform, GD3BJ empirical dispersion correction).

10. Studies of Open-Shell Species Formation

10.1. Formation of 2b from 1b in Chloroform

The NMR sample of **1b** was prepared in $CDCl_3$. The reaction was carried out according to the procedure **GP4**. NMR spectra were recorded at regular time intervals, as shown in **Fig. S99**. A slow disappearance of **1b** was observed, and after 120 h traces of **3b** appeared. EPR spectrum was recorded after 120 h (**Fig. S86**), indicating the presence of **2b**.

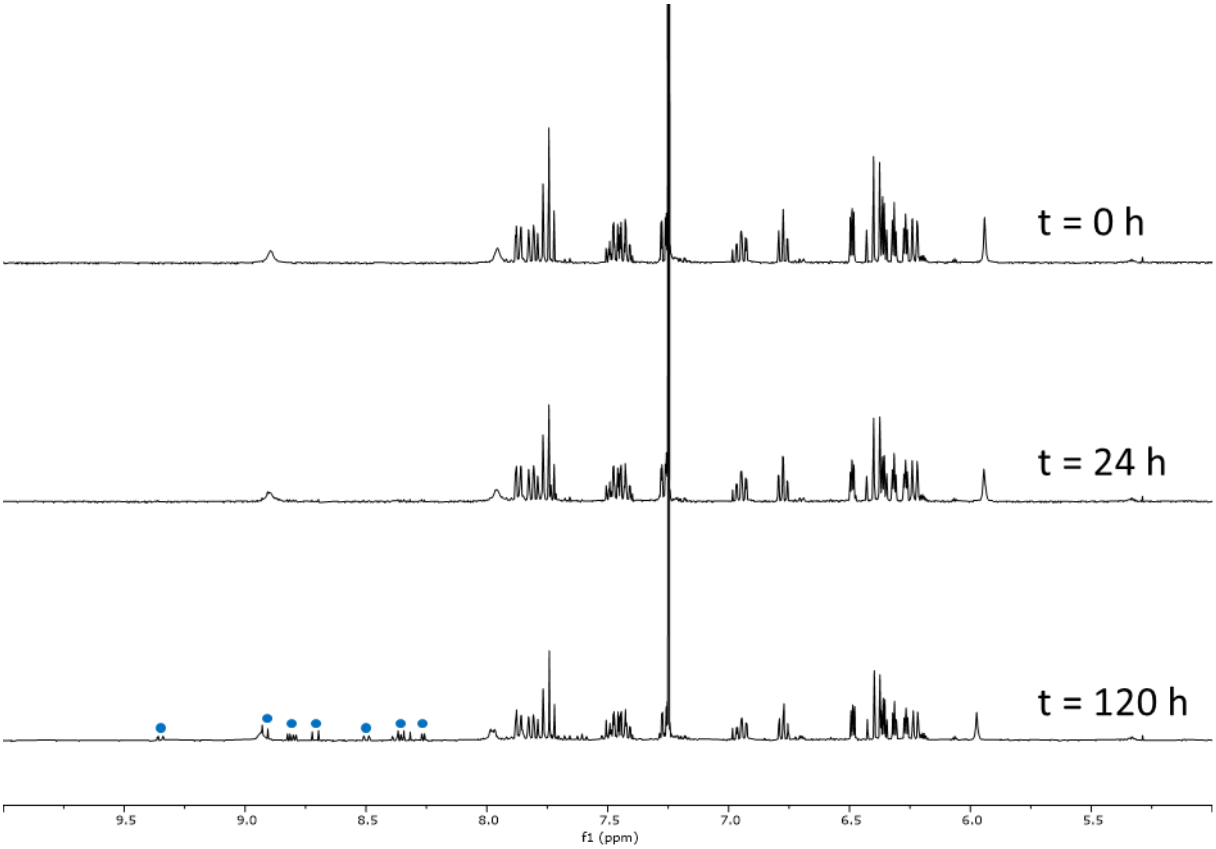

Figure S99. ^{1}H NMR spectra of **1b** recorded for a freshly prepared sample and after 24 and 120 h (400 MHz, $CDCl_3$, 293 K). Blue dots mark signals of **3b** traces.

10.2. Formation of 2a from 3a in the Presence of Moisture

The sample of **3a** was prepared according to **GP5** in dry $CDCl_3$ inside a glovebox using properly dried glassware. NMR and EPR spectra were recorded before and 24 h after exposure to air (**Fig. S100** and **Fig. S101**). After 24 hours of exposure NMR signals intensity significantly decreased, and traces of **1a** were detected. At the same time, the EPR spectrum indicated the presence of **2a**.

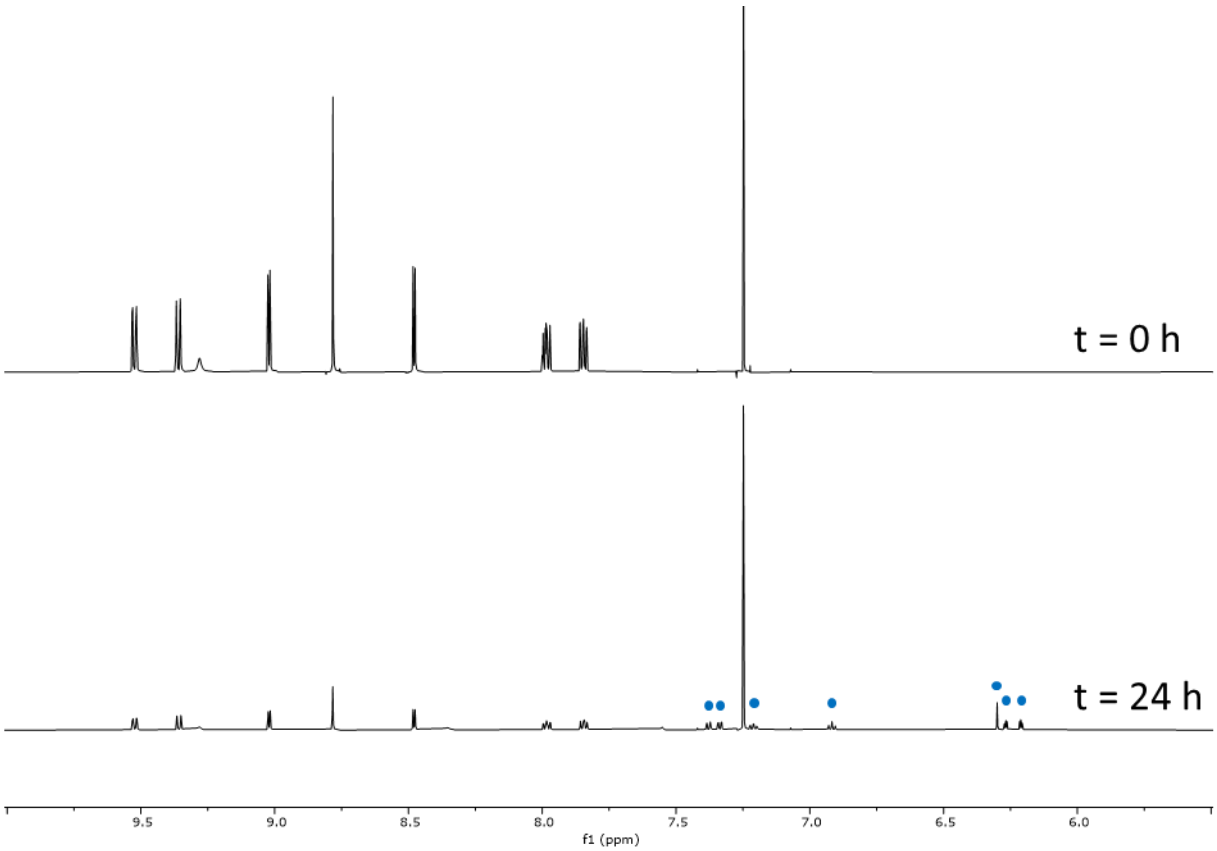

Figure S100. ^{1}H NMR spectra of **3a** recorded for a freshly prepared sample under an inert atmosphere and after 24 h of exposure to air (600 MHz, $CDCl_3$, 293 K). Blue dots mark signals of **1a** traces.

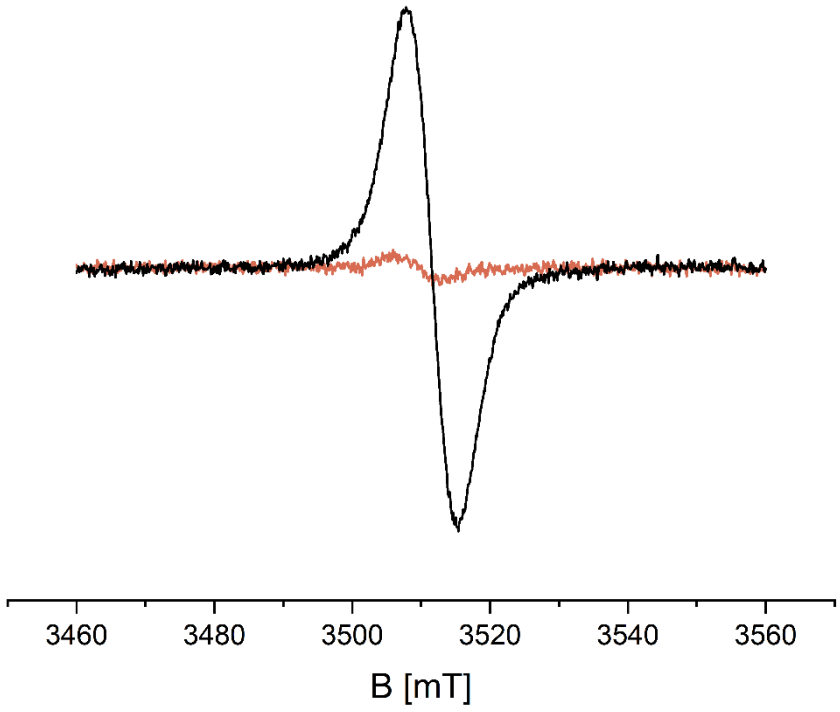

Figure S101. EPR spectrum of **3a** of a freshly prepared sample under an inert atmosphere (orange line) and after 24 h of exposure to air (black line) ($CDCl_3$, 293 K).

11. Bibliography

[1] G. M Sheldrick, *Acta Cryst. A*, **2015**, *71*, 3-8; b) G. M. Sheldrick, *Acta Cryst. C*, **2015**, *71*, 3-8.
[2] O. V. Dolomanov, L. J. Bourhis, R. J. Gildea, J. A. K. Howard, H. Puschmann, *J. Appl. Cryst.* **2009**, *42*, 339-341.
[3] S. Stoll, A. Schweiger, *J. Magn. Reson.* **2006**, *178*, 42-55.
[4] Gaussian 09, Revision E.01; M. J. Frisch et al., Gaussian, Inc.: Wallingford CT, **2009**.
[5] a) C. T. Lee, W. T. Yang, R. G. Parr, *Phys. Rev. B*, **1988**, *37*, 785-789; b) A. D. Becke, *Phys. Rev. A*, **1988**, *38*, 3098-3100.
[6] T. Lu, F. Chen, *J. Comput. Chem.* **2012**, *33*, 580-592.
[7] R.F.W. Bader, *Atoms in Molecules: A Quantum Theory*, Oxford University Press, **1990**.
[8] a) A. K. Mandadapu, M. Saifuddin, P. K. Agarwal, B. Kundu, *Org. Biomol. Chem.* **2009**, *7*, 2796-2803; b) Y. Zhang, K. Shibatomi, H. Yamamoto, *Synlett*, **2005**, *18*, 2837-2842
[9] T. Iwaki, A. Yasuhara, T. Sakamoto, *J. Chem. Soc., Perkin Trans.* **1999**, *1* 1505-1510.